

AD \_\_\_\_\_

Award Number: DAMD17-01-1-0366

TITLE: Maximizing Immune Response to Carbohydrate Antigens on Breast Tumors

PRINCIPAL INVESTIGATOR: Thomas Kieber-Emmons, Ph.D.

CONTRACTING ORGANIZATION: University of Arkansas for Medical Sciences  
Little Rock, Arkansas 72205

REPORT DATE: August 2005

TYPE OF REPORT: Final

PREPARED FOR: U.S. Army Medical Research and Materiel Command  
Fort Detrick, Maryland 21702-5012

DISTRIBUTION STATEMENT: Approved for Public Release;  
Distribution Unlimited

The views, opinions and/or findings contained in this report are those of the author(s) and should not be construed as an official Department of the Army position, policy or decision unless so designated by other documentation.

# REPORT DOCUMENTATION PAGE

*Form Approved  
OMB No. 0704-0188*

Public reporting burden for this collection of information is estimated to average 1 hour per response, including the time for reviewing instructions, searching existing data sources, gathering and maintaining the data needed, and completing and reviewing this collection of information. Send comments regarding this burden estimate or any other aspect of this collection of information, including suggestions for reducing this burden to Department of Defense, Washington Headquarters Services, Directorate for Information Operations and Reports (0704-0188), 1215 Jefferson Davis Highway, Suite 1204, Arlington, VA 22202-4302. Respondents should be aware that notwithstanding any other provision of law, no person shall be subject to any penalty for failing to comply with a collection of information if it does not display a currently valid OMB control number. PLEASE DO NOT RETURN YOUR FORM TO THE ABOVE ADDRESS.

1. REPORT DATE (DD-MM-YYYY)	2. REPORT TYPE		3. DATES COVERED (From - To)	
01-08-2005	Final		15 Jul 01 – 14 Jul 05	
4. TITLE AND SUBTITLE  Maximizing Immune Response to Carbohydrate Antigens on Breast Tumors			5a. CONTRACT NUMBER	
			5b. GRANT NUMBER DAMD17-01-1-0366	
			5c. PROGRAM ELEMENT NUMBER	
6. AUTHOR(S)  Thomas Kieber-Emmons, Ph.D.  E-Mail: tke@uams.edu			5d. PROJECT NUMBER	
			5e. TASK NUMBER	
			5f. WORK UNIT NUMBER	
7. PERFORMING ORGANIZATION NAME(S) AND ADDRESS(ES)  University of Arkansas for Medical Sciences Little Rock, Arkansas 72205			8. PERFORMING ORGANIZATION REPORT NUMBER	
9. SPONSORING / MONITORING AGENCY NAME(S) AND ADDRESS(ES)  U.S. Army Medical Research and Materiel Command Fort Detrick, Maryland 21702-5012			10. SPONSOR/MONITOR'S ACRONYM(S)	
			11. SPONSOR/MONITOR'S REPORT NUMBER(S)	
12. DISTRIBUTION / AVAILABILITY STATEMENT  Approved for Public Release; Distribution Unlimited				
13. SUPPLEMENTARY NOTES  Original contains color plates: All DTIC reproductions will be in black and white.				
14. ABSTRACT  Abstract is attached at following page.				
15. SUBJECT TERMS  Cellular (T-cell) immunology; tumor immunology; DNA immunology; IL-12, GM-CSF, cytokine				
16. SECURITY CLASSIFICATION OF:		17. LIMITATION OF ABSTRACT  UU	18. NUMBER OF PAGES  70	19a. NAME OF RESPONSIBLE PERSON USAMRMC
a. REPORT U	b. ABSTRACT U			c. THIS PAGE U

## **Table of Contents**

<b>Cover.....</b>	
<b>SF 298.....</b>	
<b>Table of Contents.....</b>	
<b>Introduction.....</b>	<b>1</b>
<b>Body.....</b>	<b>1</b>
<b>Key Research Accomplishments.....</b>	<b>18</b>
<b>Reportable Outcomes.....</b>	<b>20</b>
<b>Conclusions.....</b>	<b>20</b>
<b>References.....</b>	<b>21</b>
<b>Publications/Meeting Abstracts/Personnel.....</b>	<b>23</b>
<b>Appendices.....</b>	<b>24</b>

## ABSTRACT

Future progress to improve the overall survival of breast cancer patients will depend on introducing new therapies such as cancer vaccines. Because the majority of cell proteins and lipids are glycosylated, tumor associated carbohydrate antigens (TACA) are attractive as potential targets for cancer vaccines. However, tumor-associated carbohydrate antigens are both T-cell-independent antigens and self-antigens, impacting on their ability to induce generate strong, sustained responses against these antigens. To maximize tumor-protective immunity directed to TACA we have identified and characterized a number of peptides that mimic carbohydrate structures associated with human breast adenocarcinoma cells. Our accomplishments include 1) The induction of T cells that target naturally processed glycopeptides expressed on murine models of breast cancer; 2) Showed that these mimotopes can inhibit metastatic outgrowth in these models; 3) that the mimotopes can induce carbohydrate reactive antibodies that trigger apoptosis of human breast cancer cell lines; 4) that these peptides can cross-react with sera from breast cancer patients that have reactivity with the carbohydrate antigen. 5) Our *in vivo* studies demonstrate that the peptide mimotopes induce sustained immunity to these antigens. Collectively, these data provide the experimental foundation for evaluating peptide mimotopes as potential cancer vaccines in patients with breast cancer.

## **Introduction**

Carbohydrates are the most abundantly expressed self-antigens on tumor cells and consequently they are perceived as viable targets for immunotherapy. Examples of tumor-associated carbohydrate antigens include GD2, GD3, fucosyl GM1, Globo H, STn and the neolactoseries antigens sialyl-Lewis x (sLex), sialyl-Lewis a (sLea) and Lewis Y (LeY). A major approach to induce responses to these tumor associated carbohydrate antigens (TACA) is carbohydrate-conjugate vaccines. Representative examples of these vaccines in clinical development include those directed toward gangliosides [1-3], polysialic acid [4], Globo-H [5], Lewis Y (LeY) [6], and the STn antigen [7]. Because TACA are T-cell-independent antigens and self-antigens, conjugation to immunologic carrier protein is perceived essential to recruit T cell help for antibody generation. Conjugation of TACA does not, however, ensure an increase in immunogenicity because conjugation strategies do not uniformly enhance carbohydrate immunogenicity [8,9]. Furthermore, even with conjugation, the lack of induction of cellular immune responses that would amplify TACA-reactive humoral responses necessitates constant boosting with vaccine. Such deficiencies indicate that better ways to synthesize carbohydrate immunogens reflective of natively expressed carbohydrate structures or alternative ways to induce cross-reactive immune responses with native carbohydrate are needed.

Peptide surrogates of TACA are T-cell-dependent antigens and therefore immunization with these surrogates is predicted to facilitate cellular responses. We are demonstrating that peptides mimicking the breast cancer associated neolactoseries antigens LeY and difucoganglioside (an extended sLex structure) are capable of activating carbohydrate specific cellular immune responses that limit tumor growth *in vivo*. Thus, peptide mimotopes of TACA represent a new and very promising tool to overcome T-cell independence and to increase the efficaciousness of the immune response to glycan antigens.

## **Body**

The major goal of this application was to examine ways to maximize the tumor-protective immunity directed to carbohydrate antigens expressed on breast tumors using a DNA based vaccine approach whereby plasmids encode peptide mimotopes (Table 1) of TACA. We had defined three objectives, organized as 5 tasks. In Objective 1 we intended to optimize the peptide mimotopes (glycotope) encoded DNA vaccine by combining molecular adjuvants in the immunization procedure. In these experiments we were to immunize mice with DNA constructs encoding IL-12 to further enhance the Th1 immune response and GM-CSF to recruit Dendritic Cells that may lend to enhancement of both humoral and cellular responses. The efficacy of priming with DNA constructs and boosting with multivalent carbohydrate or multivalent peptide formulations was also to be established. In Objective 2 the protective immunity of the optimized formulation against tumor challenge was to be evaluated both *in vitro* and *in vivo*. In cytotoxic T lymphocyte (CTL) assays, as effector cells, we were to use splenocytes from experimental animals and as a target, transfected 4T1 cells that express histo-blood group related carbohydrate antigens. As control target cells we intended to use 4T1 mouse mammary cells that do not express relevant carbohydrate antigens as well as other haplotype matched murine tumor cells. Collectively, these assays would tell us about the general characteristics of Th1 and Th2 responses induced by glycotope DNA vaccines

compared to carbohydrate and peptide formulations. Using this vaccination approach we intend to magnify cellular and humoral immune responses to carbohydrate expressing tumors by augmentation of NK, CD4+ and CD8+ T cell responses. This way, we might expect to be able to clear established tumors of bigger sizes.

We made deviations from our intended tasks and objectives as warranted by obtained results or realization of unexpected results and the work was slowed down as the PI moved from the University of Pennsylvania to the University of Arkansas for Medical Sciences in 2002. Nevertheless during the funding period we published 5 manuscripts [10-14] and are at present preparing three more.

**Table I. Peptides used in our studies**

Peptide Sequence	Synthesized	DNA
104 GGIMILLIFSLWFGGA	X	
105 GGIYYPYDIYYPYDIYYPYD	X	
106 GGIYWRYDIYWRYDIYWRYD	X	X
107 GGIYYRYDIYYRYDIYYRYD	X	X
109 GGARVSFWRYSSFAPTY		
911 YRYRYGRYRSGSYRYRYGRYRSGS	X	X
D002 RGGLCYCRYRYCVCVGR	X	

**Task 1. Establish murine breast tumor model.** The purpose of this Task was to develop a breast cancer model system with two objectives. One, to use a cell type relevant to Breast cancer. The other, to use a cell line that expresses relevant carbohydrate structures. We had established by FACS analysis that murine mammary 4T1 cells do not express LeY nor sLex or sLea as determined by the usual set of monoclonal antibodies reactive with these carbohydrate antigens. The 4T1 cell line (H2-d) is highly metastatic and is weakly immunogenic in Balb/c mice. In Task 1 we planned to transfect murine 4T1 cells with the fucosyltarnsferase gene FUTIII to express sLex. However, in our initial studies we used the murine cell line Meth A (H2-d) as a model as this cell line reacted with the monoclonal antibody FH6. FH6 antibody reacted with our panel of peptide mimotopes. Meth A is a Methylcholanthrene-induced sarcoma of BALB/c origin. We identified a clone of Meth A by FACS sorting with the anti-difucoganglioside monoclonal antibody FH6. It was thought that many-proof-of-principle experiments could be conducted with this cell line early on. In our first year we established that immunization with a peptide mimetic of core structures of the neolactoseries structure that reacts with an anti-LeY monoclonal antibody, BR55-2, and with FH6 elicits a cellular response to Meth A cells [10].

During the transfection studies with FUTIII in 4T1 cells we came to realize that 4T1 was reactive with the anti-sLex monoclonal antibody KM93. This antibody is suspected to react with sLex antigen expressed on lipids. Expression of sLex and sLea on tumor cells is thought to facilitate metastasis by promoting cell adhesion to selectins on vascular endothelial cells. Experiments supporting this concept usually bypass the early steps of the metastatic process by employing tumor cells that are injected directly into the blood. As a deviation of our work we investigated the relative role of sLex oligosaccharide in the dissemination of breast carcinoma, employing the spontaneous

4T1 murine metastasis model. An sLex deficient subpopulation of the 4T1 mammary carcinoma cell line was produced by negative selection using the sLex-reactive KM93 MAb. Negatively selected 4T1 cells were to be used as a control cell line during our immunization studies. This subpopulation found to be negative for E-selectin binding but retained P-selectin binding. Both sLex-negative and -positive cells grew at the same rate; however, we found that sLex-negative cells spread more efficiently on plates and had greater motility in wound-scratch assays. We observed that mice inoculated in the mammary fat pad with sLex-negative and -positive variants produced lung metastases. However, the number of lung metastases was significantly increased in the group inoculated with the sLex-negative variant ( $p = 0.0031$ ), indicating that negative selection for the sLex epitope resulted in enrichment for a subpopulation of cells with a high metastatic phenotype. Cell variants demonstrated significant differences in cellular morphology and pattern of tumor growth in primary and secondary tumor sites. These results strongly suggest that loss of sLex may facilitate the metastatic process by contributing to escape from the primary tumor mass [14]. We are presently using this cell line in our immunization studies.

We also came to realize that the 4T1 model could also tell us something about tumorigenicity by focusing on metabolic end-products. End-products of glycolysis as well as phospholipid precursors and catabolites have been suggested as metabolic indicators of tumor progression. To test the hypothesis that increased levels of such indicators can distinguish metastatic phenotypes, we determined a limited cellular  $^1\text{H}$ -NMR metabolic profile of subpopulations of murine mammary 4T1 cells that differ in their metastatic potential. The metabolic profile of the sLex-negative subpopulation indicated higher levels of lactate and total choline metabolites than the sLex-positive subpopulation, suggesting that altered metabolism is a critical component of the malignant phenotype. Analysis of shed cellular material from the sLex-negative subpopulation displayed an increased ratio of phosphocholine to glycerophosphocholine when compared to the parental line and sLex-positive subpopulation. Serum obtained from mice inoculated with either sLex-negative or sLex-positive tumor cells contained broader methylene resonances ( $P = 0.0002$ ;  $P = 0.0003$ ) and narrower methyl resonances ( $P = 0.0013$ ;  $P < 0.0001$ ) when compared to serum of naive mice. However, line widths of methylene and methyl resonances were not useful for distinguishing between the two tumor phenotypes. Results of this study further support the notion that metabolic indicators of malignancy can correlate with *in vivo* metastatic behavior [13].

Contrary to the E-selectin reactivity, P-selectin reactivity on negatively selected 4T1 cells was found to be sLex-independent. The data indicate that E- and P-selectin react with separate ligands on the surface of 4T1 cells. Surface heparan sulfate glycosaminoglycans were the major P-selectin ligands. These ligands were significantly and stably expressed on the surface of this cell line. Heparan sulfate proteoglycans were involved in heterotypic adhesion of the 4T1 cells to HUVECs as the adhesion was clearly enhanced after P-selectin induction on the HUVECs and suppressed after heparinase treatment of tumor cells. The results suggest that therapeutics targeting sLex, even having a highly sLex-positive primary tumor, may not yield a positive outcome. When 4T1 cells were transfected with FUTIII there was a dramatic increase in the expression of sLex containing structures as determined by sLex specific monoclonal antibodies. As expected, there was an increase in E-selectin binding following FUTIII transfection.

However, FUTIII transfection caused no additional P-selectin binding. Because it is known that both E- and P-selectin can bind to sLex it is interesting that transfection with FUTIII and expression of multiple sLex epitope can increase E-selectin binding without detectable increase in P-selectin binding. This result implies that the sLex structures produced are ligands for E-selectin but not for P-selectin (manuscript in preparation).

### P-selectin reactivity with the 4T1 cells is independent of sLex expression.

To investigate the nature of carbohydrate antigens on the 4T1 cell surface, first the cells were tested for binding to E- and P-selectin receptors. Cells were incubated with recombinant mouse E- and P-selectin/Fc (human IgG) chimeras and binding was assayed by flow cytometry. Consistent with what we have reported before, both lectins bound to the 4T1 cells with P-selectin showing very strong reactivity (Fig 1A,B). Contrary to the E-selectin reactivity, P-selectin reactivity was not blocked by low concentration of EDTA. EDTA inhibited P-selectin reactivity only at high concentrations indicating Ca-independent nature of the reactivity (Fig 1A). We further treated cell with neuraminadase to see if sialylation

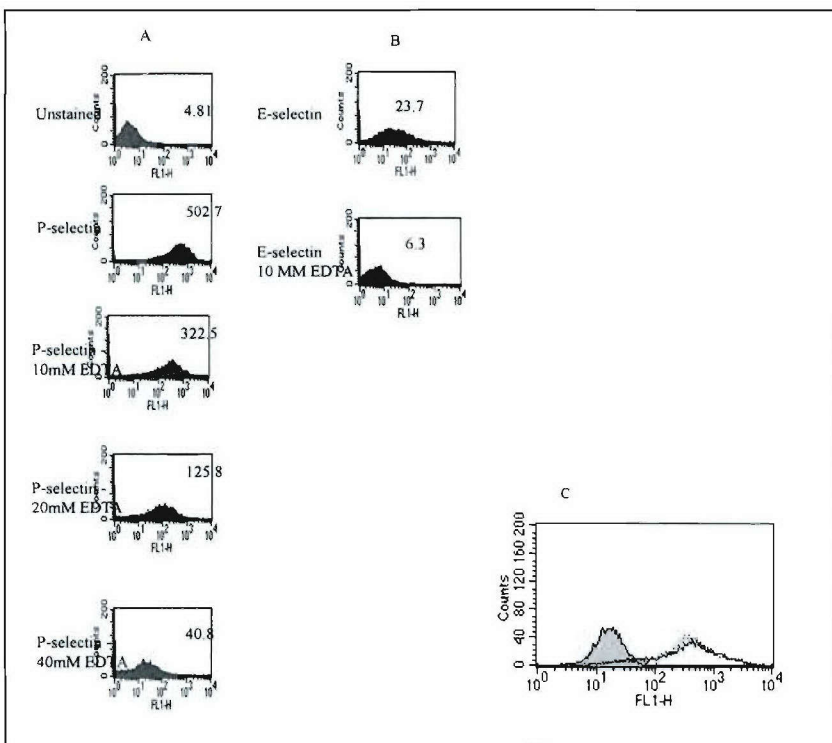


**Figure 1.** P-selectin binding to 4T1 cells is calcium independent. Cells were harvested and stained with IgG chimeric P-selectin (A) or E-selectin (B). Cells were first incubated with the chimeric proteins in the absence or presence of different concentrations of EDTA, and then stained with FITC-conjugated goat anti-human IgG. Results of One representative experiment out of three are depicted. (C). Neuraminadase treatment did not change the P-selectin reactivity. Cells were treated with neuraminadase at 50 mU/ml for 1 hour at 37°C. Filled histogram represents secondary antibody. Continuous and dotted histograms represent P-selectin reactivity without and with neuraminidase treatment,

has anything to do with reactivity of P-selectin. Neuraminidase treatment did not change the P-selectin reactivity (Fig 1C). The results indicate that E- and P-selectin react with separate ligands on the surface of 4T1 cells and contrary to the E-selectin, P-selectin binds to unsialylated ligands on these cells.

### P-selectin ligands are heparan sulfate glycosaminoglycans.

To further characterize the nature of P-selectin ligands on the surface of 4T1 cells, cells were treated with pronase or were grown in sulfate-free medium in the presence of sodium chlorate to inhibit sulfate biosynthesis and then P-selectin ligands availability was tested. Treatment with pronase dropped the P-selectin reactivity to the levels of the negative control, indicating a protein nature for the ligands (Fig 2A). Growing the cells in sulfate free medium containing sodium chlorate led to elimination of P-selectin binding in a huge proportion of the cells, indicating that most P-selectin ligands on the 4T1 cells are sulfated (Fig 2B). Sulfated glycosaminoglycans like heparan sulfate and chondroitin sulfate are carbohydrate moiety of proteoglycans, which are potential P-selectin ligands. Treatment with a mixture of glycosaminoglycan-cleaving enzymes heparinase and chondroitinase gave a clear decrease of P-selectin binding (Fig 2C). The presence of heparan sulfate was further confirmed using

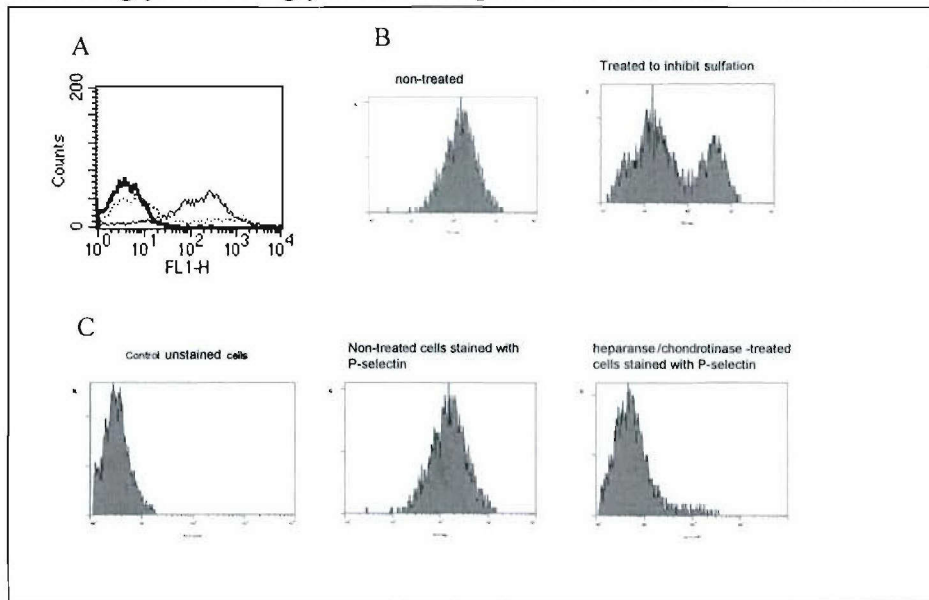


Figure 2. (A) Pronase treatment reduced P-selectin reactivity with 4T1 cells. P-selectin binding to the 4T1 cells (thin line histogram) was sharply reduced (dotted line) to the level of secondary antibody binding (thick solid line). (B) 4T1 cells were harvested and washed with sulfate-free DMEM medium for several times. Cells then were cultured in sulfate-free DMEM supplemented with 10% dialyzed FBS and 100 mM sodium chlorate. The medium was replaced with the same fresh medium after 4 hours of incubation and then incubated for another 18 hours. Then cells were harvested with enzyme-free buffer and P-selectin binding was determined and compared with cells grew in normal medium. C. Cells were left untreated or treated with a mixture of heparanase/chondroitinase at 37 degree for 1 hour. For treatment  $2 \times 10^5$  cell were re-suspended in 0.5 ml of HBSS and incubated with 25 U/ml of heparanase and 5 U/ml of chondroitinase ABC.

10E4 antibody (data not shown). The data clearly indicate that P-selectin ligands on the surface of 4T1 cells are non-sLex glycosaminoglycans.

### P-selectin ligands stably express on the surface of the 4T1 cells and are involved in interaction with HUVECs.

P-selectin binding to the cells *in vitro* and to the primary mass or metastatic cells from subpopulations *in situ* indicate that P-selectin ligands are significantly and stably expressed on the surface of this cell line (Fig 3A). We further examined 4T1 cell binding

to HUVECs and observed that interaction of P-selectin and its ligands play an important role in 4T1 cells binding to HUVECs (Fig 3B). Stimulating surface expression of P-selectin on HUVECs led to an increase in adhesion to the 4T1 cells. The adhesion to 4T1 cells was significantly inhibited by treatment with enzymes heparinase and chondritanase. There was a background adhesion to HUVECs, which was also significantly inhibited by treating the 4T1 cells with heparanase/chondritanase mix, implying a constitutive presence of P-selectin on the HUVECs at our experimental conditions. We further confirmed this point by examining P-selectin expression on HUVECs (data not shown). A low constitutive expression of P-selectin was detected on 10% of cells, which was elevated to a more intense staining on about 20% of cells after treatment with IL-4 and PGE2 (data not shown). Adhesion was clearly enhanced after P-selectin induction and suppressed after heparinase treatment of tumor cells (Fig3B). Results suggest that P-selectin ligands may play a role in hematogenous metastasis in this syngeneic breast cancer model.

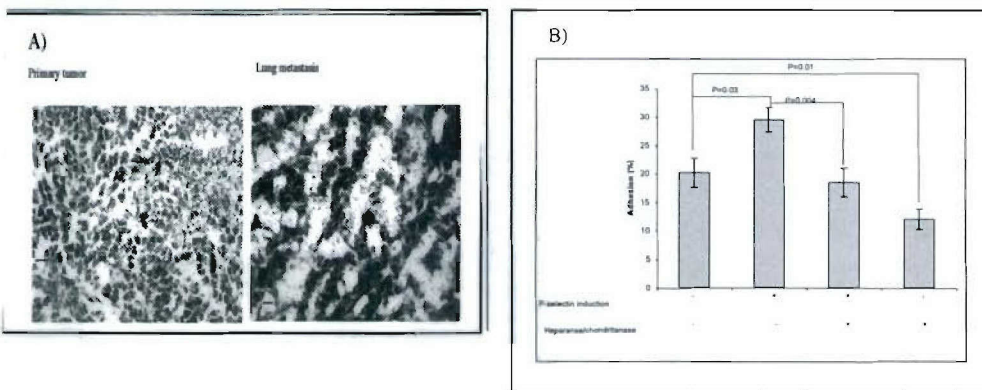


Figure 3. (A) P-selectin histochemical binding to the primary mass and metastatic pulmonary tumors. P-selectin ligands were expressed uniformly and strongly on cells of primary mass. P-selectin ligands were very strongly expressed on metastatic cells in the lung sections. (B) Monolayers of HUVECs were prepared and left untreated or treated for induction of surface presence of P-selectin receptor before conducting the experiment. The 4T1 cells were labeled with Calcein AM and left untreated or treated with a mixture of heparanase/chondritanase enzymes and added to the HUVEC monolayers and incubated at 37°C for 45 min. Unbound cells were removed by gentle washing. Percentage of adhesion was calculated based on mean fluorescence intensities and presented as average of 11 replications. Bars represent SD base on 11 replications. A representative experiment out of three is shown. Paired Student's *t* test was used to compare the means.

#### **Transfection with human fucosyltransferase III induced expression of FH6- and CSLEX-reactive sLex epitopes with no effects on P-selectin binding.**

Monoclonal antibodies defined as KM93, FH6 and CSLEX1 are supposed to recognize sLex antigen. It is shown that FH6 is specific for an extended form of sLex. CSLEX1 and KM93 antibodies are supposed to recognize the same antigen, however, there are dissimilarities regarding the specificities. The nature of molecules carrying the sLex

determinant is supposed to display distinct reactivity with these two antibodies. Among these antibodies we found that only KM93 reacted with the 4T1 tumor cell surface as detected by flow cytometry. We did not detect binding to 4T1 cells with FH6 or CSLEX1 mAbs. Therefore, the lack of relation between P-selectin binding and surface expression of sLex could be due to the specificity of the KM93-reactive epitope. In other words, CSLEX or FH6- reactive sLex epitopes, due to a possible variation in lipid or peptide backbone, may be reactive with P-selectin. In order to test this issue, a broader array of cell surface sLex epitopes was needed. Therefore, we transfected 4T1 cells with human fucosyltransferase III (FUTIII).

FUTIII and FUTVII are responsible for formation of Lewis-type structures. As FUTVII is expressed in 4T1 cells (data not shown) and still there are no detectable levels of sLea, Lea or LeY epitopes, we decided to transfect cells with FUTIII to expand the expression of Lewis epitopes to see if transfectants can produce the other epitopes.

Transfected cells were analyzed by flow cytometry (Fig. 4A). The binding of KM93 mAb was increased to 4T1-FUTIII. Most importantly, CSLEX-1 and FH6

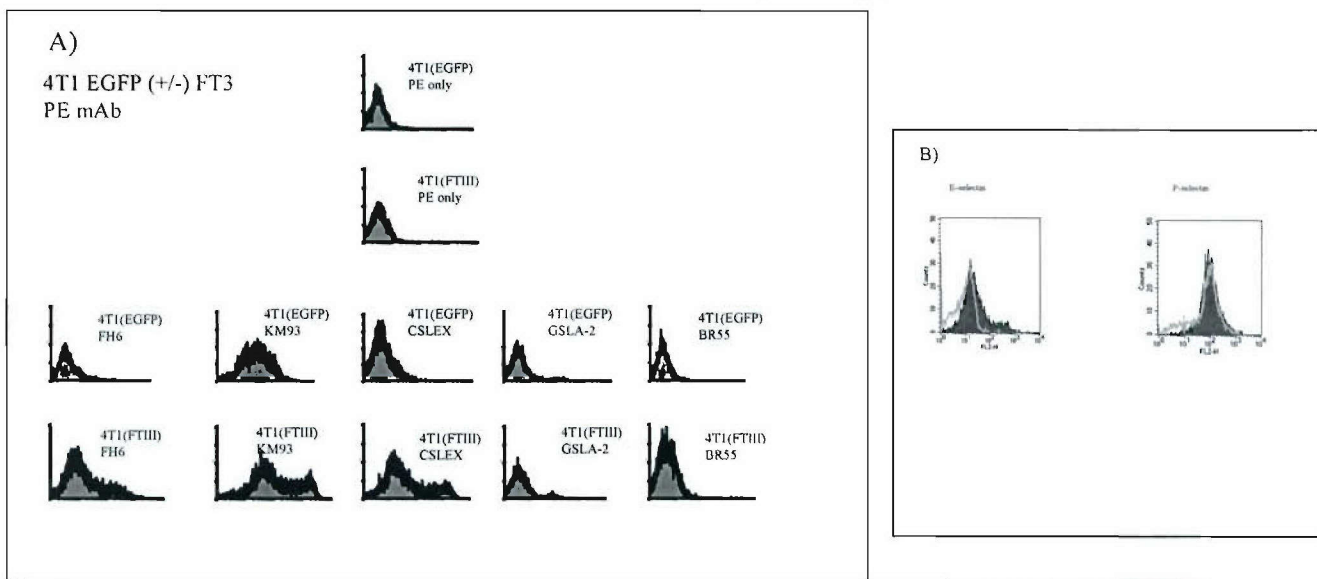


Figure 4. (A) The binding of 3 antibodies to sLex are increased in 4T1 (FUTIII) cells relative to 4T1 (EGFP). Antibodies against sLea and LeY show no difference in binding between 4T1(FUTIII) and the control 4T1(EGFP) transfectant. It is interesting that there is no significant change in sLeA (GSLA-2) or LeY (BR55) since FUT3 can produce LeA, sLeA, Leb, LeY, Lex, and sLex if the proper substrates are present. This may indicate that glycosyltransferases further upstream are not producing the required carbohydrate substrates or that the proteins needed to carry LeA or LeY are not present. (B) FUTIII transfection resulted in an increase in E-selectin but not P-selectin binding. Open histogram is non-transfected and filled histogram is transfected cells.

reactive epitopes were expressed at detectable levels in transfected cells. Since FUTIII expression can also produce other lactoseries antigens like sLea, LeY, Leb and Lex, we examined the expression of these antigens. Antibodies against sLea (GSLA-2) and LeY (BR55-2) showed no difference in binding between 4T1-FUT3 and the control 4T1-EGFP transfectants. No reactivity for the Lex-specific lectin, lotus, was observed to

either cell lines (data not shown). Griffonia simplicifolia lectin I (GSI) lectin, which is reactive with Leb and LeY as well as the  $\alpha$ Gal epitope ubiquitously expressed on murine tumors, did not react preferentially with either cell lines (data not shown). We also analyzed reactivity of some other lectins including SNA, PHA, PNA, Jac, VVA, WGA with the cell lines but no significant differences was observed (data not shown). The antibody and lectin binding data suggest that among a family of carbohydrate antigens involved in metastasis, transfection with FUTIII only improved the expression of various sLex epitopes.

To further understand whether transfection with FUTIII and subsequent expression of sLex alternates alters reactivity of P- and E-selectins with cell, we examined P- and E-selectin reactivities with parental and transfected cells. We detected little E-selectin binding in parental 4T1 cells, after FUTIII transfection the E-selectin binding was increased significantly (Fig 4B). This was expected given the increase in KM93, CSLEX and FH6 binding after transfection. P-selectin binding is more complex. P-selectin bound very well to the parental 4T1 cells and the binding did not increase significantly in transfected cells. The data indicate that P-selectin reactivity with the 4T1 cells is independent of sLex expression and that sLex presence in any form does not affect P-selectin binding.

**Task 2. To evaluate immune parameters associated with DNA vaccination of plasmids encoding glycoprotein along with molecular adjuvants.** We were interested in inducing both cross-reactive antibody and cellular responses using the mimotopes. We intended to manipulate the immune response to mimotopes by co-immunization with genes encoding IL-12 and GM-CSF. We made the peptide encoded constructs and tested them in a vaccination study. In preliminary experiments addition of recombinant IL-12 to the 911 plasmid did not affect the outcome. We established that recombinant IL-12 could enhance the efficacy of immunization with the 106 peptide eradicating established Meth A tumor cells [11]. We further established that peptide/plasmid immunization mediates a Th1 response, as did immunization with 106 peptide [10]. To further confirm a role played by T cells activated by the peptide mimotope, nude mice were transplanted with Meth A cells and injected ip with fresh splenocytes, isolated from cured mice [11]. Immune cells transferred had a dramatic effect on tumor size as by day 15 after transfer, tumor was eradicated completely. These studies suggested that the mimotopes could induce both antibodies and T cells that could eradicate establish tumors of only small size and that IL-2 was effective as an adjuvant.

#### **Peptide immunization leads to an increase in T-cell population and IL-12 responsiveness of T cells**

We observed that the T cell population was increased after immunization with peptide. We used flow cytometry to examine the expression of CD3, CD4, CD8 and NK marker (DX5) on the surface of freshly isolated splenocytes. As shown in Figure 5A, the proportion of CD4+ and CD8+ T cells increased in immunized/cured mice compared with non-immunized/tumor-bearing animals. We did not detect any difference between groups of mice regarding NK cell population using the DX5 antibody.

To determine whether this population could be stimulated by IL-12, an IL-12 responsiveness test was performed on the T-cell population. Individual mice from non-immunized/tumor-bearing, and immunized/cured groups were sacked and T-cells purified

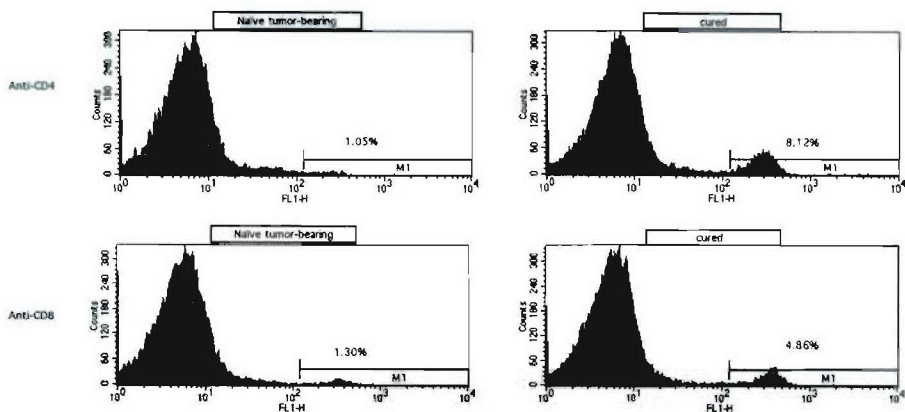


**Figure 5A.** Peptide immunization induces higher proportion of CD4<sup>+</sup> and CD8<sup>+</sup> cells among splenocytes and IL-12 responsiveness among T cells. Naïve (non-immunized), tumor bearing, and peptide immunized/IL12 treated, cured, mice were sacrificed, splenocytes collected and deleted from erythrocytes. Freshly prepared splenocytes were stained with anti-CD4 and -CD8 FITC-conjugated mAbs. The results are representative of two experiments.

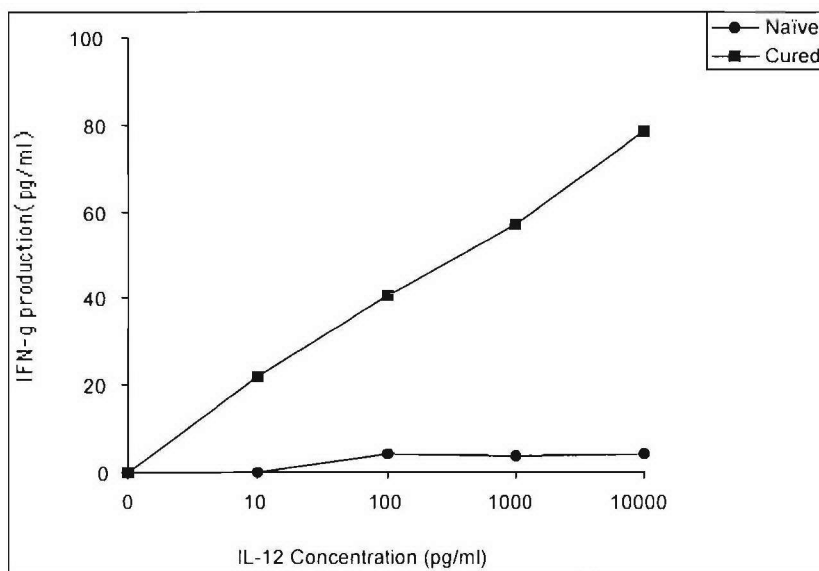
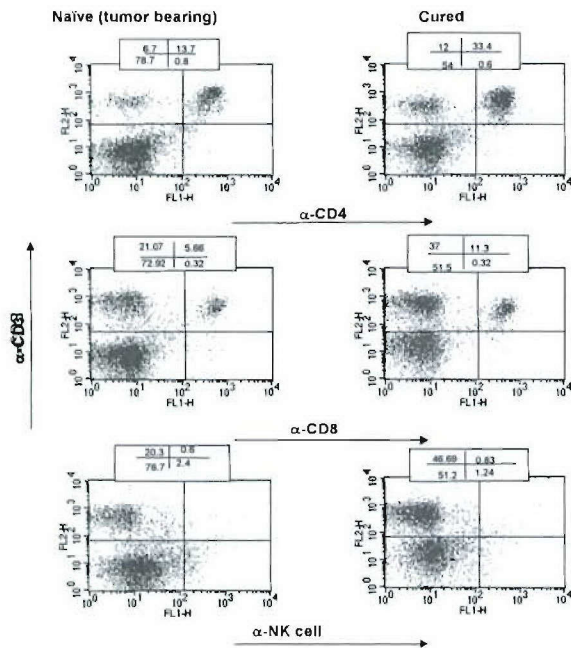


**Figure 5B.** Induction of IL-12 responsiveness in T cells of transplanted mice after peptide immunization. Non-immunized/tumor-bearing and peptide-immunized/cured mice were sacerd, splenocytes collected and T cells purified. Purified T cells were incubated with serial dilutions of rIL-12 for 48 hours. Then supernatants were collected and concentration of IFN $\gamma$  was determined. The results are representative of three independent experiments.

using nylon wool followed by depletion of NK cells and a subsequent positive selection for Thy1.2 using MACS. Purity of T cells was more than 97% as assessed by expression of CD3 molecule by FACS. Purified T cells were seeded and stimulated with various concentrations of IL-12 and induction of IL-12 responsiveness was determined by measuring IFN- $\gamma$  production. Figure 5B shows that T cells from peptide-immunized animals produced IFN- $\gamma$  upon stimulation with IL-12. As it is clear from our data regarding tumor challenge and peptide boost we had a prime and boost effect, we thought to magnify our priming by immunization with inactivated cells. In this case we replaced our first peptide immunization with inactivated Meth A-cell immunization. Tumor-bearing mice seven days after tumor inoculation first were immunized with attenuated cells ( $10^7$ /mouse, i.p.), followed by a combination of peptide/IL-12 as explained before. Unexpectedly, this immunization regimen was less efficient as we recorded 3-4 escaped mice out of 12 in each separate experiment. The data again suggested that peptide immunization is efficacious but it should be done early on, as large tumors are hard to treat. Taking advantage of other effector cells, we further tried to stimulate eradication of tumors in immunized/tumor-bearing animals by treating them with Cyclophosphamide (Cy). Cy injected littermates were immunized with the peptide mimetic after 7 days followed by 5 doses of IL-12. We speculated that using this regimen, we might activate effector cells, which may cooperate with T cells in eradicating tumors of larger size. Following Cy and peptide/IL-12 therapy a clear tumor regression was marked in two thirds of the cases (data not shown). To further understand what cell population was in charge of such distinct tumor regression, we isolated splenocytes and stained cell surface markers by flow cytometry. As shown in Figure 6, it appears T cells may be the major effector population.

Figure 6 is on following page.

**Figure 6.** Treatment with Cy and IL-12 mediate an increase in CD4+ and CD8+ cells. Immunized tumor-bearing (uncured) and a mouse that underwent Cy and IL-12 treatment after or before eradication of tumor were sacerd and freshly prepared CD3+ splenic lymphocytes were stained with anti-CD4 -CD8 and -NK cell marker. The results are representative of two experiments.



### Task 3. Evaluate priming and boosting effect of immunogens.

#### Mimotopes are superior immunogens than carbohydrates

A closer look at the above data revealed to us that mimotope immunization might induce a type of memory for generation of serum IgM, which is long lasting. To examine this issue we primed mice with 911 MAP and then boosted them with sLex (sialyl Lewis <sup>x</sup>-PAA). Serum reactivity was then checked against sLex. As shown in figure 7, 911 peptide primes for IgM-sLex reactive Abs. Immunization with sLex boosts the response and it lasts longer than it does in immunization with sugar only. Sugar boosted the response and stabilized it for a longer time period. The data suggest that there is a priming effect, with peptide immunization, for generation of cross-reactive IgM and the generated IgM is longer lasting. We also analyzed the cross-reactive IgG response during the course of experiments, as we reported before we also detected a prime and boost effect for IgG of low titer (data not shown). The results suggest that despite the induction of a state of tolerance in carbohydrate immunization, mimotope immunization induce a type of memory for the IgM portion of the serum, priming for later sugar immunization.

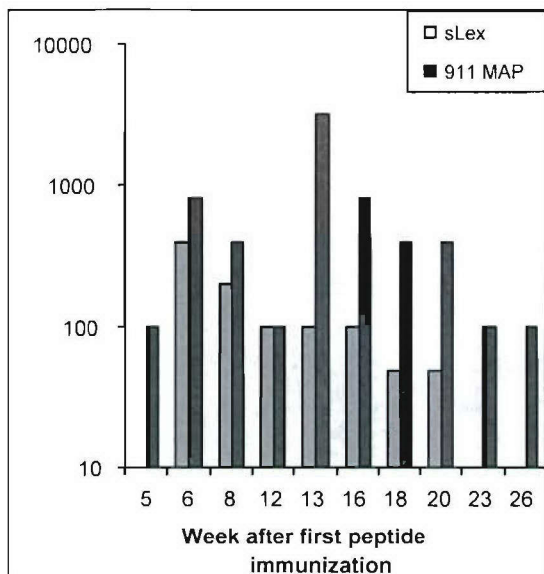
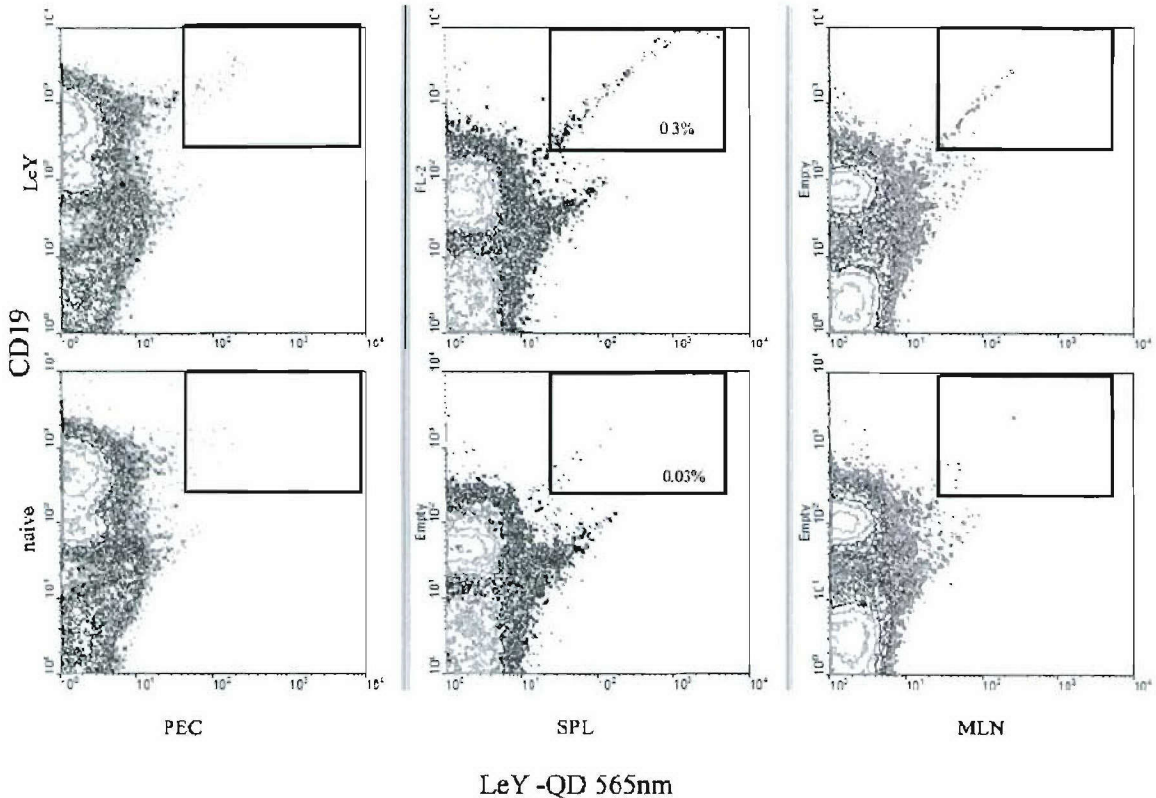


Figure 7. Peptide immunization primes for an anti-carbohydrate cross-reactive memory IgM response. Mice were pre-bled and groups of mice were immunized with 911 MAP twice at weeks one and four. Other groups were immunized with sLex (sialyl Lewis  $\alpha$ -PAA) once at week four. Serum was collected at week 0 (pre-bled), after peptide boost or after first sugar immunization for every two-three succeeding weeks. All groups received a sugar immunization at week 12. Mice were bled individually, collected sera pooled and the reactivity against indicated carbohydrates was detected by standard ELISA. The highest serum dilution with a 2SD higher OD than pre-immune serum was determined as end-point titer. Data are representative of three independent experiments.

The rationale behind a direct antigen specific staining in this model is the multiple antigenic mimotope property of the peptide that increases the frequency of observed cells. Even so frequency of about 1/10 000 are expected so the experiments are carried out with large number of cells. Successful staining of antigen specific cells of similar specificity (PC) has been reported [15]. A major difficulty visible in the experiments reported by Newman et al. is the low fluorescence intensity of the labeled cells, which will be dealt with by using quantum dot labels. Quantum dots (QDs) are stable, bright fluorophores that, under ideal conditions, can have high quantum yields, narrow fluorescence emission bands, high absorbency, very long effective Stokes shifts, high resistance to photobleaching, and can provide excitation of several different emission colors using a single wavelength for excitation [16]. Quantum dots were supplied by Quantum Dot Corporation, Hayward, CA 94545 and contained core shell zinc sulfide-cadmium selenide QDs emitting at 565nm, or at 705nm and coating coupled to streptavidin. The carbohydrate complexes were prepared by incubating QD with biotinylated Lewis X or Y polyacrylamide polymers in 5:1 or 10:1 molar ratio (excess of carbohydrate polymer). Cells were then stained with preformed complexes and analyzed by flow cytometry. When Lewis Y immunized mouse splenocytes, mesenteric lymph node cells and peritoneal exsudate cells were compared to those of a naïve mouse a 10 times increase of the QDLewisYPAA stained CD19 positive cells was observed after immunization in all three compartments.(Fig. 8 )



**Figure 8.** Flow cytometry data from samples of peritoneal exudate, spleen and mesenteric lymph node cells from LeY immunized and naïve mice stained with CD19 and Quantum Dot-Streptavidin-LeYPAAbiotin complexes. The frame indicates LeY binding B cells.

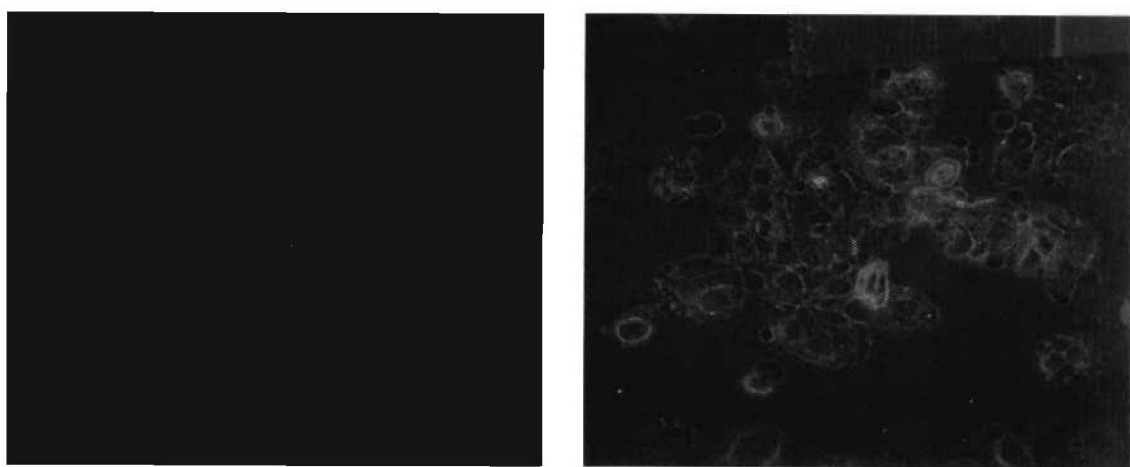
We are now testing if we can isolate B cells reactive with LeY after an initial mimotope prime. The first experiments did not show a detectable increase in Lewis x or Lewis Y binding B cells after immunization with D002MAP or 106MAP in QS21 respectively (data not shown). Experiments are under way to compare the occurrence of carbohydrate binding B cells after priming with mimotope and boosting with carbohydrate polymer as compared to priming and boosting only with carbohydrate.

#### Task 4. Perform tumor challenge experiments

The selective targeting of tumor-associated carbohydrate antigens by the induction of serum antibodies that trigger apoptosis of tumor cells as a means to reduce circulating tumor cells and micrometastases would be an advantage in cancer vaccine development. Some plant lectins like Griffonia simplicifolia lectin I and wheat germ agglutinin mediate the apoptosis of tumor cells. We investigated the possibility of using these lectins as templates to select peptide mimotopes of tumor-associated carbohydrate antigens as immunogens to generate cross-reactive antibodies capable of mediating apoptosis of tumor cells. In this study, we showed that immunization with a mimotope selected based on its reactivity with GSI and wheat germ agglutinin induced serum IgM antibodies in mice that mediated the apoptosis of murine 4T1 and human MCF7 cell lines in vitro, paralleling the apoptotic activity of the lectins. We observed that peptide

immunogen did better than the DNA encoded form. Vaccine-induced anti-carbohydrate antibodies reduced the outgrowth of micrometastases in the 4T1 spontaneous tumor model, significantly increasing survival time of tumor-bearing animals. This finding parallels suggestions that carbohydrate-reactive IgM with apoptotic activity may have merit in the adjuvant setting if the right carbohydrate-associated targets are identified [12]. This work showed that peptide immunization was more effective than DNA vaccination with encoded mimotope.

We also observed that the IgM induced by the mimotopes either peptide or DNA encoded was able to mediate apoptosis of MCF7 cells. We observed that the IgM antibodies were able to internalize into the 4T1 cells. We see this also for MCF7 cells.

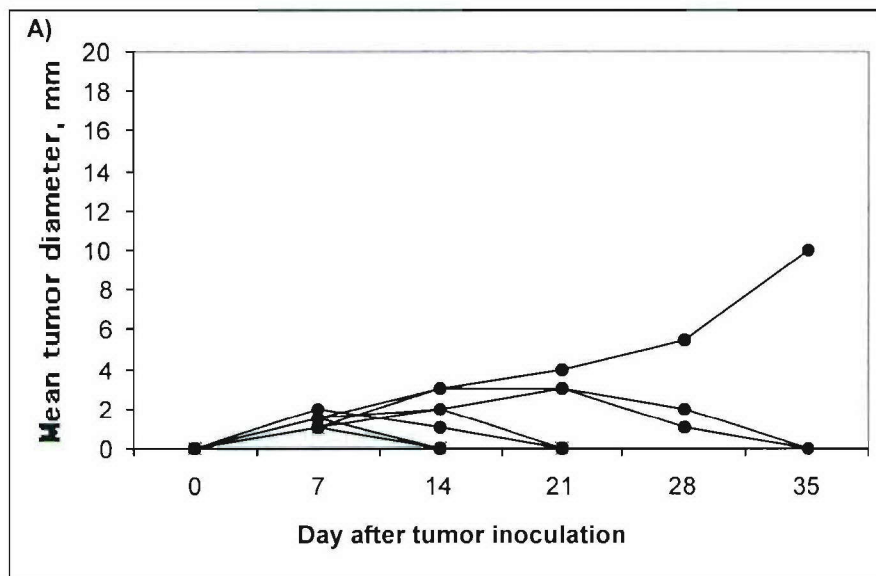


Anti-mouse IgM only

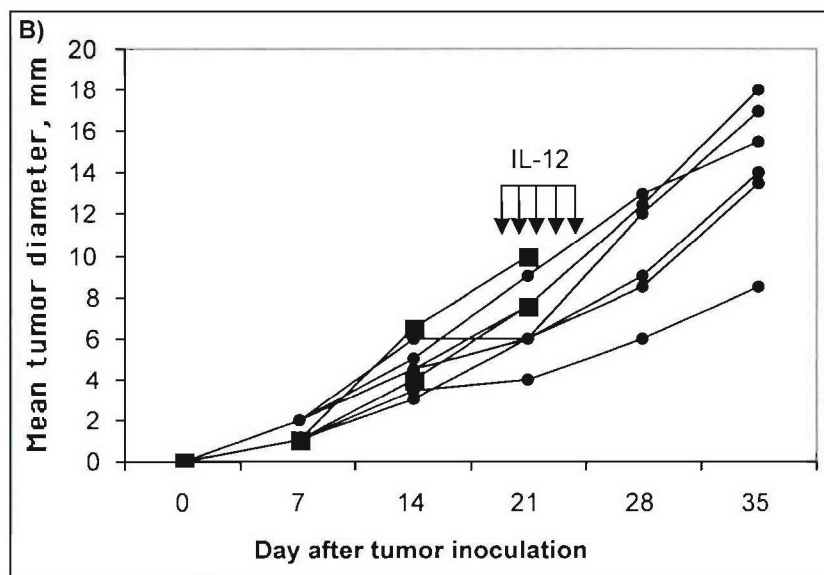
107 serum plus anti-mouse IgM

Figure 9. IgM antibodies were visualized as internalized into MCF7 cells. The immunized serum was premixed with FITC conjugated anti-mouse IgM, then the mixture was added to MCF7 cells and the distribution of staining was visualized using a Zeiss LSM 410 inverted confocal microscope. FITC-conjugated anti mouse IgM was added alone in similar conditions as negative control.

**Vaccination with peptide 106 encoded DNA inhibits tumor growth.** Using the DNA encoded sequences of peptides 106 and 109, groups of mice were immunized with respective DNA constructs. After two immunizations of the respective peptide encoded DNAs, mice (respective groups) were rested for 110 days and challenged with Meth A tumor cells (**Fig. 10**). Tumor growth inhibition was observed in mice immunized with the 106 DNA (**10A**) but not in mice immunized with the construct of peptide 911 (**10B**). Addition of IL-12 did not affect the outcome of the 911 immunized mice.



**Figure 10.** Vaccination with DNA format of the peptide suppressed tumor growth in further challenging the immunized mice with Meth A cells. Mice were immunized with DNA constructs of 106 (A) and 911 (B) peptides twice at a three-week interval. 4 months after the boost mice were challenged with  $5 \times 10^5$  Meth A cells s.c.. Tumor growth is expressed for each individual mouse.



#### Task 5. Test Peptide binding to human DC and human T cell proliferation.

As a maker for T cell binding we first looked at baseline titers to LeY and peptide mimotopes in human sera. To evaluate the potential immunogenicity of a LeY-targeted vaccine, it is important to obtain an estimate of the frequency and mean titer of LeY reactive antibodies that is preexisting within the general public. To obtain these baselines, we have started to screen serum from normal healthy individuals by ELISA to

measure the extent of reactivity by serum antibodies to LeY and to peptides 106 and 107 (Fig 11). We observed two types of patterns. In the majority of sera, the anti-LeY, -106 and -107 IgG and IgM titers were uniformly low (<0.2OD) at all dilutions of sera, suggesting that this reactivity is due to general nonspecific background of the ELISA with no specific antibody reactivity to these antigens in these individuals. In one healthy individual, significant IgG (but not IgM) anti-LeY reactivity was detected (Fig. 3A); reactivity decreased with increasing dilutions of sera, with parallel reactivity to peptides 106 and 107 (Fig. 11B). Although these responses are being further characterized, the data suggest that in this individual, a population of anti-LeY antibodies is present that also recognizes peptides 106 and 107.

We have also sera from breast cancer patients. Like the healthy population, the majority of these sera show no specific anti-LeY, anti-106, or anti-107 reactivity. However positive LeY titers was detected in 1 individual (P76; Fig. 11 C). This patient also displayed a significant peptide 106-reactive IgG titer (Fig 11 D). For this patient, we propose that vaccination with the peptide mimotope could potentially augment the existing immune response. However, the pattern of LeY/peptide 106 reactivity is heterogeneous, because in another patient (P58; Fig. 11D), we see demonstrable anti-106 titers with no apparent reactivity to LeY (P58; Fig 11 C). It is possible that in this patient, vaccination with mimotope can amplify a subpopulation of B cells with LeY reactivity.

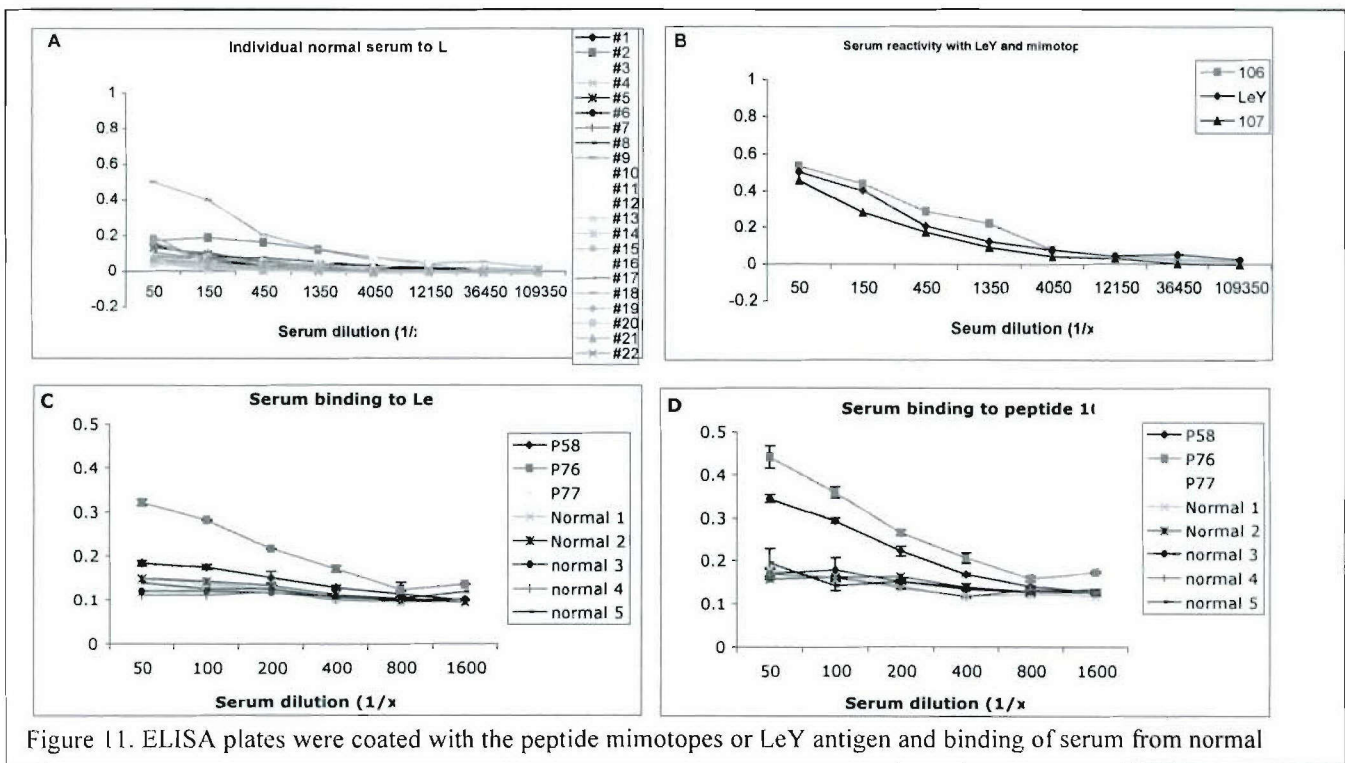
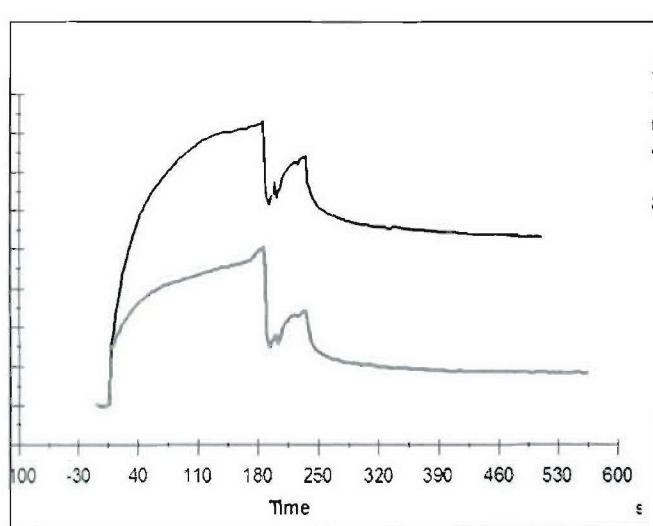


Figure 11. ELISA plates were coated with the peptide mimotopes or LeY antigen and binding of serum from normal

### Optimization of the multiple antigenic mimotope to be taken up by cells

In previous work we showed that 106MAP stimulates cellular response in splenic T cells, which is inhibited by anti-MHC class II antibodies and depends on APC presence[10].

At the same time analysis of the sequence of 106 with available algorithms identifies a H- $2K^d$  binding motif but not a class II one. In Xid mice 106MAP cross reactivity with LeY was present both in the context of TI and TD related response. Its magnitude though correlated with the ability of the immunogen to act as a TD antigen, a property, which was dependent on conjugating to BSA probably due to the introduction of potent Th epitopes. While most probably 106 peptide does stimulate a weak CD4 T cell response it does not seem enough to make it a true TD antigen. To further improve the immunogenicity of the peptide, the strategy of introducing a Th cell epitope and a protein transduction domain (PTD) by the same structure is being currently developed. To this end we synthesized a longer version of 106 (GGIYWRYDIYWRYDIYWRYDGGAYARAAARQARA) which included a PTD (AYARAAARQARA) that coincidentally rendered the structure a I-A $d$  binding motif. The ability of the 106PTD peptide to penetrate liposome layer was demonstrated by SPR using L type biosensor (Fig. 12). 4T1 mouse tumor cells treated with fluorescent 106PTD-FITC showed fluorescence indicating an efficient protein transduction (Fig. 13). In vitro 106PTD induced a stronger proliferative T cell response than 106 but weaker than 106MAP in splenocytes derived from 106MAP immunized mice (Fig. 14 left panel). Splenocytes from 106PTD immunized mice also cross-reacted with 106MAP although, the overall response was weaker than after 106MAP immunization (Fig 14 right panel). These results indicate the 106PTD induces T cells with the same specificity for MAP106 antigen. The immunogenic properties of the new peptide will be defined by comparing a 106PTDMAP version to 106MAP and proving its capacity to stimulate CD4 and CD8 T cells.



**Figure 12.** Binding of 106 (grey) and 106 PTD (black) to liposomes coated on LI chip, Biacore. The peptides were passed over the liposome surface in equal concentrations. The presence of the PTD increases the uptake of the peptide.

**Figure 13.** Uptake of 106-PTD-FITC peptide by murine breast cancer cell line 4T1 – confocal microscopy (left) compared to unstained cells (right). The upper panel shows the fluorescent channel.

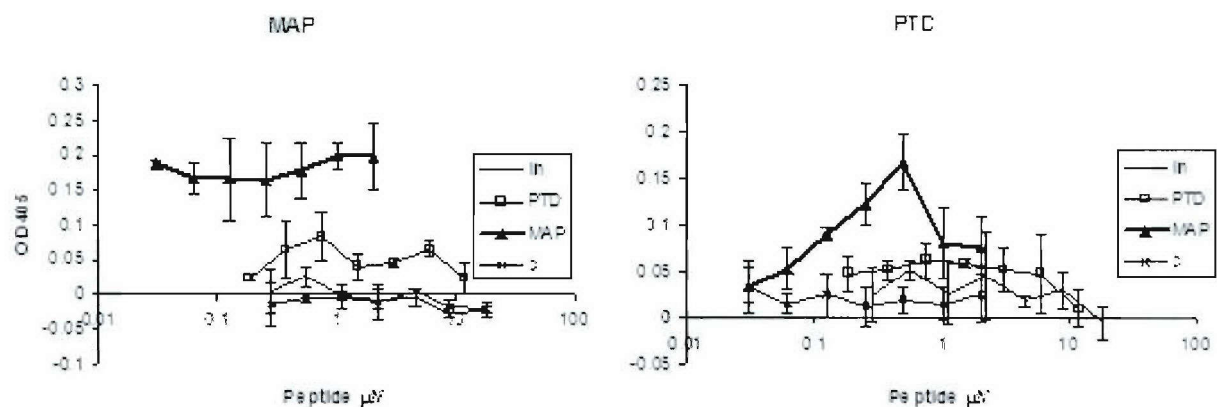
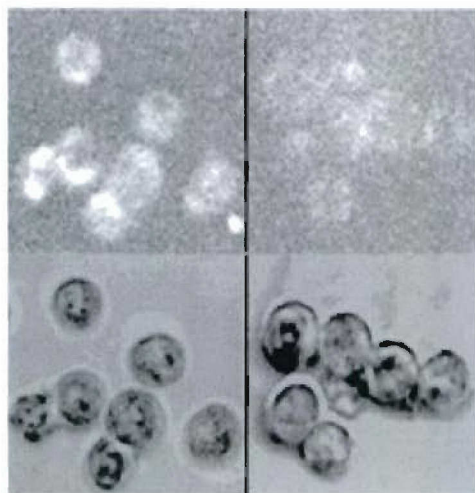


**Figure 14.** Proliferation assay (BrDU cell ELISA) of splenocytes from BALB/c mice immunized with either MAP (left) or PTD (right) versions of 106-peptide and stimulated in vitro with the linear, MAP or PTD versions as well as an irrelevant 12-mer MAP.

### Key research accomplishments

1. We observed that peptide 106 can stimulate Th1 response. We established that cell proliferation, stimulated by peptide 106, was primarily MHC Class II dependent as determined by inhibition with respective anti-MHC antibody. Cell stimulation with peptide 106 triggered IFN- $\gamma$  release suggesting that peptide immunization with QS-21 as expected polarized the Th1 subset.
2. We observed that Th1 cells activated by peptide mimetic express L-selectin. Consistent with previous studies we observed L-selectin loss on CD4+ T lymphocytes upon peptide stimulation but also saw this loss upon stimulation

with sLex. The proliferative response was peptide, sLex and Lex specific since LeY did not exhibit any cellular responses nor did splenocytes from sLex and LeY immunized animals responded to peptide 106, sLex or Lex antigens.

3. **We observed that the designed peptide 106 contained a CTL epitope.** In vivo stimulated effector cells from peptide 106 immunization displayed cytotoxicity directed toward peptide 106-pulsed MHC Class I<sup>+</sup> Class II<sup>-</sup> P815 target cells, further verifying a role for CD8<sup>+</sup> T cell reactivity with peptide 106.
4. **Peptide 106 boosting can affect Meth A directed CTL.** While Meth A cell priming and boosting can lead to CTL activity against Meth A cells, peptide boosting increased the level of cytotoxicity against Meth A cells to a statistically significant level as compared with cytotoxicity against P815 cells as control target indicating a cross-reactive nature between peptide and tumor specific CTL responses. CTL activity was inhibited by the addition of either anti-Class I or anti-L-selectin antibody.
5. **Immunization with Peptide 106 along with IL-12 can eradicate established tumors.** As it was expected, immunization with 106 MAP moderately inhibited tumor growth. It was shown that vaccination with inactivated Meth A cells had no effect on tumor growth, suggesting a superiority of 106 peptide vaccine to a cell-based one in this model. Our data proposes that immunization with only 106 peptide is not sufficient for induction of a state of reliable immunity to eradicate tumor. IL-12 is known to exhibit potent anti-tumor activity in a number of murine tumor models. Further treatment of peptide immunized mice with IL-12 or a combination of Cy and IL-12 considerably helped in stimulating eradication of tumor.
6. **Both types of T cells seem to play a role in tumor cell eradication.** Our data shows that there is a proportional increase in the CD4<sup>+</sup> and CD8<sup>+</sup> T cells among splenocytes of treated mice compared to tumor-bearing mice. We did not observe any differences between splenocytes of these two groups of mice regarding the expression of NK cell marker DX5. Therefore, we propose that 106 immunization induces a population of Th1 and CTLs with production of IFN $\gamma$ , and that IL-12 helps out with expanding the T cell population and activating IFN $\gamma$  production. As resting T cells do not express IL-12 receptor and IL-12 responsiveness is induced after TCR stimulation, purified T cells were stimulated with IL-12 in vitro. The data indicate that in tumor-bearing animals T cells were not sensitized with tumor antigens, while peptide immunization induced T-cell responsiveness to IL-12.
7. **The designed 106 sequence is superior to the 911 sequence as a means to inhibit tumor growth.** DNA immunization with the 911 sequence did not mediate tumor growth inhibit even with the addition of IL-12.
8. **Peptide immunization performs better than DNA immunization.** Immunization with mimotope was able to reduce spontaneous metastases to he

lung in the 4T1 model. Antibodies were shown to trigger apoptosis of the 4T1 cells and for the human breast cancer cell line MCF7.

9. **Cells lacking in sLex may actually be better at metastasizing.** 4T1 cells deficient in E-selectin binding ligands are observed to metastasize quicker than those that express the ligand. SLex ligand does not affect P selectin binding. Deficient expression of sLex may be associated with efficient metastases.
10. **There is limited cross-reactivity of human sera with peptide 106 mimotope.** The lack of cross-reactivity with peptide 106 suggests that the peptide is unique to the immune system.

### **Reportable Outcomes**

We have published 5 manuscripts with three more in preparation. We have shown that immunization with peptide 106 induces cellular responses that are not achievable by immunization with carbohydrate alone. Although cellular responses generated by the peptide mimotope may enhance CTL induction, vaccination with peptide alone appears not to be completely sufficient in the effector phase when challenged with a very high tumor burden. Our CTL data using effectors from peptide only immunized mice on Meth A cells as targets confirm this fact with marginal CTL activity observed.

Our results are very narrow with regards to the breadth of carbohydrate directed cellular responses. Further efforts to optimize and isolate the carbohydrate moieties associated with presented glycopeptides may facilitate vaccine applications for eradication of metastatic lesions by both antibody dependent lysis and cellular responses. This possibility has yet to be proved with the appropriate models but suggests that for certain carbohydrate antigens peptide mimetics might augment cellular responses other than delayed-type hypersensitivity like responses in future vaccine applications. The generated data support the idea of inhibiting metastatic outgrowth suggesting that targeting TACA might be useful in the adjuvant setting. Consequently, peptide mimotopes may be effective immunogens that should be clinically evaluated for their ability to amplify carbohydrate immune responses against circulating or disseminated tumor cells. We have submitted an invited proposal to the BCRP CTR program – July 2005. Our proposed translational studies will benefit breast cancer immunotherapy by using a novel immunogen to generate potent, sustained LeY-reactive responses in breast cancer patients, facilitating long-term immunosurveillance through recall of carbohydrate immune responses that should contribute to patient survival.

### **Conclusions:**

Defining new targets for designing effective and broad-based vaccines is considered crucial for the immunotherapy of solid tumors. Carbohydrates are abundantly expressed on the surface of malignant cells and induction and enhancement of a cell-mediated immune response toward these antigens has outstanding implications in vaccination and treatment of cancer. We have established that:

1. Immunization with 106 MAP induces a peptide specific cellular response.
2. Vaccination of mice with peptide 106 eradicates established tumor.
3. Immunization with DNA format of the peptide suppresses tumor growth in further challenge, but not as good as the peptide form.
4. Induced immunity has a cellular nature as it is transferred to nude mice by transferring splenocytes from cured mice.

Our results suggest that mimotopes are entering another phase in that they may be suitable to generate cellular responses to naturally processed glycopeptides providing an advantage over carbohydrate-based vaccines. The potential remains to further identify mimotopes and improve upon their immunogenicity to amplify functional carbohydrate directed immune responses against circulating or disseminated tumor cells to impact on cancer survival. We believe that this vaccine approach is particularly interesting for cancer prevention because: (a) TACA are expressed very early during neoplastic transformation rendering possible immunosurveillance by CTL ; (b) the same TACA-based vaccine can be used in a variety of tumors, circumventing the limitation of epitope mapping; and (c) by designing appropriate peptide(s) backbone sequence(s) it may be possible to target multiple supertype MHC class I alleles rendering feasible future CTL-based vaccines applicable on a large population scale.

## References

- [1] Guthmann, M. D.; Bitton, R. J.; Carnero, A. J.; Gabri, M. R.; Cinat, G. et al. Active specific immunotherapy of melanoma with a GM3 ganglioside-based vaccine: a report on safety and immunogenicity. *J Immunother* **2004**, *27*, 442-451.
- [2] Krug, L. M.; Ragupathi, G.; Hood, C.; Kris, M. G.; Miller, V. A. et al. Vaccination of patients with small-cell lung cancer with synthetic fucosyl GM-1 conjugated to keyhole limpet hemocyanin. *Clin Cancer Res* **2004**, *10*, 6094-6100.
- [3] Ragupathi, G.; Livingston, P. O.; Hood, C.; Gathuru, J.; Krown, S. E. et al. Consistent antibody response against ganglioside GD2 induced in patients with melanoma by a GD2 lactone-keyhole limpet hemocyanin conjugate vaccine plus immunological adjuvant QS-21. *Clin Cancer Res* **2003**, *9*, 5214-5220.
- [4] Krug, L. M.; Ragupathi, G.; Ng, K. K.; Hood, C.; Jennings, H. J. et al. Vaccination of small cell lung cancer patients with polysialic acid or N-propionylated polysialic acid conjugated to keyhole limpet hemocyanin. *Clin Cancer Res* **2004**, *10*, 916-923.
- [5] Slovin, S. F.; Ragupathi, G.; Fernandez, C.; Jefferson, M. P.; Diani, M. et al. A bivalent conjugate vaccine in the treatment of biochemically relapsed prostate cancer: a study of glycosylated MUC-2-KLH and Globo H-KLH conjugate vaccines given with the new semi-synthetic saponin immunological adjuvant GPI-0100 OR QS-21. *Vaccine* **2005**, *23*, 3114-3122.
- [6] Sabbatini, P. J.; Kudryashov, V.; Ragupathi, G.; Danishefsky, S. J.; Livingston, P. O. et al. Immunization of ovarian cancer patients with a synthetic Lewis(y)-protein conjugate vaccine: a phase 1 trial. *Int J Cancer* **2000**, *87*, 79-85.

- [7] Holmberg, L. A.; Sandmaier, B. M. Vaccination with Theratope (STn-KLH) as treatment for breast cancer. *Expert Rev Vaccines* **2004**, *3*, 655-663.
- [8] McCool, T. L.; Harding, C. V.; Greenspan, N. S.; Schreiber, J. R. B- and T-cell immune responses to pneumococcal conjugate vaccines: divergence between carrier- and polysaccharide-specific immunogenicity. *Infect Immun* **1999**, *67*, 4862-4869.
- [9] Gilewski, T.; Ragupathi, G.; Bhuta, S.; Williams, L. J.; Musselli, C. et al. Immunization of metastatic breast cancer patients with a fully synthetic globo H conjugate: a phase I trial. *Proc Natl Acad Sci U S A* **2001**, *98*, 3270-3275.
- [10] Monzavi-Karbassi, B.; Cunto-Amesty, G.; Luo, P.; Shamloo, S.; Blaszczyk-Thurin, M. et al. Immunization with a carbohydrate mimicking peptide augments tumor-specific cellular responses. *Int Immunol* **2001**, *13*, 1361-1371.
- [11] Monzavi-Karbassi, B.; Luo, P.; Jousheghany, F.; Torres-Quinones, M.; Cunto-Amesty, G. et al. A mimic of tumor rejection antigen-associated carbohydrates mediates an antitumor cellular response. *Cancer Res* **2004**, *64*, 2162-2166.
- [12] Monzavi-Karbassi, B.; Artaud, C.; Jousheghany, F.; Hennings, L.; Carcel-Trullols, J. et al. Reduction of spontaneous metastases through induction of carbohydrate cross-reactive apoptotic antibodies. *J Immunol* **2005**, *174*, 7057-7065.
- [13] Whitehead, T. L.; Monzavi-Karbassi, B.; Jousheghany, F.; Artaud, C.; Elbein, A. et al. <sup>1</sup>H-NMR metabolic markers of malignancy correlate with spontaneous metastases in a murine mammary tumor model. *Int J Oncol* **2005**, *27*, 257-263.
- [14] Monzavi-Karbassi, B.; Whitehead, T. L.; Jousheghany, F.; Artaud, C.; Hennings, L. et al. Deficiency in surface expression of E-selectin ligand promotes lung colonization in a mouse model of breast cancer. *Int J Cancer* **2005**, *19*, 19.
- [15] Newman, J.; Rice, J. S.; Wang, C.; Harris, S. L.; Diamond, B. Identification of an antigen-specific B cell population. *J Immunol Methods* **2003**, *272*, 177-187.
- [16] Watson, A.; Wu, X.; Bruchez, M. Lighting up cells with quantum dots. *Biotechniques* **2003**, *34*, 296-300, 302-293.

**Publications:**

Monzavi-Karbassi, B.; Cunto-Amesty, G.; Luo, P.; Shamloo, S.; Blaszczyk-Thurin, M.; et al. Immunization with a carbohydrate mimicking peptide augments tumor-specific cellular responses. *Int Immunol* 2001, 13 (11), 1361-1371.

Monzavi-Karbassi, B.; Luo, P.; Jousheghany, F.; Torres-Quinones, M.; Cunto-Amesty, G. et al. A mimic of tumor rejection antigen-associated carbohydrates mediates an antitumor cellular response. *Cancer Res.* 2004, 64, 2162-2166.

Whitehead, T.L.; Monzavi-Karbassi, B.; Jouseghany, F.; Artaud, C.; Elbein, A. et al. <sup>1</sup>H-NMR metabolic markers of malignancy correlate with spontaneous metastases in a murine a mammary tumor model. *Int J Oncol* 2005, 27, 257-263.

Monzavi-Karbassi, B.; Artaud, C.; Jousheghany, F.; Hennings, L.; Carcel-Trullols, J. et al. Reduction of spontaneous metastases through induction of carbohydrate cross-reactive apoptotic antibodies. *J Immunol* 2005, 174, 7057-7065.

Monzavi-Karbassi, B.; Whitehead, T.L.; Jouseghany, F.; Artaud, C.; Hennings, L. et al. Deficiency in surface expression of E-selectin ligand promotes lung colonization in a mouse model of breast cancer. *Int J Cancer* 2005, 117, 398-408.

**Meeting Abstracts:**

AACR American Association for Cancer Research 95<sup>th</sup> Annual Meeting  
March 27-31, 2004, Orange County Convention Center, Orlando Florida

Fourth World Congress on Vaccines and Immunization  
September 30-October 3, 2004, Tsukuba Science City/Tokyo, Japan  
Infections Control World Organization

AACR American Association for Cancer Research 96<sup>th</sup> Annual Meeting  
April 16-20, 2005, Anaheim Convention Center, Anaheim, Orange County, CA

10<sup>th</sup> World Congress on Advances in Oncology and 8<sup>th</sup> International Symposium on Molecular Medicine, 13-15 October, 2005, Creta Maris, Hersonissos, Crete Greece

**Personnel:**

Thomas Kieber-Emmons, Ph.D.  
Behjatolah Monzavi Karbassi, Ph.D.  
Stewart Macleod, Ph.D.  
Yue Jin Wen, Ph.D.  
Fariba Jousheghany  
Kathleen Thomasson

# Immunization with a carbohydrate mimicking peptide augments tumor-specific cellular responses

**Behjatolah Monzavi-Karbassi, Gina Cunto-Amesty, Ping Luo, Shahram Shamloo, Magdalena Blaszcyk-Thurin<sup>1</sup> and Thomas Kieber-Emmons**

Department of Pathology and Laboratory Medicine, University of Pennsylvania, and <sup>1</sup>The Wistar Institute, Philadelphia, PA 19104, USA

**Keywords:** cancer vaccine, carbohydrate, L-selectin, Meth A cells, peptide mimotope

## Abstract

The metastatic potential of some tumor cells is associated with the expression of the neolactoseries antigens sialyl-Lewis x (sLex) and sialyl-Lewis a (sLea) as they are ligands for selectins. We have recently shown that peptide mimetics of these antigens can potentiate IgG2a antibodies, which are associated with a T<sub>h</sub>1-type cellular response. As L-selectin is preferentially expressed on CD4<sup>+</sup> T<sub>h</sub>1 and CD8<sup>+</sup> T cell populations, specific induction of these phenotypes could augment a response to L-selectin ligand-expressing tumor cells. Here we demonstrate that immunization with a multiple antigen peptide (MAP) mimetic of sugar constituents of neolactoseries antigens induces a MHC-dependent peptide-specific cellular response that triggers IFN- $\gamma$  production upon peptide stimulation, correlating with IgG2a induction. Surprisingly, T lymphocytes from peptide-immunized animals were activated *in vitro* by sLex, also triggering IFN- $\gamma$  production in a MHC-dependent manner. Stimulation by peptide or carbohydrate resulted in loss of L-selectin on CD4<sup>+</sup> T cells confirming a T<sub>h</sub>1 phenotype. We also observed an enhancement in cytotoxic T lymphocyte (CTL) activity *in vitro* against sLex-expressing Meth A cells using effector cells from Meth A-primed/peptide-boosted animals. CTL activity was inhibited by both anti-MHC class I and anti-L-selectin antibodies. These results further support a role for L-selectin in tumor rejection along with the engagement by the TCR for most likely processed tumor-associated glycopeptides, focusing on peptide mimetics as a means to induce carbohydrate reactive cellular responses.

## Introduction

Tumor-associated carbohydrate antigens are correlated with metastatic phenotype and poor survival in epithelial malignancies of different origins. The expression of the neolactoseries antigens represented by sialyl-Lewis x (sLex), Lewis x (Lex) and Lewis Y (LeY) are increased significantly on a variety of carcinomas (1–6), with sLex and sialyl-Lewis a (sLea) also reported to be expressed on melanoma cells (7). Early studies indicated a possible relationship between metastatic properties of tumor cells and the expression of these antigens leading to tumor cell dissemination (8–11). An inhibitory effect on the establishment and growth of metastatic colonies of tumor cells expressing these antigens has been noted when anti-sLea or anti-sLex antibody was administered to mice in a pancreatic tumor murine model (12).

A cellular role played by L-selectin expressed on lympho-

cytes has also been noted in that anti-L-selectin antibody (Mel14) can influence cytotoxic T Lymphocyte (CTL) sensitization and metastatic colony formation (13), and Mel 14 can inhibit CTL activity of effector cells *in vitro* derived from immunization with selectin-ligand expressing cells (14). These results strongly suggest that blood-borne tumor cells may utilize these antigens with selectin molecules when tumor cells adhere to the endothelia at metastatic sites (1,12,15–17). Over-expression of selectin ligands on tumor cells are also targeted by NK cells (18). Consequently, targeting these antigens may thwart tumor cell dissemination.

We have recently shown that peptide mimetics of selectin ligands can induce a humoral response that targeted sLex in a murine tumor model facilitating tumor growth inhibition (19). We have gone on to show that immunization with peptide

Correspondence to: T. Kieber-Emmons

Transmitting editor: G. Trinchieri

Received 29 January 2001, accepted 20 July 2001

mimetics can elicit carbohydrate-reactive IgG2a antibodies, associated with T<sub>h</sub>1 (20,21). As QS-21 potentiates a T<sub>h</sub>1 response (22) and L-selectin is preferentially expressed on CD4<sup>+</sup> T<sub>h</sub>1 cells (23) and on CD8<sup>+</sup> T cells (14,24), we were in the first instance interested in determining if peptide mimetic immunization activated lymphocytes that expressed L-selectin. As glycopeptides are also presented by MHC class I that express carbohydrate constituents (25,26) and T cells can recognize carbohydrate moieties on MHC-associated glycopeptides (27), we were also interested in whether mimotope immunization could augment a CTL response to fibrosarcoma Meth A cells.

We observed that peptide immunization promotes a specific cellular response with IFN- $\gamma$  production upon activation of splenocytes and T lymphocytes with immunizing peptide or with sLex and its homologue Lex. More importantly, we observed that immunization with peptide mimetic facilitated a specific cellular response to Meth A cells. Peptide boosting of mice primed with sLex-expressing Meth A cells enhanced the Meth A directed *in vitro* CTL activity. This activity was blocked not only by anti-MHC class I but also by anti-L-selectin antibody. This latter observation parallels other studies describing a role for L-selectin in T cell-mediated rejection of cells that express its ligands, such as sLex (14). The possibility of boosting lymphocyte subsets that cross-react with tumor cells that express L-selectin ligands opens new perspectives in designing cancer vaccines for further reducing micrometastases.

## Methods

### *Immunization of animals*

Peptides were synthesized as multiple antigen peptides (MAP; Research Genetics, Huntsville, AL) made by Fmoc synthesis on polylysine groups, resulting in the presentation of eight peptide clusters. Multivalent sLex, Lex and LeY were obtained from GlycoTech (Rockville, MD). Each BALB/c mouse received i.p. injections with 100  $\mu$ g of MAP, or 50  $\mu$ g of carbohydrates, and 20  $\mu$ g of the adjuvant QS-21 (Aquila Biopharmaceuticals, Framingham, MA), both re-suspended in 100  $\mu$ l of PBS as we described earlier (19). QS-21 was used in all peptide and carbohydrate immunization as adjuvant. As controls we used naive mice, animals injected with QS-21 (20  $\mu$ g per mouse) or with multivalent sLex and LeY (50  $\mu$ g of carbohydrates and 20  $\mu$ g of the adjuvant QS-21 per mouse) antigens.

sLex-expressing Meth A cells were selected by sorting of positive cells with anti-sLex FH-6 antibody from an original Meth A cell line and were 100% sLex<sup>+</sup> upon prolonged culture. Meth A cells were repeatedly passed *in vitro* to decrease their tumorigenicity. Mice were immunized i.p. with 3  $\times$  10<sup>5</sup> of these cells. Non-tumor bearing mice were used for analysis or for further experiments.

### *Antibodies*

All antibodies were purchased from PharMingen (San Diego, CA). Anti mouse I-A<sup>d</sup> (AMS 32.1), H-2K<sup>d</sup> (SF1-1-1) and CD1d (1B1), and their IgG2a and IgG2b isotype controls were first dialyzed in PBS buffer and then used in the proliferation

cultures. For fluorescent staining of the splenocytes we used biotinylated rat anti-mouse anti-CD62L (anti-L-selectin Mel-14) and its isotype control IgG2a; anti-CD4-FITC (L3T4) and its isotype control IgG2b-FITC.

### *Flow cytometry*

Fresh or *in vitro* stimulated splenocytes were blocked before staining with PBS containing 1% BSA and 1% rat serum for 10 min at 4°C. Cells were subsequently stained with rat anti-mouse mAb labeled with biotin, FITC or phycoerythrin. Appropriate rat isotype controls were used to set up background fluorescence. Streptavidin-FITC or avidin-phycoerythrin (Sigma, St Louis, MO) were used after biotin-labeled antibodies, as required. Acquisition of data was performed immediately after staining by using the FACScan analyzer and analysis performed by CellQuest software (both from Becton Dickinson Immunocytometry Systems, Mansfield, MA).

### *In vitro proliferation assays*

Spleens were aseptically removed from each group. Splenocytes were harvested from spleens, and isolated as the responder cells by lysis of erythrocytes and consequent washing several times with fresh media. Prepared responder cells were used for detection of cell proliferation, as described (28,29). Briefly, cells (2.5  $\times$  10<sup>5</sup>/well) were cultured in flat-bottom 96-well plates and incubated with MAP, carbohydrates, ovalbumin (OVA) or media only. After 3 days of incubation, 1  $\mu$ Ci of [<sup>3</sup>H]thymidine was added to each well and cells were incubated for an additional 16–18 h. Cultures were then harvested and radioactive emission counted on a Betaplate liquid scintillation counter (EG & G Wallac, Turku, Finland).

Proliferation assay was also performed using CellTiter 96 Aqueous One Solution (Promega, Madison, WI) based on the manufacturer's instructions. Cell culture was exactly performed as above and at the third day of incubation the provided solution was added to each well. Plates were incubated for an additional 1–2 h in a humidified, 5% CO<sub>2</sub> incubator at 37°C. Absorbency was measured immediately at 490 nm using a 96-well plate reader (Spectra Fluor; Tecan, Triangle Park, NC) as a measure for cell proliferation.

For detection of cell proliferation in T lymphocyte-enriched populations, a single-cell suspension of isolated splenocytes was depleted of B cells by positive selection after incubation with pan-B (B220) magnetic beads (Dynal, Oslo, Norway), at 4°C, for 30 min. To separate adherent from non-adherent cells, the B cell-depleted population was resuspended in RPMI media with 20% FBS and incubated for two consecutive adherence periods of 1 h each, at 37°C in humidified atmosphere with 5% CO<sub>2</sub>. T lymphocytes were recovered and washed 3 times with RPMI/10% FBS and used in cell proliferation assays with or without mitomycin C (MMC)-treated antigen-presenting cells (APC). Adherent cells were recovered separately, treated with MMC (100  $\mu$ g/ml in RPMI supplemented with 10% FBS, for 40 min at 37°C) and used as APC in proliferation of purified T lymphocytes at 10% ratio. Purified T cell populations, checked by FACS analysis, were assessed as >95% CD3<sup>+</sup>, with no CD19<sup>+</sup> cells, and used in cell proliferation assays as explained above. Medium used for the proliferation assays was RPMI 1640 (Life Technologies,

**Table 1.** Peptides used in this study

Peptide	Sequence	Source	Predicted H-2K binding motif
106	GGIYWRYDIYWRDYDIWRYD	designed	RYDIYWRDYI (2000.0)
109	GGARVSFWRYSSFAPTY	phage display	RYSSFAPTY (60.00)
711	GGPGQPGQPGQPGQ	designed	QPGQPGQPGQ (0.144)

Values in parenthesis are estimated half-times of disassociation of a molecule containing this sequence using a subsequence of 10 for scoring (33). The score for 109 ranges from 20 to 60 for different subsequences. The score for 106 changes from 50.0 for a subsequence of 8 to 80.0 for a subsequence of 9. The score for 711 does not go above 1.0 for subsequences of 8 or 9.

Rockville, MD) supplemented with 5% heat-inactivated FCS, L-glutamine, penicillin (100 IU/ml) and streptomycin (100 µg/ml).

#### Cytokine production

Supernatants were collected from the co-cultures of splenocytes or purified T lymphocytes 72 h after *in vitro* stimulation with carbohydrate, peptides and media. The concentrations of IL-4, IL-10 and IFN-γ were measured by quantitative capture ELISA (PharMingen), according to the manufacturer's instructions.

#### CTL assay

Cytotoxic activity was measured by a 5 (P815 cells)- or 16 (Meth A cells)-h  $^{51}\text{Cr}$ -release assay, as described elsewhere (30,31). Briefly, effector cells were stimulated for 5 days in the presence of stimulator cells and 10% RAT-T-STIM without concanavalin A (Becton Dickinson Labware, Bedford, MA). Peptide-pulsed murine mastocytoma P815 cells were used as stimulators (10:1 effector:stimulator ratio) and targets in 5-h assay, as described before (30,32). Meth A cells were treated with MMC and used as stimulator in 300:1 effector:stimulator ratio. For MMC treatment,  $1 \times 10^7$  cells were treated in 1 ml of RPMI media supplemented with 10% FBS, with 100 µg MMC at 37°C for 40 min. Cells were washed 3 times after treatment.

Untreated Meth A cells were used as target cells. All target cells were labeled with 100 µCi/ml  $\text{Na}_2^{51}\text{CrO}_4$  and mixed with effector cells at E:T ratios ranging from 50:1 to 3:1. Maximum and minimum (spontaneous) releases were determined by lysis of target cells in 5% Triton X-100 and medium respectively. Lysis was calculated as  $[(\text{experimental} - \text{spontaneous}) / (\text{maximum} - \text{spontaneous})] \times 100$ . An assay was not considered valid if the values for the 'spontaneous release' count were >20% (for 5-h assay) or 30% (for 16-h assay) of the 'maximum release'. To calculate specific lysis of targets, the percent lysis of non-specific targets (P815 cells) was subtracted from the percent lysis of specific targets (peptide-pulsed P815 cells).

#### Statistical analysis

Data were analyzed by using Student's *t*-test. Values of  $P < 0.05$  were considered statistically significant. All experiments were performed at least 3 times.

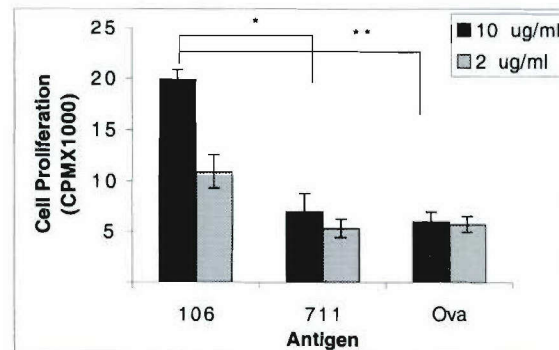


**Fig. 1.** Proliferative response of splenocytes from peptide 106-immunized mice. (A) Mice (four per group) were immunized 3 times with peptide 106 formulated in QS-21 every other week. Seven days after the third injection, spleens were collected and splenocytes were incubated with two concentrations (10 and 2 µg/ml) of the indicated MAP or OVA for 72 h. A  $^3\text{H}$ -incorporation assay was performed as described in Methods. Results represent the mean value  $\pm$  SEM based on four independent experiments with triplicate samplings. \* $P < 0.05$ ; \*\* $P < 0.025$ .

## Results

#### Peptide immunization primes for a specific cellular response

To facilitate a cellular response, we had designed peptide 106 (Table 1) with the potential to bind to H2-K<sup>d</sup> and I-A<sup>d</sup>. MHC binding prediction calculations identifies an H2-K<sup>d</sup> and I-A<sup>d</sup> binding motif centered on the RYDIYWRDYI sequence of the 106 peptide (Table 1) (33). Furthermore, the WRYDI sequence tract of the 106 peptide also displays similarity to a peptide sequence tract (DIYRW) identified in a peptide that binds to CD1 (34), which may play a role in activating NK T cells.

To analyze the cellular response upon peptide 106 immunization, BALB/c mice were immunized with the mimoepitope and the proliferative response of isolated splenocytes to the peptides 106, 711 (Table 1) as MAP forms, as well as OVA (as an additional control) was determined. As expected, *in vivo* primed splenocytes from 106 peptide-immunized animals were specifically activated by peptide 106, and not control peptides, in a statistically significant concentration-dependent manner (Fig. 1). Peptide 106 did not stimulate splenocytes from naive animals or from animals immunized with QS-21 alone (data not shown). These results indicate

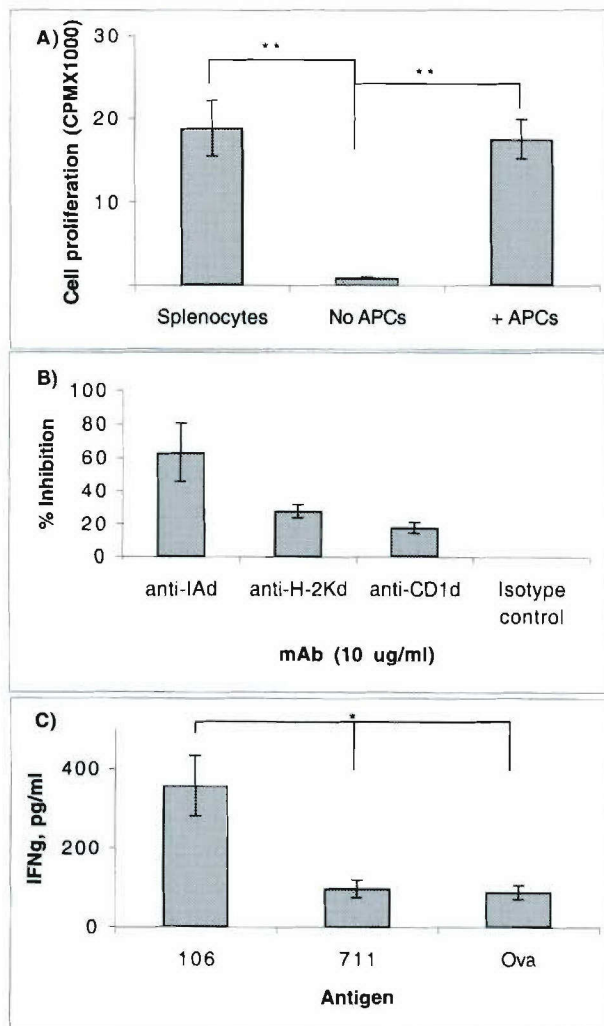


**Fig. 2.** Cell proliferation is APC dependent, and is blocked by anti-MHC class II and I antibodies. Mice were immunized with peptide 106 as explained in the legend to Fig. 1 and splenocytes were collected 7 days after the last immunization. (A) Proliferation assay was performed on splenocytes and purified T lymphocytes (with or without addition of inactivated APC) with a peptide concentration of 10 µg/ml. (B) Anti-I-A<sup>d</sup>, -H-2K<sup>d</sup> and -CD1d, and IgG2a and IgG2b isotypes were used for blocking of proliferation of splenocytes. Isotype controls acted very similarly, so just one of those is presented. (C) Splenocytes were stimulated using peptides 106, 711 and OVA (each 10 µg/ml), and IFN- $\gamma$  levels were quantified. All results are expressed as the mean  $\pm$  SEM of four independent experiments with triplicate samplings. \*P < 0.05; \*\*P < 0.01.

that immunization with peptide 106 mediates a peptide-specific cellular response.

#### Anti-MHC class II and I inhibit proliferative response

A standard cell proliferation was performed with purified T lymphocytes alone and after addition of MMC-inactivated APC (Fig. 2A). The results indicate that proliferation is APC dependent. Proliferation of the T lymphocytes was not observed in the absence of APC. Proliferation was inhibited by the addition of specific anti-I-A<sup>d</sup> anti-class II and to a lesser extent with anti-class I antibodies (Fig. 2B). The addition

of anti-CD1 antibody inhibited proliferation to almost the same extent as addition of anti-class I antibody. Therefore, the 106 peptide might be presented in multiple ways to T cells; however, MHC class II-dependent presentation appears to be the major pathway (60% inhibition by anti-class II antibody).

For analysis of cytokine profiles, plates for proliferation were doubled and the supernatant of duplicated plates were harvested after 72 h of *in vitro* activation. IFN- $\gamma$  production was found to be peptide specific (Fig. 2C), with no detectable presence of IL-4 or IL-10 (data not shown). The sensitivity for IL-4 and IL-10 detection was 7.8 and 31.3 pg/ml respectively. Taken together, these results demonstrate that 106-MAP-peptide immunization along with QS-21 potentially activates lymphocyte populations with a predominant T<sub>h1</sub> phenotype.

#### Activation down-modulates L-selectin

We examined L-selectin expression on CD4<sup>+</sup> T cells. L-selectin is preferentially expressed on T<sub>h1</sub> over T<sub>h2</sub> cells (23). The activation of T cells through the TCR results in the differential regulation of L-selectin (24). Using FACS analysis, we studied the expression of L-selectin on CD4<sup>+</sup> T cells from naive and peptide-immunized animals before and after *in vitro* stimulation with peptide 106 to assess activation (Fig. 3). In keeping with other studies, a population of cells from peptide 106-immunized mice remained clearly L-selectin<sup>+</sup> after *in vitro* stimulation (24). The demonstrated presence and loss of L-selectin on the surface of CD4<sup>+</sup> T cells occurring upon stimulation to the 106 peptide further confirms a T<sub>h1</sub> nature for these cells. It was observed that sLex could activate these cells as effectively as peptide 106 as assessed by L-selectin loss (Fig. 3).

#### Carbohydrate stimulates proliferation of 106 peptide-primed splenocytes

In separate experiments, isolated splenocytes were incubated with sLex, Lex and LeY (Fig. 4A). sLex and Lex, but not LeY stimulated a proliferative response with splenocytes from 106-immunized animals. Splenocytes from mice immunized with the carbohydrate antigens sLex or LeY did not proliferate upon incubation with peptide 106, LeY, sLex or Lex (Fig. 4B and C). This result suggests that priming with the peptide mimotope leads to a specific carbohydrate cross-reactive cellular response.

#### MHC class II molecule is involved in proliferation of peptide-primed T lymphocytes by carbohydrate

sLex-stimulated proliferation of peptide-primed T lymphocytes was inhibited by the I-A<sup>d</sup>-specific anti-MHC class II antibody, suggesting a role played by the class II molecule in the cross-reactivity between the carbohydrate antigen and peptide-primed responder cells and APC (Fig. 5A). The specificity of the antibody for I-A<sup>d</sup> has been assessed by others, indicating specific MHC class II inhibition of proliferation (35–37). IFN- $\gamma$  production for sLex activation was detected (Fig. 5B). As in the peptide case, we could not detect any IL-4 and IL-10 production after activation. This production was specific for peptide-immunized mice compared with T lymphocytes derived from mice immunized with QS-21 alone or from naive animals.

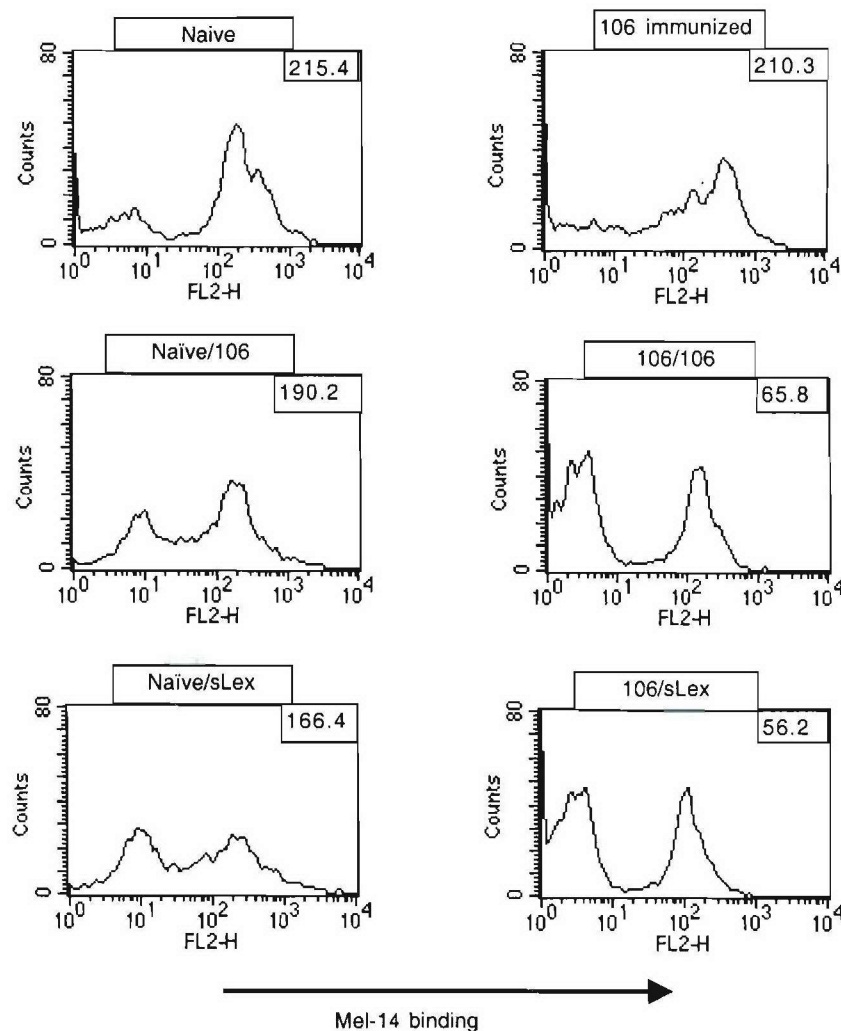


**Fig. 3.** Analysis of L-selectin expression on the surface of CD4<sup>+</sup> lymphocytes obtained from naive and 106/QS21-immunized animals. Staining was performed with phycoerythrin-conjugated anti-mouse L-selectin (Mel-14) and anti-CD4-FITC (L3T4) mAb before and after 3 days of *in vitro* stimulation. For stimulation either 106 or sLex (10 µg/ml) were used. Analysis of Mel-14 binding was performed on gated CD4<sup>+</sup> lymphocytes. Mean fluorescence values for L-selectin expression on CD4<sup>+</sup> cells are shown in the top right corner of the histograms. Naive, cells from naive mice before proliferation. 106 immunized, cells from 106-peptide immunized mice before proliferation. Naïve/106 and 106/106, cells from naive and 106 immunized mice stimulated *in vitro* for 3 days with 106 peptide. Naïve/sLex and 106/sLex, cells from naive and 106 immunized mice stimulated *in vitro* for 3 days with carbohydrate sLex.

#### Peptide boost of Meth A cell-primed animals enhances CTL activity against Meth A cells

*In vitro* stimulated effector cells from peptide 106-injected animals showed high specific lysis against peptide-pulsed P815 cells, confirming the peptide's ability to function as a MHC class I target (Fig. 6A). As expected, cytotoxicity was reduced in experiments in which CD8<sup>+</sup> cells were depleted. When Meth A cells were used as stimulators and targets, we observed moderate cell killing (Fig. 6B). In contrast, no significant cytotoxicity was detected on the P815 cells, used as a negative control. P815 cells did not express sLex, as assessed by FACS using the mAb FH-6 (data not shown) nor did serum to peptide 106 bind to P815 cells, also assessed by FACS (data not shown). We did not detect any significant increase in lysis of peptide pulsed

Meth A cells (not shown). *In vitro* stimulated splenocytes from naive or QS-21 immunized mice did not show significant cytotoxicity on Meth A cells.

To examine the hypothesis that peptide immunization could augment cellular responses to Meth A-cells, we studied the proliferative effects of peptides and Meth A cells in groups of mice immunized with Meth A cells only or primed with Meth A cells and boosted with peptide. The results are summarized in Fig. 7(A). Immunization with Meth A cells stimulated a proliferative response to the cells, as expected. Boosting of Meth A cell-immunized mice with peptide 106 increased the proliferative response to peptide 106 and to Meth A cells. As the control peptide for proliferation we used a peptide referred to as peptide 109 (Table 1). We did not detect cross-reactivity between

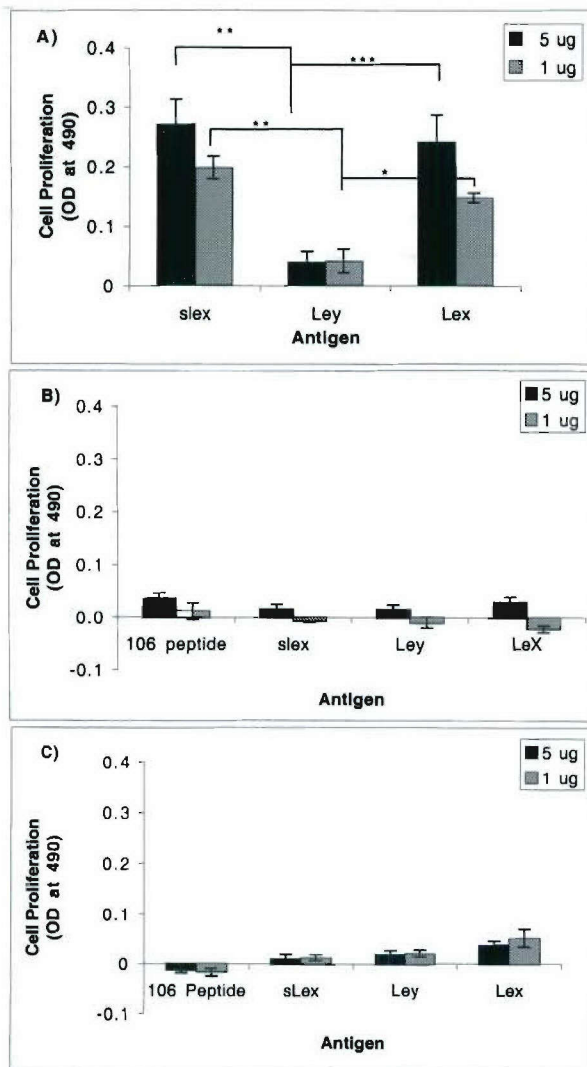


**Fig. 4.** Cell proliferative response to carbohydrates in splenocytes from 106 peptide (A), sLex (B) and LeY (C)-immunized mice. Mice (four per group) were immunized 3 times at a 2-week interval. Seven days after the last immunization spleens were removed, and splenocytes collected and prepared as explained in Methods. Cells were incubated with peptide and carbohydrates for 3 days. Proliferation was measured at the third day after incubation. For recording the proliferation response the number of viable cells was detected using the CellTiter 96 Aqueous One Solution cell proliferation assay (Promega). The absorbance in the presence of culture medium is subtracted as background proliferation. All results present the mean value  $\pm$  SD of triplicate samplings. Data are representative of three independent experiments with pooled cells from four mice. \* $P < 0.05$ ; \*\* $P < 0.025$ ; \*\*\* $P < 0.01$ .

peptide 109 and Meth A cells, but this peptide showed cross-reactivity in cellular response with 106 peptide (not shown; attributed to the sequence homology between the peptides). We investigated the role of Meth A and P815 cells in stimulation of splenocytes from mice immunized with peptide 106, sLex and OVA as control. Only splenocytes from 106 peptide immunization showed a proliferative response in co-culture with MMC-treated Meth A cells (data

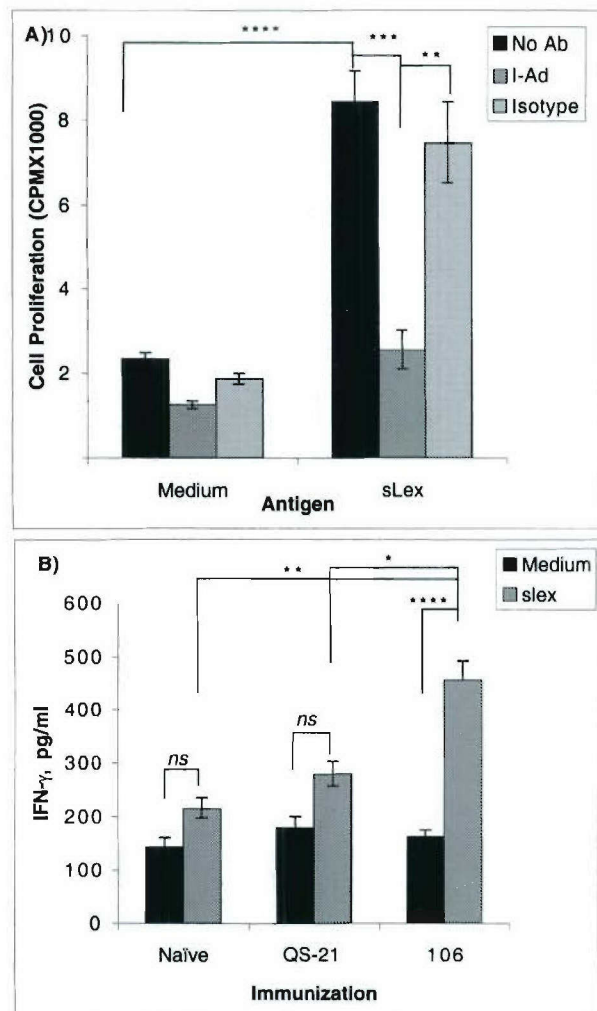


**Fig. 5.** (A) Anti-MHC class II antibody blocks activation of T cells by sLex. Purified T lymphocytes from 106 peptide/QS21-immunized (performed as explained above) animals were used in a proliferation assay with or without sLex (10  $\mu$ g/ml) in the presence or absence (No Ab) of anti-MHC class II antibody (10  $\mu$ g/ml). Isotype control was used at 10  $\mu$ g/ml. (B) IFN- $\gamma$  production in the supernatant of purified T lymphocytes stimulated with sLex (10  $\mu$ g/ml) for 3 days in the presence of MMC-treated APC. Supernatant from stimulated T lymphocytes was collected and IFN- $\gamma$  was measured. All results are presented as the mean value  $\pm$  SEM based on four independent experiments with duplicate samplings. Medium, proliferation in culture medium used as background. \* $P < 0.05$ ; \*\* $P < 0.025$ ; \*\*\* $P < 0.01$ ; \*\*\*\* $P < 0.005$ . ns, not significant.

not shown), we did not detect significant proliferation using P815 cells as stimulator (data not shown).

We observed a cytotoxic enhancement effect upon immunization with peptide 106 using effector cells from Meth A-immunized mice compared with those from Meth A-primed/peptide-boosted mice (Fig. 7B). The level of CTL was consistent with those observed in similar studies (31,32). A clear increase in lysis was observed in the cell-primed/peptide-boosted animals compared to mice immunized with Meth A cells only. We did not detect any cytotoxicity using re-

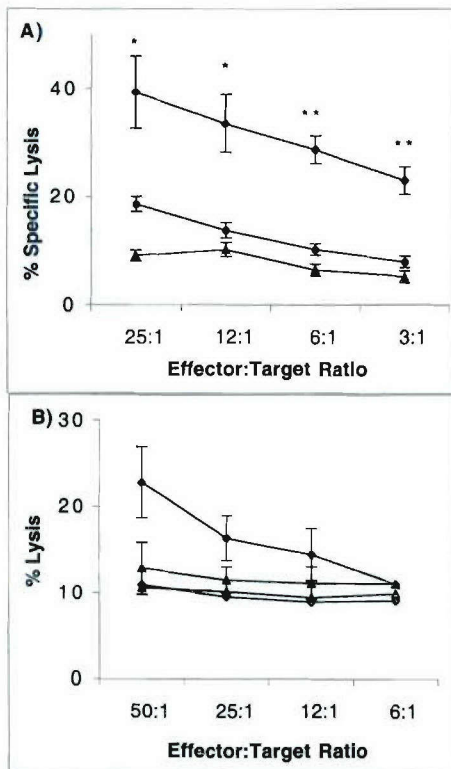


**Fig. 6.** Induction of cross-reactive CTL response to Meth A cells following immunization with peptide 106. Mice (four per group) were immunized with peptide 106 at 3 times at a 2-week interval and 7 days after the last immunization, spleens were collected and isolated effector cells were re-stimulated with either peptide pulsed P815 cells or Meth A cells *in vitro* for 5 days. CTL was performed using 106 peptide-pulsed P815 (A) or Meth A (non-pulsed) (B) cells as stimulators and targets. ◆, Bulk effector cells from 106-immunized mice; ●, CD8<sup>+</sup> T cell depleted effector cells from 106-immunized mice; ▲, Bulk effector cells from naive mice. To calculate specific lysis of targets (as shown in A), the percent lysis of non-specific targets (P815 cells) was subtracted from the percent lysis of specific targets (peptide-pulsed P815 cells). Cytotoxicity against P815 cells as control target (open symbols) is shown in (B). All error bars (SD) were calculated based on triplicates. All data are representative of three independent experiments using pooled cells from four mice. Statistically significant compare with cytotoxicity levels of naive effector cells at \* $P < 0.05$  and \*\* $P < 0.025$  respectively.

stimulated effectors from either immunization groups targeting P815 cells. Levels of cytotoxicity against Meth A cells were compared with those levels against P815 cells, statistically significant cytotoxicity against Meth A cells was detected only with effectors from peptide boosted animals. Representative results from 50:1 E:T ratio of a separate experiment are summarized in Table 2. Cytotoxicity was dependent on both CD4<sup>+</sup> and CD8<sup>+</sup> cells as assessed by respective depletion of the CD4<sup>+</sup> and CD8<sup>+</sup> subsets. Meth A cell-mediated lysis was found to be inhibited by both anti-MHC class I and L-selectin antibodies, but not by anti-class II antibody as Meth A cells do not express MHC class II molecules.

These results further suggest that immunization with peptide or Meth A cells activates CD4<sup>+</sup> and CD8<sup>+</sup> T cells that affect cytotoxicity. Meth A cells are known to activate both T cell

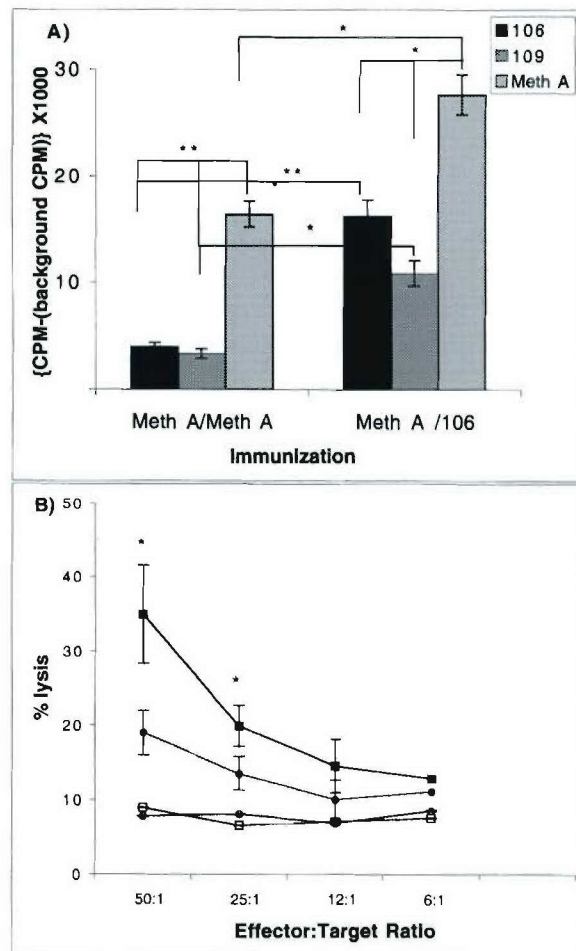


**Fig. 7.** (A) 106 peptide boosts cellular responses in the Meth A cell-primed animals. Mice were immunized with Meth A cells, rested for 1 month, and then were boosted with the 106 peptide and compared with Meth A cell primed/boosted (at the same interval) only. In each immunization regimen, splenocytes were collected 7 days after boost, and proliferative response was measured using peptides 106, 109 and Meth A cells as antigens. Meth A cells were treated with MMC and then used in the assay. Background c.p.m. is [<sup>3</sup>H]thymidine incorporation with used medium only. (B) Anti-Meth A cells CTL. Mice were primed and boosted with Meth A cells (circle) or primed with Meth A cells and boosted with 106 peptide (square), as explained above. Cytotoxicity was measured against Meth A (closed symbols) or P815 cells (open symbols). Splenocytes were stimulated *in vitro* with Meth A cells as described in Methods. All bars show SD based on three replications. All data are representative of three independent experiments using pooled cells from four mice. \* $P < 0.05$ ; \*\* $P < 0.025$ . In (B) asterisks compare the levels of cytotoxicity of effector cells from Meth A/106-immunized animals with the cytotoxicity levels of the same cells detected against P815 cells as targets.

subsets that are involved in cytotoxicity targeting Meth A cells (31,32). However, in the case of peptide mimetic boost of Meth A cell-immunized animals, MHC class I-restricted/CD8<sup>+</sup>-dependent T cells showed a predominant role in the CTL response. Our results further indicate that L-selectin may participate in the lysis process as described previously (14).

**Table 2.** Percentage of specific lysis ( $\pm$  SD)<sup>a</sup> on Meth A<sup>b</sup> cells as targets at 50:1 E:T ratio

Immunization <sup>c</sup>	Cell treatment					
	None	Anti-I-A <sup>d</sup>	Anti-H-2k <sup>d</sup>	Mel-14	CD4 <sup>+</sup> depleted	CD8 <sup>+</sup> depleted
Naive	5.7 (0.9)	ND <sup>d</sup>	ND	ND	ND	ND
Meth A/Meth A	20.98 (6)	ND	ND	3.4 (4.2)	15.8 (8)	14 (7)
Meth A/106	30.06 <sup>e</sup> (4.9)	27.8 <sup>e</sup> (4.1)	13.3 (6.7)	13.09 (7.7)	21.8 (8.5)	14.2 (6)
Meth A/QS-21	11.2 (4.2)	15 (6.36)	13.63 (2.9)	11.8 (5.8)	ND	ND

<sup>a</sup>Values are calculated means  $\pm$  SD from three replications and are representative of three independent experiments using pooled cells from four mice in each.

<sup>b</sup>P815 cells were also used as targets and no significant lysis (6%) was detected.

<sup>c</sup>Groups of mice were primed with Meth A cells, rested for 1 month and then boosted with Meth A, 106 peptide/QS-21 or QS-21 alone. Splenocytes were collected 7 days after the boost.

<sup>d</sup>ND, not determined.

<sup>e</sup>Statistically significant ( $P < 0.05$ ) as compared with cytotoxicity level of the same effectors against P815 cells as targets or of naive effectors against Meth A cells.

With naive mice and QS-21-immunized mice, as before, we did not detect any significant lysis.

## Discussion

We had previously demonstrated that immunization with a multivalent, repetitive peptide mimetic of sLex (peptide 106) induced an anti-sLex cross-reactive antibody response to Meth A tumor cells (19). Antibody responses to sLex can mediate complement-dependent killing of sLex-expressing tumor cells inhibiting the establishment and growth of metastatic colonies as observed in several animal models (12,19,38).

Meth A tumor growth inhibition upon immunization with attenuated Meth A cells is reported to be dependent on CD4<sup>+</sup> and CD8<sup>+</sup> T cell responses to undefined glycoproteins (31,32,39–41). Commitment of lymphocytes to the T<sub>H</sub>1 and to CD8<sup>+</sup> T cell phenotypes as characterized by the expression of IFN- $\gamma$ , may be critically involved in tumor rejection (42,43). However, the expression of L-selectin on these cell types may also lend to CTL activity (14). IFN- $\gamma$  and lymphocytes work together to find and eliminate tumor cells (44). As the adjuvant QS-21 promotes the T<sub>H</sub>1 phenotype, which expresses L-selectin, and peptide 106 can induce a T<sub>H</sub>1-associated humoral response, we examined if immunization with peptide 106 along with QS-21 could augment cellular responses to sLex-expressing Meth A tumor cells.

Immunization with the mimoepope led to peptide-specific cell proliferation that was concentration dependent (Fig. 1). As expected, cell proliferation was primarily MHC class II dependent as determined by inhibition with respective anti-MHC antibody (Fig. 2). Cell stimulation with peptide 106 triggered IFN- $\gamma$  release, suggesting that peptide immunization with QS-21 as expected polarized the T<sub>H</sub>1 subset (Fig. 2C). Consistent with previous studies we observed L-selectin loss on CD4<sup>+</sup> T lymphocytes upon peptide stimulation, but also saw this loss upon stimulation with sLex (Fig. 3). The proliferative response was peptide, sLex and Lex specific since LeY did not exhibit any cellular responses nor did splenocytes from sLex- and LeY-immunized animals responded to peptide 106, sLex or Lex antigens (Fig. 4).

We observed that sLex activated T lymphocytes from 106 immunized animals to proliferate and secrete IFN- $\gamma$  (Fig. 5). Cell activation by sLex was inhibited by anti-MHC class II antibody addition, suggesting a possible role for this molecule in the presentation process (Fig. 5B). *In vivo* stimulated effector cells from peptide 106 immunization displayed cytotoxicity directed toward peptide 106-pulsed MHC class I<sup>+</sup> class II<sup>-</sup> P815 target cells, further verifying a role for CD8<sup>+</sup> T cell reactivity with peptide 106 (Fig. 6). While Meth A cell priming and boosting can lead to CTL activity against Meth A cells, peptide boosting increased the level of cytotoxicity against Meth A cells to a statistically significant level as compared with cytotoxicity against P815 cells as control target (Fig. 7 and Table 2), indicating a cross-reactive nature between peptide and tumor specific CTL responses.

CTL activity was inhibited by the addition of either anti-class I or anti-L-selectin antibody (Table 2). However, we could not block CTL activity by the sLex-reactive antibody FH-6 (data not shown). It is possible that FH-6 binds to a subtype of sLex carbohydrate epitopes that do not always function as ligands for L-selectin just like it defines a subset that does not bind to E-selectin (2). This is also similar to that found for the antibody MECA 79 which binds to a subset of sulfated sLex different than that of L-selectin (45). L-selectin is known to bind to a variety of carbohydrates expressed on glycoproteins (46,47). It is possible that L-selectin functions as an auxiliary molecule (48) and by itself is not sufficient to mediate CTL killing, but requires engagement of antigen-specific TCR (14). NK cells, on the other hand, also express L-selectin and other lectin-type molecules, and NK cells appear to mediate cytolysis of tumor cells that express high levels of sLex (18). However, direct evidence that fucosylated selectin ligands play a role in tumor rejection is still lacking.

The activation of cross-reactive T cells has been described in many systems. What is the specificity of the CD8<sup>+</sup> T cells targeting Meth A? Meth A cell-primed T cells maybe glycopeptide/glycoprotein specific (32), which are cross-reactive with peptide 106, as glycopeptides are known to activate T cells that recognize the carbohydrate moiety on MHC-associated glycopeptides (49–55). Direct interaction of the TCR with the carbohydrate (27,56) is dependent on the chemical structure

of the glycan as well as its position within a peptide. Glycopeptides with GlcNAc residues known to associate with class I (25) also induce CTL responses (26). T cells primed to glycopeptides carrying more complex saccharide antigens sometimes show a complicated pattern of cross-responses to glycopeptides with simpler glycan moieties (51). It argues that the presentation of carbohydrate antigens on Meth A should be more thoroughly characterized in terms of the structure of glycopeptides, glycosphingolipids, etc., which is beyond the scope of the present paper.

Proliferation by sLex and Lex is tougher to reconcile. Carbohydrate antigens have been proposed to associate with MHC directly (57); however, this type of association has not yet been confirmed in our system. It is possible that proliferation is associated with some yet undefined superantigen-like association as we observed up-regulation of CD15s on sLex activated T cells (data not shown). Superantigens but not mitogens are capable of inducing up-regulation of E-selectin ligands on human T lymphocytes (58). Likewise, bacterial polysaccharides and mimicking peptides with a distinct charge motif involving Lys and Asp residues have been shown to activate T lymphocytes and that this activity confers immunity to a distinct pathologic response to bacterial infection (59). Peptide 106 has a Arg residue homologous to Lys, with the Asp residues identical to peptides that induce cross-reactive cellular responses in bacterial studies (59). The molecular details of how this occurs are not as yet known. Further analysis of binding affinities of peptide and carbohydrate with I-A<sup>d</sup> will be illuminating. However, immunization with sLex did not induce T lymphocytes that reacted with peptide 106 nor itself, an effect of sLex being a T cell-independent antigen.

Immunization with peptide 106 induces cellular responses that are not achievable by immunization with carbohydrate alone. Nevertheless, the induction of optimal systemic anti-tumor immunity involves the priming of both CD4<sup>+</sup> and CD8<sup>+</sup> T cells specific for tumor-associated antigens. Although cellular responses generated by the peptide mimotope may enhance CTL induction, vaccination with peptide alone appears not to be completely sufficient in the effector phase when challenged with a very high tumor burden (19). Our CTL data using effectors from peptide-only-immunized mice on Meth A cells as targets (Fig. 6B) confirm this fact with marginal CTL activity observed. Consequently, we did not observe complete tumor protection in our previous study (19).

Our results are very narrow with regard to the breadth of carbohydrate directed cellular responses. However, constituents of sLex and sLea are proposed to be influential to the metastatic properties of a variety of human tumor cells. Consequently, further efforts to optimize and isolate the carbohydrate moieties associated with presented glycopeptides may facilitate vaccine applications for eradication of metastatic lesions by both antibody-dependent lysis and cellular responses. This possibility has yet to be proved with the appropriate models but suggests that for certain carbohydrate antigens, peptide mimetics might augment cellular responses other than delayed-type hypersensitivity like responses (60) in future vaccine applications.

## Acknowledgements

This work was supported by NIH grant AI45133 and by US Army Material Command grant DAMD 17-01-0366. We thank Charlotte Read Kensil of Aquila Biopharmaceuticals, Inc. (Framingham, MA) for supplying the QS-21

## Abbreviations

APC	antigen-presenting cell
CTL	cytotoxic T lymphocyte
LeY	Lewis Y
MAP	multiple antigen peptide
Meth A cells	methylcholanthrene-induced fibrosarcoma
MMC	mitomycin C
OVA	ovalbumin
sLex	sialylated Lewis x
sLea	sialylated Lewis a

## References

- Dabelsteen, E. 1996. Cell surface carbohydrates as prognostic markers in human carcinomas [Review]. *J. Pathol.* 179:358.
- Nemoto, Y., Izumi, Y., Tezuka, K., Tamatani, T. and Irimura, T. 1998. Comparison of 16 human colon carcinoma cell lines for their expression of sialyl LeX antigens and their E-selectin-dependent adhesion. *Clin. Exp. Metast.* 16:569.
- Davidson, B., Gotlieb, W. H., Ben-Baruch, G., Kopolovic, J., Goldberg, I., Nesland, J. M., Berner, A., Bjamer, A. and Bryne, M. 2000. Expression of carbohydrate antigens in advanced-stage ovarian carcinomas and their metastases—a clinicopathologic study. *Gynecol. Oncol.* 77:35.
- Burdick, M. D., Harris, A., Reid, C. J., Iwamura, T. and Hollingsworth, M. A. 1997. Oligosaccharides expressed on MUC1 produced by pancreatic and colon tumor cell lines. *J. Biol. Chem.* 272:24198.
- Hey, N. A. and Aplin, J. D. 1996. Sialyl-Lewis x and sialyl-Lewis a are associated with MUC1 in human endometrium. *Glycoconj. J.* 13:769.
- Shimizu, T., Yonezawa, S., Tanaka, S. and Sato, E. 1993. Expression of Lewis X-related antigens in adenocarcinomas of lung. *Histopathology* 22:549.
- Ravindranath, M. H., Amiri, A. A., Bauer, P. M., Kelley, M. C., Essner, R. and Morton, D. L. 1997. Endothelial-selectin ligands sialyl Lewis(x) and sialyl Lewis(a) are differentiation antigens immunogenic in human melanoma. *Cancer* 79:1686.
- Hoff, S. D., Irimura, T., Matsushita, Y., Ota, D. M., Cleary, K. R. and Hakomori, S. 1990. Metastatic potential of colon carcinoma. Expression of ABO/Lewis-related antigens. *Arch. Surg.* 125:206.
- Matsuura, N., Narita, T., Mitsuoka, C., Kimura, N., Kannagi, R., Imai, T., Funahashi, H. and Takagi, H. 1997. Increased level of circulating adhesion molecules in the sera of breast cancer patients with distant metastases. *Jpn. J. Clin. Oncol.* 27:135.
- Narita, T., Funahashi, H., Satoh, Y., Watanabe, T., Sakamoto, J. and Takagi, H. 1993. Association of expression of blood group-related carbohydrate antigens with prognosis in breast cancer. *Cancer* 71:3044.
- Bresalier, R. S., Ho, S. B., Schoepfner, H. L., Kim, Y. S., Slesinger, M. H., Brodt, P. and Byrd, J. C. 1996. Enhanced sialylation of mucin-associated carbohydrate structures in human colon cancer metastasis. *Gastroenterology* 110:1354.
- Kawarada, Y., Ishikura, H., Kishimoto, T., Kato, H., Yano, T. and Yoshiiki, T. 2000. The role of sialylated Lewis antigens on hematogenous metastases of human pancreas carcinoma cell lines *in vivo*. *Pathol. Res. Pract.* 196:259.
- Rosato, A., Zambon, A., Macino, B., Mandruzzato, S., Bronte, V., Milan, G., Zanovello, P. and Collavo, D. 1996. Anti-L-selectin monoclonal antibody treatment in mice enhances tumor growth by preventing CTL sensitization in peripheral lymph nodes draining the tumor area. *Int. J. Cancer* 65:847.
- Biancone, L., Stamenkovic, I., Cantaluppi, V., Boccellino, M., De Martino, A., Bussolino, F. and Camussi, G. 1999. Expression of

L-selectin ligands by transformed endothelial cells enhances T cell-mediated rejection. *J. Immunol.* 162:5263.

- 15 Tozeren, A., Kleinman, H. K., Grant, D. S., Morales, D., Mercurio, A. M. and Byers, S. W. 1995. E-selectin-mediated dynamic interactions of breast- and colon-cancer cells with endothelial-cell monolayers. *Int. J. Cancer* 60:426.
- 16 Takada, A., Ohmori, K., Yoneda, T., Tsuyuoka, K., Hasegawa, A., Kiso, M. and Kannagi, R. 1993. Contribution of carbohydrate antigens sialyl Lewis A and sialyl Lewis x to adhesion of human cancer cells to vascular endothelium. *Cancer Res.* 53:354.
- 17 Renkonen, J., Paavonen, T. and Renkonen, R. 1997. Endothelial and epithelial expression of sialyl Lewis(x) and sialyl Lewis(a) in lesions of breast carcinoma. *Int. J. Cancer* 74:296.
- 18 Ohyama, C., Tsuboi, S. and Fukuda, M. 1999. Dual roles of sialyl Lewis x oligosaccharides in tumor metastasis and rejection by natural killer cells. *EMBO J.* 18:1516.
- 19 Kieber-Emmons, T., Luo, P., Qiu, J., Chang, T. Y., O, I., Blaszczyk-Thurin, M. and Steplewski, Z. 1999. Vaccination with carbohydrate peptide mimotopes promotes anti-tumor responses. *Nat. Biotechnol.* 17:660.
- 20 Cunto-Amesty, G., Luo, P., Monzavi-Karbassi, B., Lees, A. and Kieber-Emmons, T. 2001. Exploiting molecular mimicry to broaden the immune response to carbohydrate antigens for vaccine development. *Vaccine* 19:2361.
- 21 Kieber-Emmons, T., Monzavi-Karbassi, B., Wang, B., Luo, P. and Weiner, D. B. 2000. Cutting edge: DNA immunization with minigenes of carbohydrate mimotopes induce functional anti-carbohydrate antibody response. *J. Immunol.* 165:623.
- 22 Wong, C. P., Okada, C. Y. and Levy, R. 1999. TCR vaccines against T cell lymphoma: QS-21 and IL-12 adjuvants induce a protective CD8<sup>+</sup> T cell response. *J. Immunol.* 162:2251.
- 23 Wely, C. A., Beverley, P. C., Brett, S. J., Britten, C. J. and Tite, J. P. 1999. Expression of L-selectin on Th1 cells is regulated by IL-12. *J. Immunol.* 163:1214.
- 24 Chao, C. C., Jensen, R. and Dailey, M. O. 1997. Mechanisms of L-selectin regulation by activated T cells. *J. Immunol.* 159:1686.
- 25 Kastrup, I. B., Stevanovic, S., Arsequell, G., Valencia, G., Zeuthen, J., Rammensee, H. G., Elliott, T., Haurum, J. S., Sun, Y., Hwang, Y. and Nahm, M. H. 2000. Lectin purified human class I MHC-derived peptides: evidence for presentation of glycopeptides *in vivo*. *Tissue Antigens* 56:129.
- 26 Haurum, J. S., Hoier, I. B., Arsequell, G., Neisig, A., Valencia, G., Zeuthen, J., Neefjes, J. and Elliott, T. 1999. Presentation of cytosolic glycosylated peptides by human class I major histocompatibility complex molecules *in vivo*. *J. Exp. Med.* 190:145.
- 27 Gilthero, A., Tormo, J., Haurum, J. S., Arsequell, G., Valencia, G., Edwards, J., Springer, S., Townsend, A., Pao, Y. L., Wormald, M., Dwek, R. A., Jones, E. Y. and Elliott, T. 1999. Crystal structures of two H-2D<sup>b</sup>/glycopeptide complexes suggest a molecular basis for CTL cross-reactivity. *Immunity* 10:63.
- 28 Kim, J., Ayyavoo, V., Bagarazzi, M., Chattergoon, M., Dang, K., Wang, B., Boyer, J. and Weiner, D. 1997. *In vivo* engineering of a cellular immune response by coadministration of IL-12 expression vector with a DNA immunogen. *J. Immunol.* 158:816.
- 29 Kim, J. J., Trivedi, N. N., Wilson, D. M., Mahalingam, S., Morrison, L., Tsai, A., Chattergoon, M. A., Dang, K., Patel, M., Ahn, L., Boyer, J. D., Chalian, A. A., Schoemaker, H., Kieber-Emmons, T., Agadjanyan, M. A., Weiner, D. B. and Shoemaker, H. 1998. Molecular and immunological analysis of genetic prostate specific antigen (PSA) vaccine [published erratum appears in *Oncogene* 1999;18:2411]. *Oncogene* 17:3125.
- 30 Agadjanyan, M. G., Kim, J., N., Wilson, D., Monzavi-Karbassi, B., Morrison, L. K., Nottingham, L. K., Dentchev, T., Tsai, A., Dang, K., Chalian, A. A., Maldonado, M. A., Williams, W. V. and Weiner, D. B. 1999. CD86 (B7-2) can function to drive MHC-restricted antigen-specific CTL responses *in vivo*. *J. Immunol.* 162:3417.
- 31 Jiao, Y. and Fujimoto, S. 1998. Sequential T cell response involved in tumor rejection of sarcoma, Meth A, in syngeneic mice. *Jpn. J. Cancer Res.* 89:657.
- 32 Frassanito, M. A., Mayordomo, J. I., DeLeo, R. M., Storkus, W. J., Lotze, M. T. and DeLeo, A. B. 1995. Identification of Meth A sarcoma-derived class I major histocompatibility complex-associated peptides recognized by a specific CD8<sup>+</sup> cytotoxic T lymphocyte. *Cancer Res.* 55:124.
- 33 Parker, K. C., Bednarek, M. A. and Coligan, J. E. 1994. Scheme for ranking potential HLA-A2 binding peptides based on independent binding of individual peptide side-chains. *J. Immunol.* 152:163.
- 34 Castano, A. R., Tangri, S., Miller, J. E., Holcombe, H. R., Jackson, M. R., Huse, W. D., Kronenberg, M. and Peterson, P. A. 1995. Peptide binding and presentation by mouse CD1 [see Comments]. *Science* 269:223.
- 35 Bedford, P., Garner, K. and Knight, S. C. 1999. MHC class II molecules transferred between allogeneic dendritic cells stimulate primary mixed leukocyte reactions. *Int. Immunol.* 11:1739.
- 36 Chesney, J., Bacher, M., Bender, A. and Bucala, R. 1997. The peripheral blood fibrocyte is a potent antigen-presenting cell capable of priming naive T cells *in situ*. *Proc. Natl. Acad. Sci. USA* 94:6307.
- 37 Nashar, T. O., Betteridge, Z. E. and Mitchell, R. N. 2001. Evidence for a role of ganglioside GM1 in antigen presentation: binding enhances presentation of *Escherichia coli* enterotoxin B subunit (EtxB) to CD4<sup>+</sup> T cells. *Int. Immunol.* 13:541.
- 38 Tsuyuoka, K., Yago, K., Hirashima, K., Ando, S., Hanai, N., Saito, H., Yamasaki, K. M., Takahashi, K., Fukuda, Y., Nakao, K. and Kannagi, R. 1996. Characterization of a T cell line specific to an anti-Id antibody related to the carbohydrate antigen, sialyl SSEA-1, and the immundominant T cell antigenic site of the antibody. *J. Immunol.* 157:661.
- 39 Inagawa, H., Nishizawa, T., Honda, T., Nakamoto, T., Takagi, K. and Soma, G. 1998. Mechanisms by which chemotherapeutic agents augment the antitumor effects of tumor necrosis factor: involvement of the pattern shift of cytokines from Th2 to Th1 in tumor lesions. *Anticancer Res.* 18:3957.
- 40 Manki, A., Ono, T., Uenaka, A., Seino, Y. and Nakayama, E. 1998. Vaccination with multiple antigen peptide as rejection antigen peptide in murine leukemia. *Cancer Res.* 58:1960.
- 41 Noguchi, Y., Richards, E. C., Chen, Y. T. and Old, L. J. 1995. Influence of interleukin 12 on p53 peptide vaccination against established Meth A sarcoma. *Proc. Natl. Acad. Sci. USA* 92:2219.
- 42 Aruga, A., Aruga, E., Cameron, M. J. and Chang, A. E. 1997. Different cytokine profiles released by CD4<sup>+</sup> and CD8<sup>+</sup> tumor-draining lymph node cells involved in mediating tumor regression. *J. Leuk. Biol.* 61:507.
- 43 Khar, A., Kausalya, S. and Kamal, M. A. 1996. AK-5 tumor-induced modulation of host immune function: upregulation of Th1-type cytokine response mediates early tumor regression. *Cytokines Mol. Ther.* 2:39.
- 44 Shankaran, V., Ikeda, H., Bruce, A. T., White, J. M., Swanson, P. E., Old, L. J. and Schreiber, R. D. 2001. IFNgamma and lymphocytes prevent primary tumour development and shape tumour immunogenicity. *Nature* 410:1107.
- 45 Bruehl, R. E., Bertozzi, C. R. and Rosen, S. D. 2000. Minimal sulfated carbohydrates for recognition by L-selectin and the MECA-79 antibody. *J. Biol. Chem.* 275:32642.
- 46 Crottet, P., Kim, Y. J. and Varki, A. 1996. Subsets of sialylated, sulfated mucins of diverse origins are recognized by L-selectin. Lack of evidence for unique oligosaccharide sequences mediating binding. *Glycobiology* 6:191.
- 47 Rosen, S. D. 1999. Endothelial ligands for L-selectin: from lymphocyte recirculation to allograft rejection. *Am. J. Pathol.* 155:1013.
- 48 Bohm, C. M., Mulder, M. C., Zennadi, R., Notter, M., Schmitt-Graff, A., Finn, O. J., Taylor-Papadimitriou, J., Stein, H., Clausen, H., Riecken, E. O. and Hanski, C. 1997. Carbohydrate recognition on MUC1-expressing targets enhances cytotoxicity of a T cell subpopulation. *Scand. J. Immunol.* 46:27.
- 49 Abdel-Motal, U., Berg, L., Rosen, A., Bengtsson, M., Thorpe, C. J., Kihlberg, J., Dahmen, J., Magnusson, G., Karlsson, K. A. and Jondal, M. 1996. Immunization with glycosylated K<sup>b</sup>-binding peptides generates carbohydrate-specific, unrestricted cytotoxic T cells. *Eur. J. Immunol.* 26:544.
- 50 Carbone, F. R. and Gleeson, P. A. 1997. Carbohydrates and antigen recognition by T cells. *Glycobiology* 7:725.

51 Galli-Stampino, L., Meinjohanns, E., Frische, K., Meldal, M., Jensen, T., Werdelin, O. and Mouritsen, S. 1997. T-cell recognition of tumor-associated carbohydrates: the nature of the glycan moiety plays a decisive role in determining glycopeptide immunogenicity. *Cancer Res.* 57:3214.

52 Haurum, J. S., Tan, L., Arsequell, G., Frodsham, P., Lelouch, A. C., Moss, P. A., Dwek, R. A., McMichael, A. J. and Elliott, T. 1995. Peptide anchor residue glycosylation: effect on class I major histocompatibility complex binding and cytotoxic T lymphocyte recognition. *Eur. J. Immunol.* 25:3270.

53 Jensen, T., Galli, S. L., Mouritsen, S., Frische, K., Peters, S., Meldal, M. and Werdelin, O. 1996. T cell recognition of Tn-glycosylated peptide antigens. *Eur. J. Immunol.* 26:1342.

54 Jensen, T., Hansen, P., Galli, S. L., Mouritsen, S., Frische, K., Meinjohanns, E., Meldal, M. and Werdelin, O. 1997. Carbohydrate and peptide specificity of MHC class II-restricted T cell hybridomas raised against an O-glycosylated self peptide. *J. Immunol.* 158:3769.

55 Michaelsson, E., Broddefalk, J., Engstrom, A., Kihlberg, J. and Holmdahl, R. 1996. Antigen processing and presentation of a naturally glycosylated protein elicits major histocompatibility complex class II-restricted, carbohydrate-specific T cells. *Eur. J. Immunol.* 26:1906.

56 Speir, J. A., Abdel-Motal, U. M., Jondal, M. and Wilson, I. A. 1999. Crystal structure of an MHC class I presented glycopeptide that generates carbohydrate-specific CTL. *Immunity* 10:51.

57 Forestier, C., Moreno, E., Meresse, S., Phalipon, A., Olive, D., Sansonetti, P. and Gorvel, J. P. 1999. Interaction of *Brucella abortus* lipopolysaccharide with major histocompatibility complex class II molecules in B lymphocytes. *Infect. Immun.* 67:4048.

58 Zollner, T. M., Nuber, V., Duijvestijn, A. M., Boehncke, W. H. and Kaufmann, R. 1997. Superantigens but not mitogens are capable of inducing upregulation of E-selectin ligands on human T lymphocytes. *Exp. Dermatol.* 6:161.

59 Tzianabos, A. O., Finberg, R. W., Wang, Y., Chan, M., Onderdonk, A. B., Jennings, H. J. and Kasper, D. L. 2000. T cells activated by zwitterionic molecules prevent abscesses induced by pathogenic bacteria. *J. Biol. Chem.* 275:6733.

60 Ravindranath, M. H., Bauer, P. M., Amiri, A. A., Miri, S. M., Kelley, M. C., Jones, R. C. and Morton, D. L. 1997. Cellular cancer vaccine induces delayed-type hypersensitivity reaction and augments antibody response to tumor-associated carbohydrate antigens [sialyl Le(a), sialyl Le(x), GD3 and GM2] better than soluble lysate cancer vaccine. *Anti-Cancer Drugs* 8:217.

# A Mimic of Tumor Rejection Antigen-Associated Carbohydrates Mediates an Antitumor Cellular Response

Behjatolah Monzavi-Karbassi,<sup>1</sup> Ping Luo,<sup>2</sup> Fariba Jousheghany,<sup>1</sup> Marta Torres-Quiñones,<sup>2</sup> Gina Cunto-Amesty,<sup>2</sup> Cecile Artaud,<sup>1</sup> and Thomas Kieber-Emmons<sup>1</sup>

<sup>1</sup>University of Arkansas for Medical Sciences, Little Rock, Arkansas, and <sup>2</sup>Department of Pathology and Laboratory Medicine, University of Pennsylvania, Philadelphia, Pennsylvania

## ABSTRACT

Tumor-associated carbohydrate antigens are typically perceived as inadequate targets for generating tumor-specific cellular responses. Lectin profile reactivity and crystallographic studies demonstrate that MHC class I molecules can present to the immune system posttranslationally modified cytosolic peptides carrying O- $\beta$ -linked N-acetylglucosamine (GlcNAc). Here we report that a peptide surrogate of GlcNAc can facilitate an *in vivo* tumor-specific cellular response to established Meth A tumors that display native O-GlcNAc glycoproteins on the tumor cell surface. Peptide immunization of tumor-bearing mice had a moderate effect on tumor regression. Inclusion of interleukin 12 in the immunization regimen stimulated complete elimination of tumor cells in all of the mice tested, whereas interleukin 12 administration alone afforded no tumor growth inhibition. Adoptive transfer of immune T cells into tumor-bearing nude mice indicates a role for CD8+ T cells in tumor regression. This work postulates that peptide mimetics of glycosylated tumor rejection antigens might be further developed for immune therapy of cancer.

## INTRODUCTION

The presence of carbohydrate antigens on the surface of common human malignant tumor cells has led to studies directed toward the development of synthetic carbohydrate-based anticancer vaccines (1). Although these vaccines elicit antibody responses, it would also be advantageous if T cells could be directed to tumor-associated carbohydrate antigens (2–6). Posttranslationally modified cytosolic peptides carrying O- $\beta$ -linked N-acetylglucosamine (GlcNAc) can be presented by class I MHC molecules to the immune system that activate CTLs, as resolved by wheat germ agglutinin (WGA)-binding profiles reacting with GlcNAc containing glycopeptides in the MHC Class I binding site (7, 8). Crystal structure analysis of T-cell receptor binding to model glycopeptides has indeed shown that T cells can recognize GlcNAc-linked glycopeptides bound by the MHC molecule (9, 10). T cells, therefore, have the potential to react with the GlcNAc moiety of glycopeptide antigens, suggesting that T cells can target to presented carbohydrate antigens on tumor cells.

In an effort to further define strategies to augment immune responses to tumor cells, we have been developing peptide mimics of tumor-associated carbohydrate antigens and have demonstrated that peptides synthesized as multivalent peptides can emulate or mimic the native clustering or presentation of tumor cell-displayed carbohydrate antigens (11). We have shown that prophylactic vaccination with a peptide surrogate, having the sequence GGIYWRYDIYWRYDIWRYD (and referred to as peptide 106), induces a tumor-specific humoral response inhibiting tumor growth of a methylcholanthrene-induced sarcoma cell line (Meth A) *in vivo* (11). This peptide also

activates an *in vitro* Meth A-specific cellular response with IFN- $\gamma$  production on activation of lymphocytes with peptide (12). Characterization of the cellular response indicated that peptide-specific CD8+ T cells played an important role in mediating the tumor-specific CTL response that was inhibited by anti-Class I antibody (12).

Here, we demonstrate the ability of this peptide to stimulate the regression of established Meth A tumor in a murine model via the activation of specific antitumor cellular responses. We demonstrate that peptide 106 is a mimic of O-GlcNAc, an antigen presented on Meth A surface-expressed glycoproteins as resolved by reactivity with WGA to which the peptide also binds. Immunohistochemistry demonstrates infiltrates of lymphocytes targeting Meth A tumor cells in peptide-immunized mice and adoptive transfer of peptide-specific T cells into tumor-bearing nude mice verifies a role for CD8+ T cells in mediating tumor regression. These studies highlight a new function for peptide mimotopes of carbohydrate-associated antigens by demonstrating that they possess *in vivo* antitumor activity with CD8+ T cells as the primary effector cells.

## MATERIALS AND METHODS

**Mice and Tumor Inoculation.** BALB/c female mice, 6–8 weeks old, were purchased from The Jackson Laboratory (Bar Harbor, ME). BALB/c nude mice (BALB/cAnNTac-Foxn1nu N9, *nu/nu*) were purchased from Taconic Farm Inc. (Germantown, NY). To establish tumor, each mouse was inoculated s.c. into the right flank with  $5 \times 10^5$  Meth A cells (Methylcholanthrene-induced sarcoma of BALB/c origin; Ref. 11). Tumor growth was measured using a caliper and was recorded as the mean of two orthogonal diameters [( $a + b$ )/2].

**Immunization.** As in our previous studies (11, 12), peptide 106, having the sequence GGIYWRYDIYWRYDIWRYD, was synthesized as a multiple-antigen peptide (Research Genetics, Huntsville, AL). Each mouse received 100  $\mu$ g of 106 multiple-antigen peptide and 20  $\mu$ g of QS-21 (Antigenics Inc., Framingham, MA) i.p., both resuspended in 100  $\mu$ l of PBS three times at 5-day intervals. Recombinant murine interleukin (IL)-12 (Sigma, St. Louis, MO) was administered i.p. once daily for 5 days, starting on the day of the last peptide immunization.

**Flow Cytometry.** Acquisition and analysis were performed as described earlier (12). Cells were resuspended in a buffer containing, Dulbecco's PBS, 1% BSA, and 0.1% sodium azide and incubated with biotinylated peanut agglutinin or WGA (10  $\mu$ g/ml; Vector laboratories, Burlingame, CA) for 30 min on ice. Cells were then stained with FITC-conjugated streptavidin at 1:50 dilution for another 30 min on ice.

**ELISA and Inhibition Assays.** ELISA was performed as described previously (11). Briefly, plates were coated with 106 multiple-antigen peptide. Biotinylated WGA was added, and binding was visualized with streptavidin-horseradish peroxidase (Sigma, St. Louis, MO). Absorbance was read, using a Bio-Tek ELISA reader (Bio-Tek instruments, Inc, Highland Park, Vermont). For inhibition assay, GlcNAc and *N*-acetylgalactosamine, attached to a polyacrylamide polymer (GlycoTech Corporation, Rockville, MD), were used as carbohydrate competitor. Biotinylated WGA (2.5  $\mu$ g/ml) combined with serial concentrations of carbohydrates and incubated overnight at +4°C. Lectin/carbohydrate mix was added to the peptide-coated plates, and lectin binding was visualized by streptavidin-horseradish peroxidase as above. Mean absorbance was calculated from duplicates for

Received 5/28/03; revised 10/2/03; accepted 1/7/04.

**Grant support:** NIH Grant CA089480 and Department of Defense Grant DAMD17-01-0366.

The costs of publication of this article were defrayed in part by the payment of page charges. This article must therefore be hereby marked *advertisement* in accordance with 18 U.S.C. Section 1734 solely to indicate this fact.

**Requests for reprints:** Thomas Kieber-Emmons, Arkansas Cancer Research Center, University of Arkansas for Medical Sciences, 4301 West Markham Street slot 824, Little Rock, AR 72205. Phone: (501) 526-5930; Fax: (501) 526-5934; E-mail: tke@uams.edu.

each carbohydrate concentration, and percentage of inhibition was calculated as:  $\{1 - (\text{mean of test wells}/\text{mean of control wells})\} \times 100$ .

**T-Cell Purification.** Splenocytes were harvested from spleens and prepared by lysis of erythrocytes and consequent washing several times with fresh medium (12). Splenocytes were first passed through nylon wool and then, using MiniMACS (Miltenyi Biotec, Auburn, CA), natural killer cells were depleted using anti-natural killer cell (DX5) microbeads. Finally, T cells were positively purified by Thy1.2-coated beads. Purified T cells were tested for purity as >97% positive for anti-CD3 antibody. For cell transfer experiments, after nylon wool passage, cells were enriched in CD4+ or CD8+ population using MiniMACS and depletion of unwanted cell populations.

**IFN- $\gamma$  Production by Purified T Cells.** Purified T cells ( $1 \times 10^6/\text{ml}$ ) were cultured in 96-well or 24-well plates with various doses of recombinant IL-12. After 48 h of stimulation, supernatant was harvested and stored at  $-20^\circ\text{C}$  until use. Concentration of IFN- $\gamma$  was measured using a quantitative ELISA kit (BioSource International Inc., Camarillo, CA) according to the manufacturer's instructions.

**Adoptive Transfer of Cells.** Splenocytes were collected from cured mice after tumor eradication and were used in transfer experiments. Immune splenocytes ( $1.5 \times 10^7$ ) were transferred i.p. to syngeneic nude tumor-bearing mice 7 to 10 days after inoculation of  $0.5 \times 10^6$  Meth A cells into the right flank. To *in vitro* deplete CD4+ and CD8+ cells, splenocytes ( $1.5 \times 10^7/\text{each sample}$ ) were first passed through nylon wool column, and then, using MACS, we depleted CD4+ and CD8+ cells.

**Histology.** Tumors with surrounding tissues were excised and fixed in 10% formalin. Fixed samples were embedded in paraffin, sectioned, and stained with H&E. Sections were analyzed histologically for lymphocyte infiltration.

**Statistical Analysis.** Statistical analyses were performed using Student's *t* test and the  $\chi^2$  test;  $P < 0.05$  were regarded as statistically significant. EXCEL and Statistica softwares were used for analyses. All of the experiments were performed at least three times.

## RESULTS

**Peptide Mimic of GlcNAc Moiety.** It has become evident that both CD4+ and CD8+ T cells can recognize glycopeptides carrying mono- and disaccharides in a MHC-restricted manner provided the glycan group is attached to the peptide at suitable positions (13). Reactivity patterns of lectins with Meth A cells indicate that GlcNAc glycosyl epitopes are more highly expressed on Meth A tumor cells than the T antigen Gal $\beta$ 1-3 N-acetylgalactosamine epitope, because WGA displays greater reactivity with Meth A cells than peanut agglutinin (Fig. 1, *A* and *B*). WGA binds to the peptide 106 mimotope in a concentration-dependent manner as assessed by ELISA (Fig. 1*C*). This binding is selectively and significantly inhibitable by WGA-reactive GlcNAc in a concentration-dependent manner (Fig. 1*D*), further indicating that the peptide mimotope is reactive with the GlcNAc-binding site of WGA, and, therefore, peptide 106 is an effective antigenic mimic of GlcNAc.

**Therapeutic Peptide Immunization Induces Tumor Regression.** To study the outcome of peptide immunization on the growth of solid tumors *in vivo*, we evaluated the antitumor effect of the peptide 106 on established Meth A tumors. BALB/c females were inoculated s.c. with Meth A cells, and 7 days later, treatment was started with the peptide. As shown in Fig. 2*A*, immunization moderately affected the growth of Meth A sarcoma, because 6 mice of 11 immunized were cured ( $\chi^2$  test,  $P = 0.01$ , as compared with animals that were given IL-12 only). Fig. 2*B* demonstrates that treatment of animals with IL-12 after peptide immunization tended to enhance the immune response and was successful in mediating complete eradication of established tumors ( $\chi^2$  test,  $P = 0.008$ , as compared with peptide-immunized only). Treatment of tumor-bearing mice with only IL-12 did not affect tumor growth (Fig. 2*C*) in keeping with other such studies (14).

We further determined that peptide/IL-12 combination therapy is

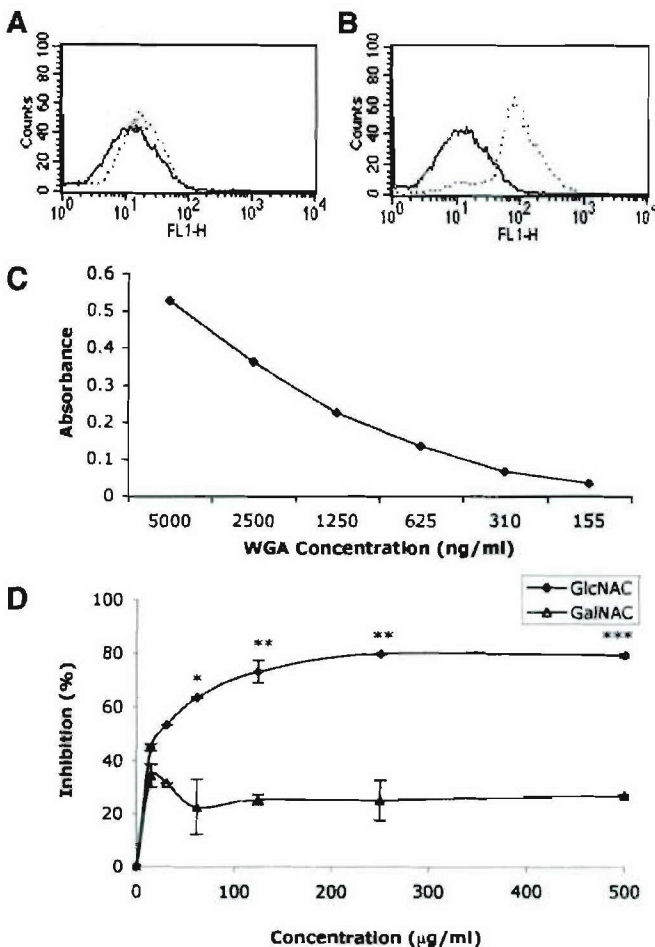
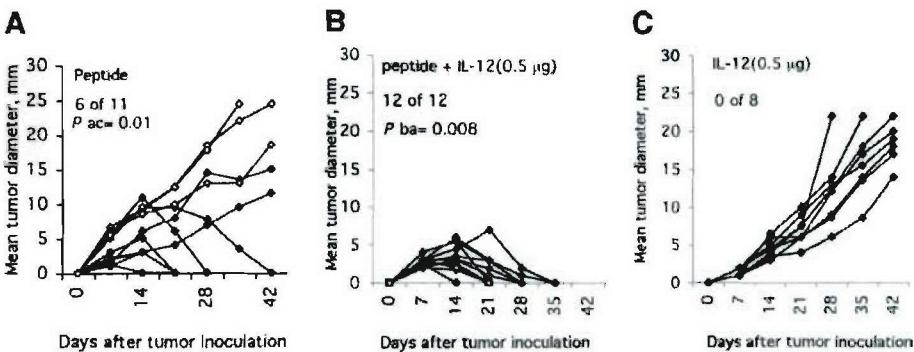


Fig. 1. Binding of wheat germ agglutinin (WGA) to the peptide and Meth A cells and the inhibition of WGA binding to the peptide. Meth A cells were incubated with biotinylated peanut agglutinin (*A*) or WGA (*B*) and were washed and stained with streptavidin-FITC for fluorescence-activated cell sorting (FACS) assay. Continuous and broken lines show streptavidin-FITC and lectin plus streptavidin-FITC, respectively. *C*, 96-well ELISA plates were coated with the peptide (50  $\mu\text{g}/\text{ml}$ ) and were incubated with biotinylated WGA; after washing, the plate binding was visualized by adding streptavidin-horseradish peroxidase. *D*, inhibition of binding of WGA to the peptide was performed by competitive carbohydrate N-acetylglucosamine (GlcNAc). N-acetylgalactosamine (GalNAc) was used as a negative control. WGA was preincubated with serial dilutions of carbohydrates overnight at  $+4^\circ\text{C}$  and then added to peptide-coated plates as above. Results present the mean value  $\pm$  SD. \*,  $P < 0.05$ ; \*\*,  $P < 0.01$ . \*\*\*,  $P < 0.0005$ , as compared with the inhibition of GalNAc at the same concentration.

highly effective even at lower doses of IL-12, because 100 ng of daily IL-12 treatment in the combined therapy, but not alone ( $\chi^2$  test,  $P = 0.001$ ), eradicated tumors in five mice of five challenged (Fig. 3, *A* and *B*). The time of the beginning of immunization and the size of tumor at the time of immunization affect the efficacy of immunization. When immunizations were started at day 14 or later or when treating tumors with a mean diameter larger than 7 mm, the efficacy of immunization dropped (Fig. 3*C*), ruling out the possible effect of hyperimmunization *per se* on the outcome of the challenge experiments. To further rule out nonspecific effects of hyperimmunization, we observed that cell-based vaccination using  $10^6$  mitomycin-C-inactivated Meth A cells, followed by IL-12 administration, also failed to induce tumor regression (Fig. 3*D*). This latter result confirmed a previous study in which Meth A immunization along with IL-12 failed to induce tumor regression (14). Our results are in agreement with other therapeutic vaccine studies on Meth A cells, in which enhancement of antitumor T-cell responses led to quick eradication of established tumors (15, 16).

**Fig. 2.** Effect of peptide immunization on Meth A tumor growth and regression. BALB/c female mice were inoculated s.c. with  $5 \times 10^5$  Meth A cells on day 0. *A* and *B*, 7 days after tumor inoculation peptide immunization started, mice were immunized i.p. with 106 multiple-antigen peptide/QS21 three times. Interleukin 12 was administered alone (*C*) or after peptide immunization (*B*) at indicated doses daily for 5 days, starting on the day of the last peptide immunization. Tumor growth is expressed as the mean diameter for each individual mouse.  $P_{ac}$  and  $P_{ba}$ ,  $P$ s of  $\chi^2$  tests comparing *A* with *C* and *B* with *A*, respectively.



**Adoptive Transfer of Splenocytes Stimulates Eradication of Tumors in Nude Mice.** To further assess whether the antitumor activity mediated by peptide/IL-12 therapy is T-cell dependent, we evaluated our therapeutic strategy in nude mice. BALB/c-*nu/nu* mice bearing Meth A tumors were immunized with the peptide followed by IL-12 treatment. Combined peptide/IL-12 therapy had no effect on tumor growth of nude mice, indicating the dependence of mediated tumor regression on T cells (data not shown). Next, nude mice were transplanted with Meth A cells and were given injections i.p. of fresh splenocytes, isolated from cured mice, 10 days later (Fig. 4). Immune cells transferred had a dramatic effect on tumor size because by day 15 after transfer, tumor was eradicated completely in all four mice tested ( $\chi^2$  test,  $P = 0.005$ ).

In a follow-up study, splenocytes were depleted of B cells and enriched for CD4+ or CD8+ cells, *in vitro*, and then were transferred

to tumor-bearing nude mice. Our data indicate that CD8+ cells are required for efficient eradication of tumor; however, the process seems dependent on both CD4+ and CD8+ cells (Fig. 5). Histological sections of tumor sites and surrounding tissues were prepared (Fig. 6). Contrary to nonimmunized tumor-bearing mice, we detected lymphocytes around the periphery and infiltrating into tumor mass of immunized mice (Fig. 6, *A* and *B*). Staining of sections obtained from the tumor site of a cured mouse shows the presence of lymphocytes, although no tumor is detectable microscopically (Fig. 6*C*).

## DISCUSSION

Carbohydrates are abundantly expressed on the surface of malignant cells, and induction and enhancement of a cell-mediated immune response toward these antigens has outstanding implications in vaccination for and treatment of cancer. T-cell recognition of nonpeptidic and modified peptide antigens is, however, still poorly understood. Peptide mimetics of carbohydrate antigens can activate peptide-specific cellular responses, but they have also been shown to activate cellular responses that might be cross-reactive with carbohydrate moieties (12, 17). The induction of carbohydrate-reactive T-lymphocytes with peptide mimics is based on a functional definition of T-cell mimotopes. One possible explanation is that the peptide mimotope activates cross-reactive CTLs that recognize a processed O-linked glycopeptide associated with MHC class I. It is also possible to generate carbohydrate-specific unrestricted CTL responses with MHC class I-binding carrier peptides (18). However, we previously showed that anti-MHC Class I antibody blocks CTL killing of Meth A cells *in vitro* by T cells derived from peptide 106 immunized mice (12).

Immunization with cells in combination with IL-12 had no obvious enhancement of antitumor immune effects. Our data propose that replacing cell immunization with peptide 106 enhanced a potential immune responses resulting in a significant but moderate tumor eradication. Further treatment of peptide-immunized mice with IL-12 helped significantly in stimulating eradication of established tumor in all of the animals tested. Lack of tumor shrinkage on cell-based immunization rules out the possibility that hyperimmunization had a bearing on tumor regression. Taken together, these results indicate that peptide immunization enables an effective antitumor immune response, the potential of which can be significantly enhanced with IL-12 administration. Other groups have performed therapeutic immunization on Meth A cells by immunization with p53 mutant epitope, starting the immunizations 7 days after tumor inoculations, and have demonstrated an efficient enhancement of antitumor cellular immune responses leading to eradication of tumor mass in the majority of animals within 2 weeks after the first immunization (15, 16). Our findings are in concert with the results of these studies.

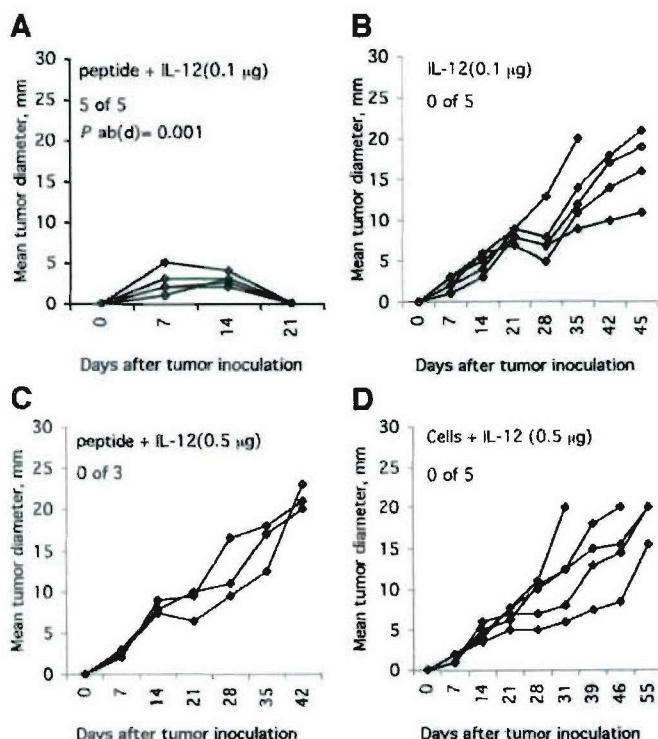


**Fig. 3.** Effect of late peptide or cell immunizations on the growth of the tumor. Tumor was established as explained in legend to Fig. 2. *A* and *B*, the same immunization as performed in Fig. 2 but with lower doses of interleukin (IL)-12. *C*, peptide immunization was started 14 days after tumor inoculation. *D*, 7 days after tumor inoculation, mice were immunized i.p. with  $10^6$  mitomycin-C-inactivated Meth A tumor cells for three times at 4–5-day intervals. IL-12 was administered alone (*B*), after peptide immunization (*A* and *C*), or after cell immunization (*D*) at indicated doses daily for 5 days, starting on the day of last peptide or cell immunization.  $P_{ab(d)}$ ,  $P$ s of  $\chi^2$  tests comparing *A* with *B* or *D*.

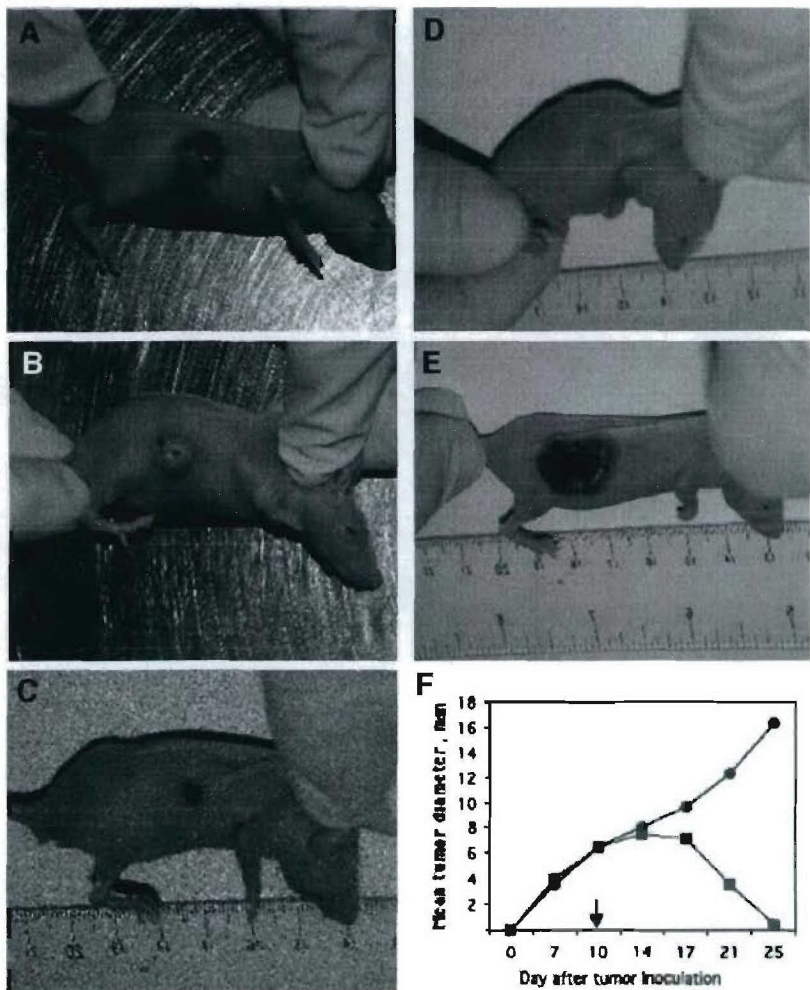


Fig. 4. Adoptive transfer of fresh immune splenocytes eradicated established tumors in nude mice. Two groups (four per group) of nude mice were inoculated s.c. with  $5 \times 10^5$  Meth A cells into the right flank. Ten days after inoculation when average of tumors diameter was about 7 mm, one group was given injections i.p. of  $1.5 \times 10^7$  of fresh splenocytes collected from already immunized and cured BALB/c animals. Splenocytes were prepared by lysis of erythrocytes and consequent washing several times with fresh medium. Pictures shown are taken from a representative individual on the day of cell transfer (A), 7 days later (B), 12 days later (C), and 17 days later (D). E, tumor size in control group 25 days after transplant as one representative individual of four is shown. F, average of tumor diameter for four mice per group in naïve control (●) and splenocyte-transferred groups (■). Arrow, the date of injection of splenocytes.

Because resting T cells do not express the IL-12 receptor (19) and IL-12 responsiveness is only activated after T-cell receptor stimulation (20), we observed that purified peptide-specific T cells were stimulated with IL-12 *in vitro* (data not shown). IL-12 treatment is ineffective in the Meth A tumor model (14) as further observed in our

studies. Because IL-12 responsiveness of T cells is induced after T-cell receptor stimulation, the lack of IL-12 responsiveness suggests that T cells in Meth A-bearing mice are not sensitized to Meth A tumor antigen on immunization with Meth A cells. In contrast, our data suggest that peptide immunization can sensitize tumor-reactive T cells that are responsive to IL-12. It is possible that peptide immunization further expands B and T cells that have been primed via shed glycoprotein(s) processing. We propose that peptide 106 immunization activated a population of Th1 and CTLs with production of IFN $\gamma$  (12), and *in vivo* IL-12 treatment further helps to expand the T-cell population and IFN $\gamma$  production. In previous studies, the failure of IL-12 treatment to induce tumor regression was also considered to be associated with the lack of T-cell migration to tumor sites (14). It was argued that sensitization of T cells to tumor antigens and generation of IL-12 responsiveness are insufficient to induce tumor regression when sensitized T cells are not allowed to migrate to tumor sites. In our studies, we observe lymphocyte migration to tumor sites.

In summary, this work further postulates the occurrence of carbohydrate epitopes for T cells linked to peptides with anchoring motifs for MHC Class I (6, 13). Although analogous to the haptens trinitrophenyl and O- $\beta$ -linked acetyl-glucosamine, the potential implications of natural carbohydrates as antigenic epitopes for CTL in biology are considerable and are understudied. Consequently, it might be possible for peptide mimetics to activate T cells that recognize carbohydrate moieties on native glycopeptides (21). Peptides that mimic carbohydrate structures attached to class I or class II anchoring peptides would

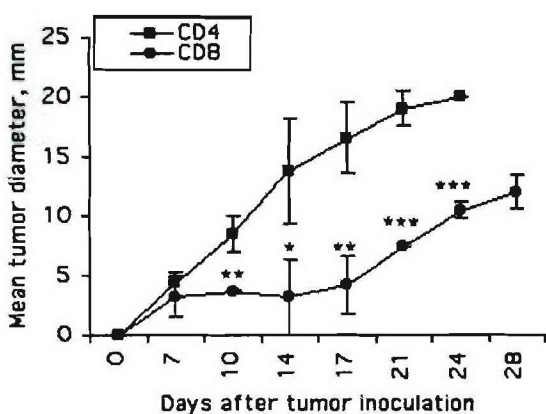


Fig. 5. CD8 $+$  T cells are required for successful adoptive therapy of established tumors. Solid tumors were established in nude mice, and at day 7, enriched splenocytes were transferred i.p. For enrichment, splenocytes were passed through nylon wool after which the percentage of CD19 $+$  cells that remained were less than 7%. Results present the mean value  $\pm$  SD. \*, P < 0.05; \*\*, P < 0.01. \*\*\*, P < 0.0005, as compared with mean tumor diameter of CD4 $+$ -transferred animals.

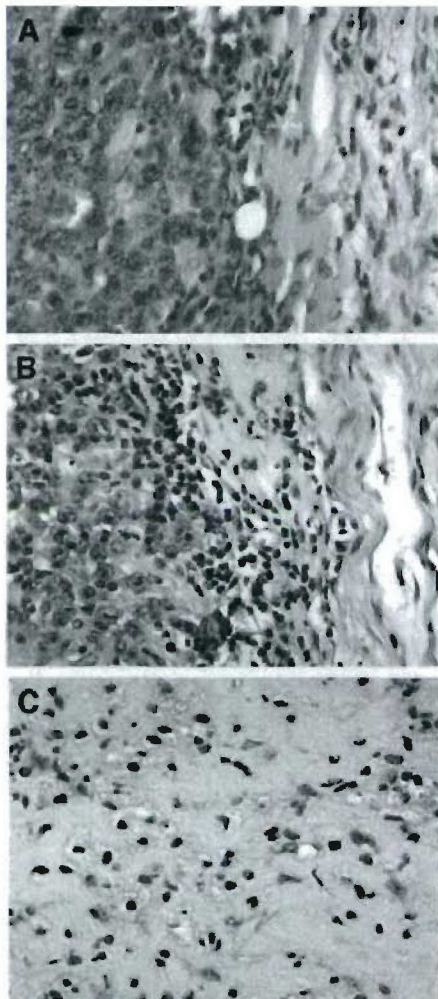


Fig. 6. Lymphocytes infiltrate the Meth A challenge site in immunized mice. Fixed sections from tumor site of nonimmunized tumor-bearing mice (A), immunized tumor-shrinking mice (B), and immunized tumor-eliminated mice (C) stained with H&E. Mice were transplanted, and immunization started 7 days later. Samples were obtained when tumor was 16 mm (A) and 2 mm (B) and at 5 days after tumor eradication (C).

extend our notion of vaccine design for cancer immunotherapy in the adjuvant setting.

#### ACKNOWLEDGMENTS

We thank Charlotte Read Kensil of Antigenics Inc. (Framingham, MA) for the QS-21. We thank Eric Siegel of the department of Biometry, University of Arkansas for Medical Sciences, for advise on the statistical analysis.

#### REFERENCES

- Danishefsky SJ, Allen JR. From the laboratory to the clinic: a retrospective on fully synthetic carbohydrate-based anticancer vaccines [frequently used abbreviations are listed in the appendix]. *Angew Chem Int Ed Engl* 2000;39:836–63.
- Jensen T, Galli SL, Mouritsen S, et al. T cell recognition of Tn-glycosylated peptide antigens. *Eur J Immunol* 1996;26:1342–9.
- Jensen T, Hansen P, Galli SL, et al. Carbohydrate and peptide specificity of MHC class II-restricted T cell hybridomas raised against an O-glycosylated self peptide. *J Immunol* 1997;158:3769–78.
- Haurum JS, Arsequell G, Lelouch AC, et al. Recognition of carbohydrate by major histocompatibility complex class I-restricted, glycopeptide-specific cytotoxic T lymphocytes. *J Exp Med* 1994;180:739–44.
- Galli-Stempina L, Meinjohanns E, Frische K, et al. T-cell recognition of tumor-associated carbohydrates: the nature of the glycan moiety plays a decisive role in determining glycopeptide immunogenicity. *Cancer Res* 1997;57:3214–22.
- Zhao XJ, Cheung NK. GD2 oligosaccharide: target for cytotoxic T lymphocytes. *J Exp Med* 1995;182:67–74.
- Haurum JS, Hoier IB, Arsequell G, et al. Presentation of cytosolic glycosylated peptides by human class I major histocompatibility complex molecules in vivo. *J Exp Med* 1999;190:145–50.
- Kastrup IB, Stevanovic S, Arsequell G, et al. Lectin purified human class I MHC-derived peptides: evidence for presentation of glycopeptides in vivo. *Tissue Antigens* 2000;56:129–35.
- Gilthero A, Tormo J, Haurum JS, et al. Crystal structures of two H-2Db/glycopeptide complexes suggest a molecular basis for CTL cross-reactivity. *Immunity* 1999;10:63–74.
- Speir JA, Abdel-Motal UM, Jondal M, Wilson IA. Crystal structure of an MHC class I presented glycopeptide that generates carbohydrate-specific CTL. *Immunity* 1999;10:51–61.
- Kieber-Emmons T, Luo P, Qiu J, et al. Vaccination with carbohydrate peptide mimotopes promotes anti-tumor responses. *Nat Biotechnol* 1999;17:660–5.
- Monzavi-Karbassi B, Cunto-Amesty G, Luo P, Shamloo S, Blaszczyk-Thurin M, Kieber-Emmons T. Immunization with a carbohydrate mimicking peptide augments tumor-specific cellular responses. *Int Immunopharmacol* 2001;13:1361–71.
- Werdelin O, Meldal M, Jensen T. Processing of glycans on glycoprotein and glycopeptide antigens in antigen-presenting cells. *Proc Natl Acad Sci USA* 2002;99:9611–3.
- Gao P, Uekusa Y, Nakajima C, et al. Tumor vaccination that enhances antitumor T-cell responses does not inhibit the growth of established tumors even in combination with interleukin-12 treatment: the importance of inducing intratumoral T-cell migration. *J Immunother* 2000;23:643–53.
- Noguchi Y, Richards EC, Chen YT, Old LJ. Influence of interleukin 12 on p53 peptide vaccination against established Meth A sarcoma. *Proc Natl Acad Sci USA* 1995;92:2219–23.
- Mayordomo JL, Loftus DJ, Sakamoto H, et al. Therapy of murine tumors with p53 wild-type and mutant sequence peptide-based vaccines. *J Exp Med* 1996;183:1357–65.
- Tzianabos AO, Finberg RW, Wang Y, et al. T cells activated by zwitterionic molecules prevent abscesses induced by pathogenic bacteria. *J Biol Chem* 2000;275:6733–40.
- Abdel-Motal U, Berg L, Rosen A, et al. Immunization with glycosylated Kb-binding peptides generates carbohydrate-specific, unrestricted cytotoxic T cells. *Eur J Immunol* 1996;26:544–51.
- Desai BB, Quinn PM, Wolitzky AG, Mongini PK, Chizzonite R, Gately MK. IL-12 receptor. II. Distribution and regulation of receptor expression. *J Immunol* 1992;148:3125–32.
- Maruo S, Toyo-oka K, Oh-hora M, et al. IL-12 produced by antigen-presenting cells induces IL-2-independent proliferation of T helper cell clones. *J Immunol* 1996;156:1748–55.
- Sandmaier BM, Oparin DV, Holmberg LA, Reddish MA, MacLean GD, Longenecker BM. Evidence of a cellular immune response against sialyl-Tn in breast and ovarian cancer patients after high-dose chemotherapy, stem cell rescue, and immunization with Theratope STn-KLH cancer vaccine. *J Immunother* 1999;22:54–66.

# **<sup>1</sup>H-NMR metabolic markers of malignancy correlate with spontaneous metastases in a murine mammary tumor model**

TRACY L. WHITEHEAD<sup>1</sup>, BEHJATOLAH MONZAVI-KARBASSI<sup>1</sup>, FARIBA JOUSHEGHANY<sup>1</sup>,  
CECILE ARTAUD<sup>1</sup>, ALAN ELBEIN<sup>2</sup> and THOMAS KIEBER-EMMONS<sup>1</sup>

<sup>1</sup>Arkansas Cancer Research Center and Department of Pathology and <sup>2</sup>Department of Cell and Molecular Biology,  
University of Arkansas for Medical Sciences, Little Rock, AR 72205, USA

Received February 10, 2005; Accepted March 22, 2005

**Abstract.** End-products of glycolysis as well as phospholipid precursors and catabolites have been suggested as metabolic indicators of tumor progression. To test the hypothesis that increased levels of such indicators can distinguish metastatic phenotypes, we determined a limited cellular <sup>1</sup>H-NMR metabolic profile of subpopulations of murine mammary 4T1 cells that differ in their metastatic potential. Subpopulations with differing metastatic phenotypes were identified by sorting for the expression of the cell surface adhesion oligosaccharide sialylated Lewis x (sLe<sup>x</sup>). The sLe<sup>x</sup>-negative subpopulation metastasizes to the lung of syngeneic mice more rapidly than the sLe<sup>x</sup>-positive subpopulations. The metabolic profile of the sLe<sup>x</sup>-negative subpopulation indicated higher levels of lactate and total choline metabolites than the sLe<sup>x</sup>-positive subpopulation, suggesting that altered metabolism is a critical component of the malignant phenotype. Analysis of shed cellular material from the sLe<sup>x</sup>-negative subpopulation displayed an increased ratio of phosphocholine to glycerophosphocholine when compared to the parental line and sLe<sup>x</sup>-positive subpopulation. Serum obtained from mice inoculated with either sLe<sup>x</sup>-negative or sLe<sup>x</sup>-positive tumor cells contained broader methylene resonances ( $P=0.0002$ ;  $P=0.0003$ ) and narrower methyl resonances ( $P=0.0013$ ;  $P<0.0001$ ) when compared to serum of naïve mice. However, line widths of methylene and methyl resonances were not useful for distinguishing between the two tumor phenotypes. Results of this study further support the notion that metabolic indicators of malignancy can correlate with *in vivo* metastatic behavior.

## **Introduction**

It is well known that cancer cell metabolism differs from that of normal tissue. High rates of glycolysis lead to anaerobic-like conditions, which result in the production of elevated levels of lactate (Lac) and pyruvate, a process historically referred to as the Warburg effect (1). Glycolytic rates in cultured cell lines correlate with tumor aggressiveness suggesting that altered metabolism is a critical component of the malignant phenotype (2). Glucose metabolism is observed to be a significant negative biomarker of prognosis and overall survival, with high concentrations of lactate in primary tumors correlating with a high incidence of distant metastasis in cancer patients (3).

Mechanistically, enhanced glycolysis has been implicated in facilitating tumor invasion, primarily as a result of decreased pH (2). Other mechanisms associated with end-product metabolites that are viewed to be important in malignant processes include the activation of hyaluronan synthesis by tumor-associated fibroblasts, up-regulation of vascular endothelial growth factor and of hypoxia-inducible factor 1α, and direct enhancement of cellular motility that generates favorable conditions for metastatic spread (3,4). By the same token, diverse molecular alterations such as metastasis-suppressor gene expression, oncogene expression, and malignant transformation converge at common end-points in choline phospholipid metabolism, demonstrating the important role of choline phospholipid metabolites in cancer progression (5). Thus, end-product metabolites and aberrant choline phospholipid metabolism might actively enhance and therefore may be markers for malignancy.

The metabolic shifts of cancer cells partly mediated by hypoxia-inducible factors significantly enhance the adhesion of tumor cells to vascular endothelial cells through both selectin- and integrin-mediated pathways, suggesting that this enhancement further facilitates hematogenous metastasis of cancers and tumor angiogenesis (6,7). Cell adhesion mediated by selectins and their carbohydrate ligands, sialyl Lewis X (sLe<sup>x</sup>) and sialyl Lewis A (sLeA) figures heavily in the metastatic process with these antigens being linked to the Warburg effect (6,7). These antigens are also influenced by tumor suppressor gene expression (8). Other studies have suggested, however, that aggressive metastatic behavior of

**Correspondence to:** Dr Thomas Kieber-Emmons, Arkansas Cancer Research Center, University of Arkansas for Medical Sciences, 4301 West Markham St. Slot #824, Little Rock, AR 72205, USA  
E-mail: tke@uams.edu

**Key words:** mammary carcinoma, solution state NMR, carbohydrate antigens, Warburg effect

human breast tumor cells can result from a lack of sLe<sup>X</sup> and sLe<sup>A</sup> antigens (9,10), diminishing homotypic (tumor cell-tumor cell) and perhaps heterotypic (tumor cell-endothelial cell) binding.

Paralleling these latter studies, we have identified a subpopulation of murine 4T1 mammary cells, a spontaneous tumor model whose growth and metastatic spread closely mimics stage IV breast cancer, with diminished expression of sLe<sup>X</sup> and have observed that this subpopulation metastasizes to the lung more efficiently than sLe<sup>X</sup>-positive subpopulations. To better distinguish between rapidly growing tumors and metastatic phenotypes, we have characterized a limited  $^1\text{H}$ -NMR metabolic profile of the 4T1 subpopulations that displays different metastatic phenotypes while maintaining similar *in vitro* and *in vivo* tumor growth profiles. Our results confirm a positive association between elevated *in vitro* levels of Lac and choline-containing compounds and increased malignant behavior of the sLe<sup>X</sup>-negative subpopulation *in vivo*. The characteristic differences in Lac and choline membrane metabolism observed here between these breast cancer cell subpopulations support further investigation of the role of glycolytic end-products and choline phospholipid metabolism in primary and metastatic disease. However, it is clear that our understanding of the relationship between the Warburg effect coupled with gene regulation and carbohydrate antigen expression on tumor cells is far from complete and in need of additional study.

#### Materials and methods

**Cell lines and reagents.** 4T1 cells were purchased from ATCC (Manassas, VA, USA). The KM93 and CSLEX1 antibodies were purchased from Kamiya Biomedical Co. (Seattle, WA) and BD Pharmingen (San Diego, CA), respectively. The anti-sLe<sup>A</sup> CA 19-9 and extended sLe<sup>X</sup> FH6 antibodies were purchased from Glycotech (Gaithersburg, MD). Recombinant mouse E- and P-selectin/Fc (human IgG) chimera were purchased from R&D System (Minneapolis, MN) and used in 10  $\mu\text{g}/\text{ml}$  aliquots for FACS assays. Deuterium oxide and 3-(trimethylsilyl)-1-propane sulfonic acid (TMSP) were purchased from Sigma Chemical Co. (St. Louis, MO).

**Flow cytometry and cell sorting.** Staining, acquisition, and analysis were performed as described in a previous study (11). In brief, cells were re-suspended in a buffer containing Dulbecco's phosphate-buffered saline, 1% BSA and 0.1% sodium azide, and were then incubated with biotinylated lectins or monoclonal antibodies (10  $\mu\text{g}/\text{ml}$ ) for 30 min on ice. Following this, cells were stained with FITC-conjugated streptavidin (2  $\mu\text{g}/\text{ml}$ ) or anti-mouse-FITC IgM or IgG (Sigma) for an additional 30 min on ice. For cell sorting, sodium azide was removed from the buffer and 10% of the most positive and the most negative cells (based on reactivity with KM93 Ab) were sorted. Sorting was repeated 4 times. For visualization of E- and P-selectin, anti-human IgG-FITC (Sigma) was used as secondary antibody. Negative controls were set using either biotin or mouse IgG/IgM as primaries.

**Growth conditions.** The 4T1 cell line and sorted subpopulations either positively-selected (sLe<sup>X</sup>-positive) or negatively-selected

(sLe<sup>X</sup>-negative) for KM93 antibody binding were cultured at 37°C in 5% CO<sub>2</sub> in DMEM (Cellgro) culture medium (pH 7.2) supplemented with 1% (v/v) penicillin-streptomycin (Cellgro), 1% (w/v) L-glutamine (Cellgro), and 10% (v/v) fetal bovine serum (FBS) (Atlas).

**Mice: tumor inoculation and metastasis assays.** 6-8 week-old BALB/c female mice were purchased from The Jackson Laboratory (Bar Harbour, ME). To establish tumors, each mouse was inoculated subcutaneously in the abdominal mammary gland with 1.0x10<sup>4</sup> 4T1 cells. Tumor growth was measured using a caliper and was recorded as the mean of two orthogonal diameters ((a+b)/2). Spontaneous metastases were assayed as described (10). Briefly, 26 days after inoculation mice were sacrificed and the lungs were harvested. Following this, the number of clonogenic cells was determined by growing collected cells in medium containing 6-thioguanine (13). Serum was collected from cardiac puncture post-sacrifice. All mouse studies were approved by the University of Arkansas for Medical Sciences animal use committee.

**Preparation of cells and cellular shed materials.** For preparation of pre-shed cell samples for  $^1\text{H}$ -NMR, 1.0x10<sup>8</sup> sub-confluent cells were harvested, washed twice in 3-5 ml of PBS (pH 7.2), and re-suspended in PBS/D<sub>2</sub>O to give a final volume of 500  $\mu\text{l}$ . Cellular shed materials including macromolecules and vesicles were prepared based on methods reported in the literature (14); in brief, 1.0x10<sup>8</sup> sub-confluent cells were harvested, washed twice in 3-5 ml of PBS, and re-suspended in 1 ml of PBS. Cells were then incubated at 37°C for 40 min. Following this, cells were removed by spinning at 800 g for 5 min and the resulting supernatant containing the cellular shed materials was spun for an additional 10 min at 12000 g to remove the remaining cell debris.

**Sample preparation for NMR measurements.** For intact cell analysis, 400  $\mu\text{l}$  aliquots of a solution comprised of 1.0x10<sup>8</sup> viable cells suspended in PBS/D<sub>2</sub>O (pH 7.2) were added as slurries to 5 mM NMR sample tubes containing 100  $\mu\text{l}$  of a 1.0 mg/ml solution of TMSP for use as an internal reference ( $\delta = 0.00$  ppm). For the analysis of shed cell samples, 200  $\mu\text{l}$  of sample were added to 200  $\mu\text{l}$  of PBS/D<sub>2</sub>O (pH 7.2) and 100  $\mu\text{l}$  of the internal reference solution, bringing the final sample volume to 500  $\mu\text{l}$ . Serum samples were prepared by mixing 300  $\mu\text{l}$  of D<sub>2</sub>O containing 0.05% TSP with 200  $\mu\text{l}$  of serum that had been thawed after storage at -80°C.

**High-resolution  $^1\text{H}$ -NMR measurements.** All  $^1\text{H}$ -NMR spectra were collected using a Varian Mercury-400 MHz spectrometer operating at a proton frequency of 399.84 MHz and at a temperature of 20°C (Note: spectra were also collected at 37°C with no discernable difference; therefore, samples were maintained at 20°C to prolong cell viability). One dimensional  $^1\text{H}$  data were collected without spinning so that solvent suppression of the residual water resonance could be achieved using the 3-9-19 Watergate (Water suppression by Gradient Tailored Excitation) pulse sequence (15). Initial spectra were collected with 1024 transients using a 45° pulse

Table I. Reactivity of anti-carbohydrate antibodies with sLe<sup>x</sup>-negative and -positive 4T1 subpopulations.<sup>a</sup>

	KM93	CSLEX-1	FH6	CA 19.9	E-selectin	P-selectin	IgG	IgM
sLe <sup>X</sup> -positive	63.69(±5)	6.96(±2.2)	5.63(±0.8)	5.76(±1.18)	17.92(±0.64)	89.25(±17.34)	5.33(±1.64)	6.36(±1.34)
sLe <sup>X</sup> -negative	12.3(3.6)	5.28(±1.6)	5.38(±1)	6.74(±0.5)	6.06(±3.04)	121.14(±30.7)	5.05(±1.39)	7.14(±2.17)

<sup>a</sup>Mean fluorescence intensities of flow cytometry assay are shown.

Table II. NMR analysis of mouse serum.

Metabolite	Serum	Mean line width 1/2 ht. (Hz)	Standard deviation	t-test (vs. control)	P-value
Lactate	sLe <sup>X</sup> -positive	48.822	8.20327	-4.37	0.0003
	sLe <sup>X</sup> -negative	46.613	6.90233	-4.61	0.0002
	Naïve mouse	34.287	5.65683		
Methyl	sLe <sup>X</sup> -positive	31.955	12.53858	6.88	<0.0001
	sLe <sup>X</sup> -negative	31.629	5.98718	3.79	0.0013
	Naïve mouse	47.939	4.50721		
Choline	sLe <sup>X</sup> -positive	23.195	4.25905	0.27	0.7932
	sLe <sup>X</sup> -negative	20.162	3.17524	-1.39	0.1824
	Naïve mouse	20.599	4.11113		

and a 2-sec relaxation delay. The spectral width was 4803.1 Hz and a 1.0 Hz line broadening was applied prior to processing.

Two-dimensional  $^1\text{H}$  COSY (Correlated SpectroscopY) spectra were acquired using a  $90^\circ\text{-}t_1\text{-}90^\circ\text{-}t_2$  pulse sequence with either presaturation of the water resonance or the WET (Water suppression Enhanced by  $T_1$  effects) water suppression method (16) coupled to a gradient COSY (gCOSY) pulse sequence with 256 repetitions in 128  $t_1$  increments. Data was processed using a square sine bell window function in both dimensions prior to transformation. All NMR spectra were processed using VNMR (Varian, Palo Alto, CA) operating on a Sun Ultra 6 workstation.

**Statistical analyses.** Statistical analysis for serum was performed using the two-population paired t-test (Microcal Origin<sup>®</sup>) with a 95% confidence interval ( $\alpha = 0.05$ ). Differences in population means were considered to be significant for  $P < 0.001$  (Table II). Primary tumor size and established lung lesions were compared using the Student's t-test option in Excel<sup>®</sup>. Differences between groups were considered significant if  $P < 0.05$ . All experiments were repeated in triplicate.

## Results

*Tumor cell selection and metastasis in vivo.* The murine mammary 4T1 cell line is a spontaneous tumor model that

metastasizes to the major organs in mice (12). The 4T1 cell line was tested for binding to the sLe<sup>x</sup>-reactive monoclonal antibodies KM93 (17), CSLEX-1 (18) and FH6 (19) and to the sLe<sup>A</sup>-reactive monoclonal antibody CA19-9 (20). Only the KM93 monoclonal antibody was found to be reactive with 4T1 cells (Table I). Sorting of the 4T1 cell line into two subpopulations was performed based on reactivity with the KM93 antibody. The sLe<sup>X</sup>-negative cells displayed weak reactivity with E-selectin but retained P-selectin binding (Table I); the KM-93-reactive epitope appears to be more associated with E-selectin binding on HUVEC cells (8).

*In vitro* proliferation studies suggest that the sLe<sup>x</sup>-negative and sLe<sup>x</sup>-positive cells grow at very similar rates (data not shown). To compare the *in vivo* growth and metastatic potential of the respective cell lines, two groups of mice (N=10/group) were inoculated with either sLe<sup>x</sup>-positive or sLe<sup>x</sup>-negative tumor cells. Subcutaneous tumor growth evaluated by tumor size was not different among the subpopulations throughout most of the study. As shown in Fig. 1A, we observed a slight increase in the size of tumors ( $P=0.05$ ) in the sLe<sup>x</sup>-negative inoculated mice near the end of the experiment, at days 21 and 26 post-transplant. While statistically significant, differences are not dramatic suggesting that these cells are growing at near equivalent rates *in vivo*. With regards to metastasis, we observed that the number of tumor cells colonized in the lung increased dramatically for sLe<sup>x</sup>-negative cells (Fig. 1B and C). These data indicate that sLe<sup>x</sup>-negative cells are highly metastatic to the lung.

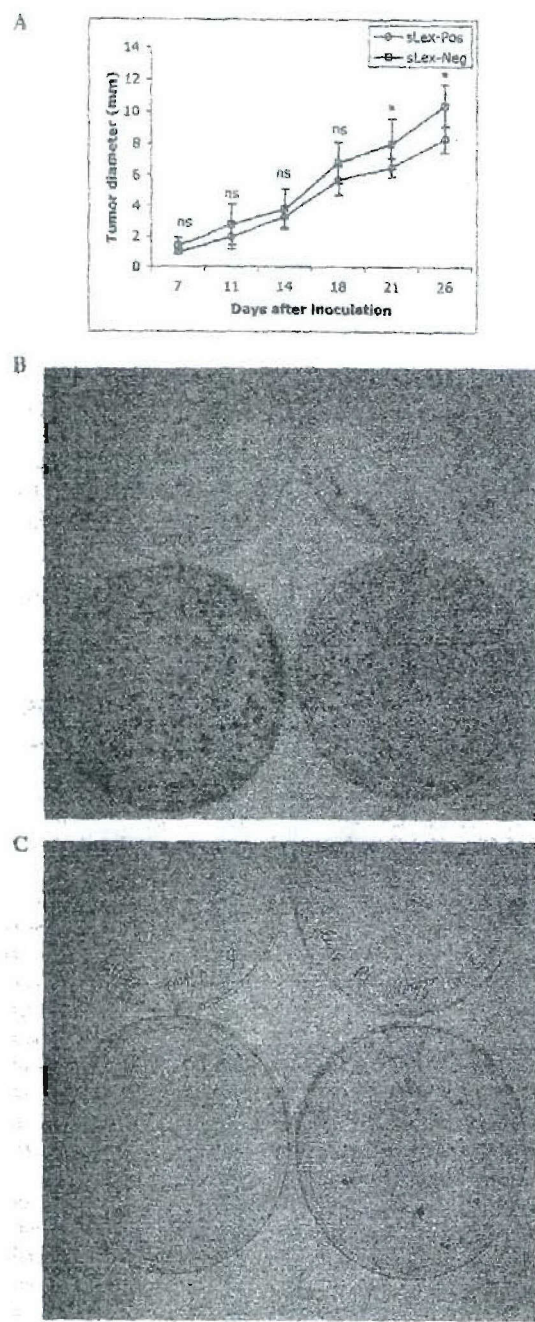


**Figure 1.** sLe $\chi$ -negative subpopulation displayed more malignant characteristics *in vivo*. Mice were inoculated into the mammary fat pads and tumor growth was measured. (A) Average of tumor diameter for mice in each group is presented. The symbol \* denotes significance at  $P < 0.05$  as performed by Student's *t*-test. Mice were then sacrificed at day 26, the lungs removed, and cell suspensions prepared and cultured. The number of clonogenic lesions was visualized and is depicted for two representative mice out of ten for each group: (B), sLe $\chi$ -negative tumors, and (C), sLe $\chi$ -positive tumors.

**Assignment of *in vitro*  $^1\text{H}$ -NMR spectra.**  $^1\text{H}$ -NMR spectra were collected and interpreted for all three populations of the 4T1 cells (wild-type, sLe $\chi$ -positive, sLe $\chi$ -negative) as well as for

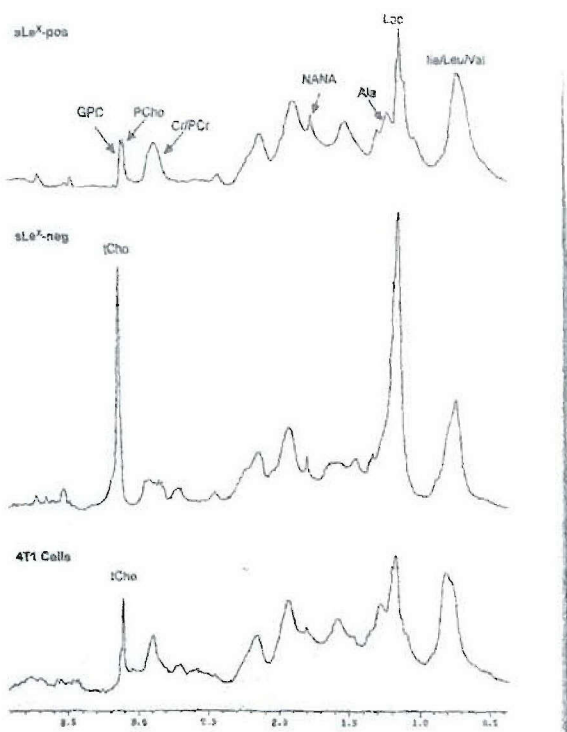


**Figure 2.** Comparison of 400 MHz  $^1\text{H}$ -NMR spectra for the alkyl regions of  $1.0 \times 10^8$  4T1 cells, sLe $\chi$ -negative cells, and sLe $\chi$ -positive cells in PBS/D<sub>2</sub>O. Note the increased level of total choline compounds and lactate in sLe $\chi$ -negative cells [tCho, total choline; PC, phosphocholine; GPC, glycerophosphocholine; lac, lactate; ala, alanine; ile, isoleucine; leu, leucine; val, valine; Cr, creatine; PCr, phosphocreatine; NANA, N-acetylneurameric acid (sialic acid)]. Also note that the tCho peak is resolved into two constituents; GPC and PCho, in sLe $\chi$ -pos cells.

shed cellular materials from the same populations. Assignments of several resonances were made using high-resolution assignments of intact breast tumor tissue and perchloric acid (PCA) extract data found in the literature (21-24) and by collection of one-dimensional and two-dimensional NMR spectra for compounds expressed on the tumor cell surface based upon lectin-binding analyses that have been performed in our laboratory (data not shown).

NMR spectra of the intact cells confirmed higher levels of total choline (tCho)-containing compounds on both parental 4T1 cells and sLe $\chi$ -negative cells when compared with the sLe $\chi$ -positive variant (Fig. 2) based on peak areas of resonances observed at 3.18 ppm. Analysis of shed cellular material provides more detailed information with respect to the composition of the tCho resonance, indicating an increase in the ratio of phosphocholine (PCho) to glycerophosphocholine (GPC). A reduction of GPC and an increase of PCho are typical for increased malignancy (25). For both wild-type 4T1 and sLe $\chi$ -positive cells, the ratio of PCho/GPC is roughly 1:1, while sLe $\chi$ -negative cells have a ratio closer to 2:1 (Fig. 3). This increase in PCho suggests that sLe $\chi$ -negative cells should be the most aggressive of the three cell lines studied.

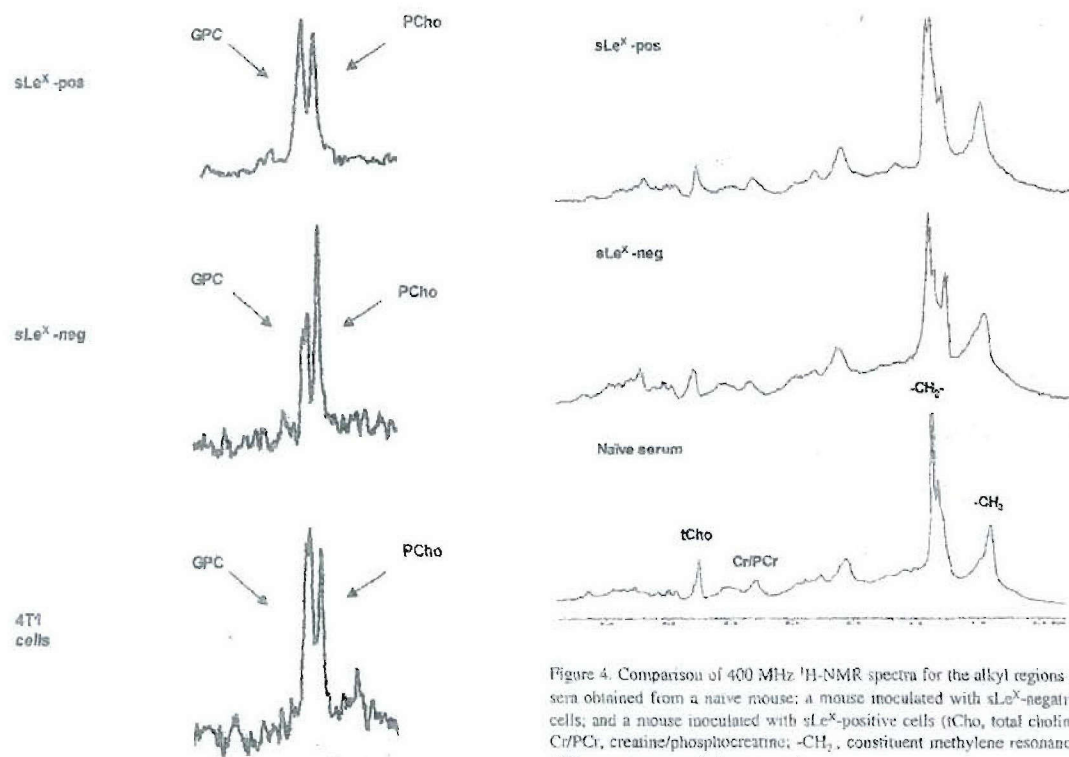


Figure 3. Comparison of PCho/GPC ratio taken from 400 MHz  $^1\text{H}$ -NMR spectra of shed cellular material from  $1.0 \times 10^8$  cells for murine 4T1, sLe $^X$ -neg; and sLe $^X$ -pos. Note the PCho/GPC ratio for the sLe $^X$ -neg cell line (increased malignancy) is approximately 2.1 when compared to a 1:1 ratio for 4T1 and sLe $^X$ -pos cells.

The most notable difference in metabolites between cell lines (with the exception of tCho level) is that of the glycolytic end-product lactate (Lac, 1.3 ppm). Cells that are sLe $^X$ -negative display a 2.5-fold increase in Lac production when compared to both sLe $^X$ -positive and wild-type 4T1 cells, indicating an increase in anaerobic glycolysis (Fig. 2). In addition, there is an approximate 50% reduction in the intensity of the composite creatine/phosphocreatine (Cr/PCr) peak (~3.0 ppm) of sLe $^X$ -negative cells when compared to both sLe $^X$ -positive cells and wild-type 4T1 cells (Fig. 2), suggesting a decrease in oxidative metabolism for the sLe $^X$ -negative subpopulation. Finally, *N*-acetylneurameric acid (sialic acid, 1.91 ppm) levels remain fairly consistent between sLe $^X$ -positive and 4T1 cell lines; however, a slight reduction is observed for sLe $^X$ -negative cells (Fig. 2), suggesting diminished sialylation of this subpopulation and correlating well with lectin binding analysis (data not shown).

$^1\text{H}$ -NMR spectra of mouse serum. In addition to *in vitro* analysis, spectra were collected for serum from mice inoculated with sLe $^X$ -positive or sLe $^X$ -negative tumor cells as well as for naive mouse (control) serum (Fig. 4). Dominant resonances observed included composite methyl (Val, Ile, Leu, HDL), methylene (Lac, LDL), Cr/PCr and tCho resonances. Spectra

Figure 4. Comparison of 400 MHz  $^1\text{H}$ -NMR spectra for the alkyl regions of sera obtained from a naive mouse; a mouse inoculated with sLe $^X$ -negative cells; and a mouse inoculated with sLe $^X$ -positive cells (tCho, total choline; Cr/PCr, creatine/phosphocreatine; -CH<sub>2</sub>, constituent methylene resonance; -CH<sub>3</sub>, constituent methyl resonance).

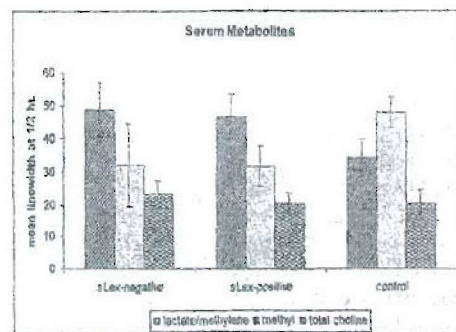


Figure 5. Comparison of average line widths at half-height for key metabolites present in serum of sLe $^X$ -positive, sLe $^X$ -negative; and naive mouse serum.

were referenced using TMSP as an internal standard. Statistical data for the analysis of serum spectra are given in Table II. Line widths were measured at half-height and compared for statistical significance, indicating fundamental differences between the three cell lines (Fig. 5).

Analysis of serum obtained from mice inoculated with sLe $^X$ -positive or sLe $^X$ -negative tumor cells using these resonances (normalized against TMSP) indicated that the line width at half height of composite methyl and methylene peaks of both sLe $^X$ -positive and sLe $^X$ -negative tumor bearing mice can be useful in distinguishing sera from these two groups of mice from that of naive mice (sLe $^X$ -negative,  $P=0.0002$ ; sLe $^X$ -

positive,  $P=0.0003$ ), with a broader methylene resonance and narrower methyl resonance both commonly observed in cancerous sera and known to be linked to abnormal distributions of plasma lipoproteins. Past studies have suggested that the ratio of line widths between these two resonances may be useful in detecting cancer in blood, commonly referred to as the *Fossel Index* (26). However, in our study, it was a direct comparison of the line widths of methylene and methyl resonances to those found in control mouse sera, and not the ratio of the two, that provided the most useful information.

In contrast, the direct comparison of methyl and methylene resonance line widths did not result in a statistically significant difference between sLe $\alpha$ -negative and sLe $\alpha$ -positive serum samples ( $P=0.5229$ ). These data indicate that the use of  $^1\text{H}$ -NMR spectroscopy line width data of methyl and methylene resonances in sera is not suitable for distinguishing between sLe $\alpha$ -positive and sLe $\alpha$ -negative tumor-bearing mice. Levels of tCho metabolites were found to not be significantly different between the two subpopulations and controls (sLe $\alpha$ -negative,  $P=0.1824$ ; sLe $\alpha$ -positive,  $P=0.7932$ ) or between the two populations alone ( $P=0.0877$ ). Finally, line widths of the composite methyl resonance were significantly different between serum from tumor bearing mice and control serum (sLe $\alpha$ -negative,  $P=0.0013$ ; sLe $\alpha$ -positive,  $P<0.0001$ ) but not to one another ( $P=0.9417$ ).

Analysis of peak intensity normalized in the same manner provided similar results with two key exceptions. As in the case with half-height line width data, the area of the composite methylene resonance was found to be statistically different between both sLe $\alpha$ -negative and sLe $\alpha$ -positive sera when compared with controls (sLe $\alpha$ -negative,  $P=0.0012$ ; sLe $\alpha$ -positive,  $P=0.0018$ ), but not to each other ( $P=0.4247$ ). Similarly, the area of the composite methyl resonance was also different between models and controls (sLe $\alpha$ -negative,  $P=0.0003$ ; sLe $\alpha$ -positive,  $P=0.0008$ ) but not between two models ( $P=0.2297$ ). However, a statistical difference was observed for the tCho resonance area between both models and controls (sLe $\alpha$ -negative,  $P=0.0004$ ; sLe $\alpha$ -positive,  $P=0.0011$ ) as well as between the two models ( $P=0.0137$ ), suggesting that mice inoculated with sLe $\alpha$ -positive tumor cells have slightly elevated levels of tCho in their sera. Finally, the composite Cr/PCr peak also displayed a statistical difference between sLe $\alpha$ -negative cells and controls ( $P=0.217$ ), while sLe $\alpha$ -positive did not ( $P=0.7643$ ), indicating a reduction in oxidative metabolism in sLe $\alpha$ -negative cells compared to the parental cells. There was no statistical difference between the Cr/PCr peak intensity between the two models ( $P=0.1874$ ).

## Discussion

In the present study, we observe that a subpopulation of 4T1 cells selected as sLe $\alpha$ -negative displays a metabolic profile indicative of a highly malignant phenotype. *In vitro*, both intact cells and supernatant display higher levels of Lac, with an elevated PCho/GPC ratio compared to parental 4T1 cells and the sLe $\alpha$ -positive subpopulation. This was confirmed *in vivo* where mice inoculated with sLe $\alpha$ -positive cells developed tumors with 'typical' metastatic and colonization ability while those inoculated with sLe $\alpha$ -negative cells developed

tumors with enhanced ability to metastasize. Therefore, the observed modified metabolite profile observed for the sLe $\alpha$ -negative subpopulation is associated with its more malignant behavior *in vivo*.

Serum obtained from mice inoculated with these cells displayed broader methylene resonances (1.3 ppm), suggestive of altered lipid metabolism and potentially of increased serum Lac levels when compared to naïve animals. We could not definitively discriminate differences in Lac and choline metabolite levels in serum among the subpopulations in tumor bearing mice; nevertheless, we could discriminate tumor-bearing mice from control animals, based upon NMR line widths of methylene and methyl resonances.

Investigating molecules involved in the metastatic potential in an inflammatory breast carcinoma model, others have shown that a decrease or lack of sLe $\alpha$ /A promotes metastatic dissemination of tumor cells (9,10). Our results support this observation. While an argument can be made that the lack of expression of sLe $\alpha$  contributes to a decrease in homotypic cell binding, therefore affecting the kinetics of cell dissemination, the observation of higher metabolite levels for the sLe $\alpha$ -negative subpopulation suggests that metabolic factors may contribute to malignancy facilitating metastasis in ways not yet defined. This observation is in accordance with studies indicating that elevated Lac and choline phospholipid metabolite levels are predictors of malignancy (5,27). Therefore, although the predictive value of such metabolites is still obscure, they deserve attention, considering the importance of metabolism to tumor cells. The ability to identify cells with increased metastatic capabilities by measuring levels of metabolic end products in serum may compliment the assessment of accepted tumor markers to facilitate identifying patients who harbor micrometastatic lesions.

## Acknowledgments

This work was supported in part by an American Cancer Society Institutional Research Grant (271/G1-11262-01E) (TLW), by CA089480 from NIH (TKE) and Department of Defense Breast Cancer Initiative - DAMD17-01-1-0366 (TKE).

## References

1. Warburg O: On the origin of cancer cells. *Science* 123: 309-314, 1956.
2. Gatenby RA and Gillies RJ: Why do cancers have high aerobic glycolysis? *Nat Rev Cancer* 4: 891-899, 2004.
3. Walenta S and Mueller-Klieser W: Lactate: mirror and motor of tumor malignancy. *Semin Radiat Oncol* 14: 267-274, 2004.
4. Lu H, Forbes RA and Verma A: Hypoxia-inducible factor 1 activation by aerobic glycolysis implicates the Warburg effect in carcinogenesis. *J Biol Chem* 277: 23111-23115, 2002.
5. Ackerstaff E, Glunde K and Bhujwalla ZM: Choline phospholipid metabolism: a target in cancer cells? *J Cell Biochem* 90: 525-533, 2003.
6. Kannagi R: Molecular mechanism for cancer-associated induction of sialyl Lewis X and sialyl Lewis A expression - The Warburg effect revisited. *Glycoconjugate J* 20: 353-364, 2004.
7. Koike T, Kimura N, Miyazaki K, Yabuta T, Kumamoto K, Takenoshita S, Chen J, Kobayashi M, Hosokawa M, Taniguchi A, Kojima T, Ishida N, Kawakita M, Yamamoto H, Takematsu H, Suzuki A, Kozutsumi Y and Kannagi R: Hypoxia induces adhesion molecules on cancer cells: a missing link between Warburg effect and induction of selectin-ligand carbohydrates. *Proc Natl Acad Sci USA* 101: 8132-8137, 2004.

8. Liu F, Zhang Y, Zhang XY and Chen HL: Transfection of the nm23-H1 gene into human hepatocarcinoma cell line inhibits the expression of sialyl Lewis X, alpha 1, 3 fucosyltransferase VII, and metastatic potential. *J Cancer Res Clin Oncol* 128: 189-196, 2003.
9. Alpaugh ML, Tomlinson JS, Ye Y and Barsky SH: Relationship of sialyl-Lewis(x/a) underexpression and E-cadherin over-expression in the lymphovascular embolus of inflammatory breast carcinoma. *Am J Pathol* 161: 619-628, 2002.
10. Alpaugh ML and Barsky SH: Reversible model of spheroid formation allows for high efficiency of gene delivery *ex vivo* and accurate gene assessment *in vivo*. *Hum Gene Ther* 13: 1245-1258, 2002.
11. Monzavi-Karbassi B, Cunto-Amesty G, Luo P, Shamloo S, Blaszczyk-Thurin M and Kieber-Emmons T: Immunization with a carbohydrate mimicking peptide augments tumor-specific cellular responses. *Int Immunopharmacol* 13: 1361-1371, 2001.
12. Pulaski BA and Ostrand-Rosenberg S: Mouse 4T1 breast tumor model. In: Current Protocols in Immunology. Coligan JE, Kruisbeek AM, Margulies DH, Shevach E and Strober W (eds). John Wiley & Sons, Inc., 3. 20.2.1-20.2.16, 2000.
13. Aslakson CJ and Miller FR: Selective events in the metastatic process defined by analysis of the sequential dissemination of subpopulations of a mouse mammary tumor. *Cancer Res* 52: 1399-1405, 1992.
14. Lean CL, Mackinnon WB, Delikatny J, Whitehead RH and Mountford CE: Cell-surface fucosylation and magnetic resonance spectroscopy characterization of human malignant colorectal cells. *Biochemistry* 31: 11095-11105, 1992.
15. Piotto M, Saudek V and Sklenar V: Gradient-tailored excitation for single-quantum NMR spectroscopy of aqueous solutions. *J Biomol NMR* 2: 661-665, 1992.
16. Ogg RJ, Kingley PB and Taylor JS: WET, a  $T_1$ - and  $B_1$ -insensitive water-suppression method for *in vivo* localized  $^1\text{H}$ -NMR spectroscopy. *J Magn Reson B* 104: 1-10, 1994.
17. Hanai N, Shitara K and Yoshida H: Generation of monoclonal antibodies against human lung squamous cell carcinoma and adenocarcinoma using mice rendered tolerant to normal human lung. *Cancer Res* 46: 4438-4443, 1986.
18. Fukushima K, Hirota M, Terasaki PI, Wakisaka A, Togashi H, Chu D, Suyama N, Fukushi Y, Nudelman E and Hakomori S: Characterization of sialosylated Lewis x as a new tumor-associated antigen. *Cancer Res* 44: 5279-5285, 1984.
19. Fukushi Y, Nudelman E, Levery SB, Hakomori S and Rauvala H: Novel fucolipids accumulating in human adenocarcinoma III. A hybridoma antibody (FH6) defining a human cancer-associated difucoganglioside (VI3NeuAc3II3Fuc2nLe6). *J Biol Chem* 259: 10511-10517, 1984.
20. Haglund C, Lindgren J, Roberts PJ and Nordling S: Tissue expression of the tumor marker CA 50 in benign and malignant pancreatic lesions: a comparison with CA19-9. *Int J Cancer* 38: 841-846, 1986.
21. Mackinnon WB, Russell P, May GL and Mountford CE: Characterization of human epithelial tumors (*ex vivo*) by proton magnetic resonance spectroscopy. *Int J Gynecol Cancer* 5: 211-221, 1995.
22. Mackinnon WB, Delbridge L, Russell P, Lean CL, May GL, Doran S, Dowd S and Mountford CE: Two-dimensional proton magnetic resonance spectroscopy for tissue characterization of thyroid neoplasms. *World J Surg* 20: 841-847, 1996.
23. Gribbestad I, Sitter B, Lundgren S, Krane J and Axelsson D: Metabolite composition in breast tumors examined by proton nuclear magnetic resonance spectroscopy. *Anticancer Res* 19: 1737-1746, 1999.
24. Sitter B, Sonnewald U, Spraul M, Fjösne HE and Gribbestad IS: High-resolution magic angle spinning MRS of breast cancer tissue. *NMR Biomed* 15: 327-337, 2002.
25. Aboagye EO and Bhujwalla ZM: Malignant transformation alters membrane choline phospholipid metabolism of human mammary epithelial cells. *Cancer Res* 59: 80-84, 1999.
26. Fossel ET, Carr JM and McDonagh J: Detection of malignant tumors. Water-suppressed proton nuclear magnetic resonance spectroscopy of plasma. *N Engl J Med* 315: 1369-1376, 1986.
27. Walenta S, Wetterling M, Lehrke M, Schwickert G, Sundfor K, Rostad EK and Mueller-Klieser W: High lactate levels predict likelihood of metastases, tumor recurrence, and restricted patient survival in human cervical cancers. *Cancer Res* 60: 916-921, 2000.

# Reduction of Spontaneous Metastases through Induction of Carbohydrate Cross-Reactive Apoptotic Antibodies<sup>1</sup>

Behjatolah Monzavi-Karbassi, Cecile Artaud, Fariba Jousheghany, Leah Hennings, Jaime Carcel-Trullols, Saeid Shaaf, Soheila Korourian, and Thomas Kieber-Emmons<sup>2</sup>

The selective targeting of tumor-associated carbohydrate Ags by the induction of serum Abs that trigger apoptosis of tumor cells as a means to reduce circulating tumor cells and micrometastases would be an advantage in cancer vaccine development. Some plant lectins like *Griffonia simplicifolia* lectin I and wheat germ agglutinin mediate the apoptosis of tumor cells. We investigated the possibility of using these lectins as templates to select peptide mimotopes of tumor-associated carbohydrate Ags as immunogens to generate cross-reactive Abs capable of mediating apoptosis of tumor cells. In this study, we show that immunization with a mimotope selected based on its reactivity with *Griffonia simplicifolia* lectin I and wheat germ agglutinin induced serum IgM Abs in mice that mediated the apoptosis of murine 4T1 and human MCF7 cell lines in vitro, paralleling the apoptotic activity of the lectins. Vaccine-induced anti-carbohydrate Abs reduced the outgrowth of micrometastases in the 4T1 spontaneous tumor model, significantly increasing survival time of tumor-bearing animals. This finding parallels suggestions that carbohydrate-reactive IgM with apoptotic activity may have merit in the adjuvant setting if the right carbohydrate-associated targets are identified. *The Journal of Immunology*, 2005, 174: 7057–7065.

**N**atural carbohydrate-reactive IgM Abs are implicated in mediating the apoptosis of tumor cells, and these circulating natural Abs are suggested as a mechanism of innate immune surveillance against cancer cells (1). mAbs directed against carbohydrate Ags expressed on tumor cells that trigger apoptosis have been described (2, 3) and provide a possibility for their application in the immunotherapy of disseminated cancer cells. The selective targeting of tumor-associated carbohydrate Ags by the induction of serum Abs that trigger apoptosis as a means to eradicate metastases could therefore be an advantage in vaccine development (4).

In our approach to induce sustained immunity against cancer cells, we are developing peptide mimotopes of tumor-associated carbohydrate Ags. Toward this end, we have shown that peptide mimotopes can induce humoral responses that mediate tumor-specific complement-dependent cytotoxicity (CDC)<sup>3</sup> (5, 6) and tumor-specific cellular responses (7). We have also shown that priming with peptide mimotopes followed by boosting with carbohydrate Ag can prolong the IgM response in mice, a benefit that is perceived to be of value for cancer vaccines in humans (8). Because it is expected that complement inhibitors expressed on a tumor cell surface can impair CDC, we have turned our attention to a strategy

of developing mimotopes that will induce Abs that trigger apoptotic mechanisms.

The lectins *Griffonia simplicifolia* I (GS-I), reactive with the  $\alpha$ -galactose ( $\alpha$ Gal) and  $\alpha$ -N-acetylgalactosamine ( $\alpha$ GalNAc) moieties, and wheat germ agglutinin (WGA), reactive with N-acetylglucosamine (GlcNAc) and sialic acid moieties, mediate apoptosis of various murine and human tumor cell lines (9–14). Screening combinatorial peptide libraries expressing a large collection of peptide sequences with lectins or anti-carbohydrate Abs has indicated a feasible strategy to produce immunogens for inducing carbohydrate cross-reactive immune responses (15). We hypothesize that using GS-I and WGA as templates to define and select peptide mimotopes will enable us to induce serum Abs capable of mediating apoptosis of tumor cells upon mimotope immunization.

The feasibility of this immunological strategy is presented in the current study, in which we find that carbohydrate-reactive IgM induced by a peptide mimotope in a DNA vaccine format or synthesized as a multiple Ag peptide (MAP) suppresses the outgrowth of metastases in the spontaneous murine mammary tumor 4T1 model. These observations further support the premise that Ab-inducing vaccines against carbohydrates can be used in the adjuvant setting, where circulating tumor cells and micrometastases are the primary targets (16, 17).

## Materials and Methods

### Cell lines, culture medium, and reagents

The 4T1 and MCF7 cell lines were purchased from American Type Culture Collection. The 4T1 cells were maintained in complete DMEM medium (Cellgro; Mediatech), supplemented with 100  $\mu$ g/ml penicillin-streptomycin (Cellgro), 2 mM L-glutamine (Cellgro), and 10% (v/v) FBS (ATLAS Biologicals). The MCF7 cells were maintained in American Type Culture Collection complete growth medium, which contains MEM (Eagle) supplemented with 0.1 mM nonessential amino acids, 1 mM sodium pyruvate, 0.01 mg/ml bovine insulin, 100  $\mu$ g/ml penicillin-streptomycin, and 10% FBS. The ARK cell line was established at the Arkansas Cancer Research Center from bone marrow aspirate of a patient with multiple myeloma (18). This cell line was kept in a complete RPMI 1640 medium supplemented with 100  $\mu$ g/ml penicillin-streptomycin, 1 mM sodium pyruvate, 10% FBS, and 2500 mg/ml glucose. Biotinylated GS-I and WGA lectins were purchased from Vector Laboratories. FITC-conjugated streptavidin was

Arkansas Cancer Research Center and Department of Pathology, University of Arkansas for Medical Sciences, Little Rock, AR 72205

Received for publication January 19, 2005. Accepted for publication March 19, 2005.

The costs of publication of this article were defrayed in part by the payment of page charges. This article must therefore be hereby marked *advertisement* in accordance with 18 U.S.C. Section 1734 solely to indicate this fact.

<sup>1</sup> This work was supported by grants from the U.S. Army Breast Cancer Program (DAMD17-01-1-0366) and the National Institutes of Health (CA-089480) to T.K.-E.

<sup>2</sup> Address correspondence and reprint requests to Dr. Thomas Kieber-Emmons, Arkansas Cancer Research Center, University of Arkansas for Medical Sciences, 4301 West Markham Street, Slot #824, Little Rock, AR 72205. E-mail address: tke@uams.edu

<sup>3</sup> Abbreviations used in this paper: CDC, complement-dependent cytotoxicity; GS-I, *Griffonia simplicifolia* lectin I; Gal, galactose; GalNAc, N-acetylgalactosamine; GlcNAc, N-acetylglucosamine; WGA, wheat germ agglutinin; MAP, multiple Ag peptide; PAA, polyacrylamide; PI, propidium iodide.

purchased from Sigma-Aldrich. Peptides were synthesized as MAP (Bio-Synthesis). Synthetic carbohydrate probes incorporated into a polyacrylamide (PAA) matrix were purchased from Glycotech. Vybrant apoptosis kit no. 3 was purchased from Molecular Probes. Fluorometric caspase activity detection kit was purchased from BD Biosciences. Apoptag, In Situ Apoptosis Detection kit S7100, was purchased from Chemicon International.

#### *Construction of expression vectors*

Oligonucleotides were synthesized and inserted into a secretory plasmid vector. First, the oligonucleotides were cloned between the restriction site *Not*I and *Hind*III in an intermediate shuttle vector pSL1180 (Amersham Biosciences) and then transferred to pSecTag2/HygroB (Invitrogen Life Technologies). Cloning was confirmed in each step by DNA sequencing. Constructs were designated as 104-, 105-, and 107-pSec based on the cloned peptide sequence.

#### *Mice, tumor inoculation, immunization, and metastases assay*

Six- to 8-wk-old BALB/c female mice were purchased from The Jackson Laboratory. To establish tumor, each mouse was inoculated s.c. in the abdominal mammary gland with  $1 \times 10^5$  4T1 cells. Tumor growth was measured using a caliper and was recorded as the mean of two orthogonal diameters ( $(a + b)/2$ ) (7). DNA immunization was performed as described earlier with minor modifications (6). Each mouse received three i.m. injections (weekly intervals) of 50- $\mu$ g DNA construct resuspended in 100  $\mu$ l of PBS. Immunization started 4 days posttumor transplant. Peptide immunization was performed as described earlier (5). Each mouse received 50  $\mu$ g of MAP and 10  $\mu$ g of QS-21 (Antigenics, Inc.) i.p., both resuspended in 100  $\mu$ l of PBS.

Spontaneous metastases were measured by methods described by Pulkaski and Ostrand-Rosenberg (19, 20) as clonogenic assays. Briefly, 4 wk after tumor inoculation, mice were sacrificed, and the lungs and the livers were harvested. Following this, the number of clonogenic cells was determined by growing harvested cells in medium containing 6-thioguanine (21). The animal studies have been reviewed and approved by Institutional Animal Care and Use Committee of University of Arkansas for Medical Sciences.

#### *Flow cytometry*

Staining, acquisition, and analysis were performed as described earlier (22). Briefly, cells were incubated with biotinylated GS-I and WGA lectins (10  $\mu$ g/ml) for 30 min and then stained with FITC-conjugated streptavidin at 2  $\mu$ g/ml for another 30 min on ice. For inhibition assay, biotinylated GS-I lectin (10  $\mu$ g/ml) was combined with serial concentrations of the peptide and incubated overnight at +4°C. Lectin/peptide mix was then added to the cells, and lectin binding was visualized as above. Mean fluorescence intensity was calculated from duplicates for each carbohydrate concentration, and percentage of inhibition was calculated as follows:  $(1 - (\text{mean of test tubes}/\text{mean of control tubes (only GS-I)})) \times 100$ .

#### *ELISA*

ELISA was performed as described before (5). Inhibition ELISA was performed as described earlier (7). Mean absorbance was calculated from duplicates for each carbohydrate concentration, and percentage of inhibition was calculated as follows:  $(1 - (\text{mean of test wells}/\text{mean of control wells})) \times 100$ .

#### *Cytotoxicity and apoptosis*

4T1 cells were plated into wells of a 96-well plate in medium containing 5% FBS. Lectins were added to some wells at various concentrations, and after overnight incubation, wells were washed; cells were fixed, stained with trypan blue, and counted; and the percentage of cytotoxicity was calculated using the following formula:  $(1 - (\text{alive cells in experimental wells}/\text{alive cells in control wells})) \times 100$ . Cytotoxicity of MCF7 cells was assayed by using Celltiter 96 Aqueous One Solution (Promega) according to the manufacturer's instructions. Briefly, 3–5  $\times 10^4$  cells were seeded in wells of 96-well plates, and lectins were added and incubated overnight. Then, the provided solution was added, absorbance was read, and the percentage of cytotoxicity was calculated using the following formula:  $(1 - (\text{absorbance of test well}/\text{absorbance of control well})) \times 100$ . To assess apoptosis, we used Vybrant apoptosis kit no. 3 (Molecular Probes) based on manufacturer's instructions. Briefly, cells were incubated with or without the lectins and then harvested and stained with red-fluorescent propidium iodide (PI) and FITC-conjugated annexin V. After staining, dead cells show red and green fluorescence, apoptotic cells show green fluorescence, and live cells show no fluorescence. For detection of serum-medi-

ated cytotoxicity or apoptosis, cell culture was established in complete medium overnight, and then the medium was replaced with the medium supplemented with 5% heat-inactivated mouse serum, and incubation was continued. Caspase activity was assayed by a fluorometric kit (BD Biosciences) using the manufacturer's instructions. Briefly, cells were coin cubated with medium supplemented with the lectins or the mice sera. Then, cells were trypsinized and counted, and cell lysate was prepared. Total protein was quantitated using a BCA Protein Assay kit (Pierce). Activity of each caspase was detected by using the specific fluorogenic substrates peptides VDVA (caspase 2), DEVD (caspase 3), IETD (caspase 8), and LEHD (caspase 9) conjugated to 7-amino-4-methyl-coumarin. Fluorescence intensity was measured using FLx 800 Microplate Fluorescence Reader (Bio-Tek Instruments) and corrected in regard to protein concentration. Lysates of nontreated cells (in case of lectins) or cells treated with normal mouse serum prepared at the same time points were used as negative controls.

#### *Fluorescence microscopy*

Cells were grown in 24-well plates on coverslips overnight. Culture medium was replaced with fresh medium containing 1% BSA and premixed 5% immunized mouse serum and anti-mouse IgM-FITC and incubated for 4 h. Slides were then washed in PBS and scanned with an inverted confocal microscope (Zeiss LSM 410) to a maximum depth of 25  $\mu$ m, and representative images were captured.

#### *Histopathology and in situ apoptosis detection*

Sections of lung and primary tumor from mice at 7, 14, and 21 days postinoculation were fixed in 10% neutral buffered formalin, processed, and embedded in paraffin, sectioned at 6  $\mu$ m, stained with H&E, and examined under a light microscope. Serial sections were stained by the TUNEL method using Apoptag Peroxidase In Situ Apoptosis Detection kit S7100 (Chemicon International) based on the manufacturer's instructions. Briefly, 6- $\mu$ m sections were deparaffinized, rehydrated, and treated with 20  $\mu$ g/ml Proteinase K for 15 min at room temperature. Sections were washed with two changes of dH<sub>2</sub>O for 2 min each. Endogenous peroxidases were blocked with 3% H<sub>2</sub>O<sub>2</sub> in PBS for 5 min and washed with three changes of PBS. Equilibration buffer containing digoxigenin-conjugated nucleotides was placed directly onto the section for 10 s. Sections were incubated with TdT enzyme in a humidified chamber at room temperature for 1 h. Sections were then incubated for 10 min at room temperature in stop-wash buffer, rinsed in three changes of PBS for 1 min each, and incubated with anti-digoxigenin conjugate for 30 min at room temperature. Sections were washed in four changes of PBS, stained with 0.5% (w/v) methyl green counterstain, and evaluated with a light microscope.

#### *Statistical analysis*

The Kaplan-Meier method was used to estimate survival rates, and the log-rank test was performed to compare two groups. Fisher exact test was used for comparisons made between animals regarding liver metastasis. Other statistical comparisons between means were performed using Student's *t* test. Differences between groups were considered significant if  $p < 0.05$ . Statistica software was used for analyses.

## **Results**

#### *WGA and GS-I lectins mediated cytotoxicity and apoptosis in select breast cancer cell lines*

Both WGA and GS-I bound to murine 4T1 and human MCF-7 breast cell lines with WGA showing stronger reactivity for both cell lines as assessed by flow cytometry (Fig. 1A). Both lectins mediated cell death upon coinubcation overnight with either cell line, validating the induction of cytotoxicity by the lectins (9–11, 14) (Fig. 1B). Supplementary experiments demonstrated that the cytotoxicity effect of the GS-I and WGA lectins was mediated through an apoptotic pathway as measured by an annexin V assay (Fig. 1C), with WGA displaying a more dramatic apoptotic effect on MCF7 cells than GS-I.

Using 4T1 cells, we further confirmed the induction of apoptosis, measuring activation of caspases 2, 3, 8, and 9. Overnight incubation of 4T1 cells with GS-I and WGA activated all indicated caspases (Fig. 1D). Activation was observed to start as early as 4 h postincubation for all caspases. Activation of caspases 2 and 3

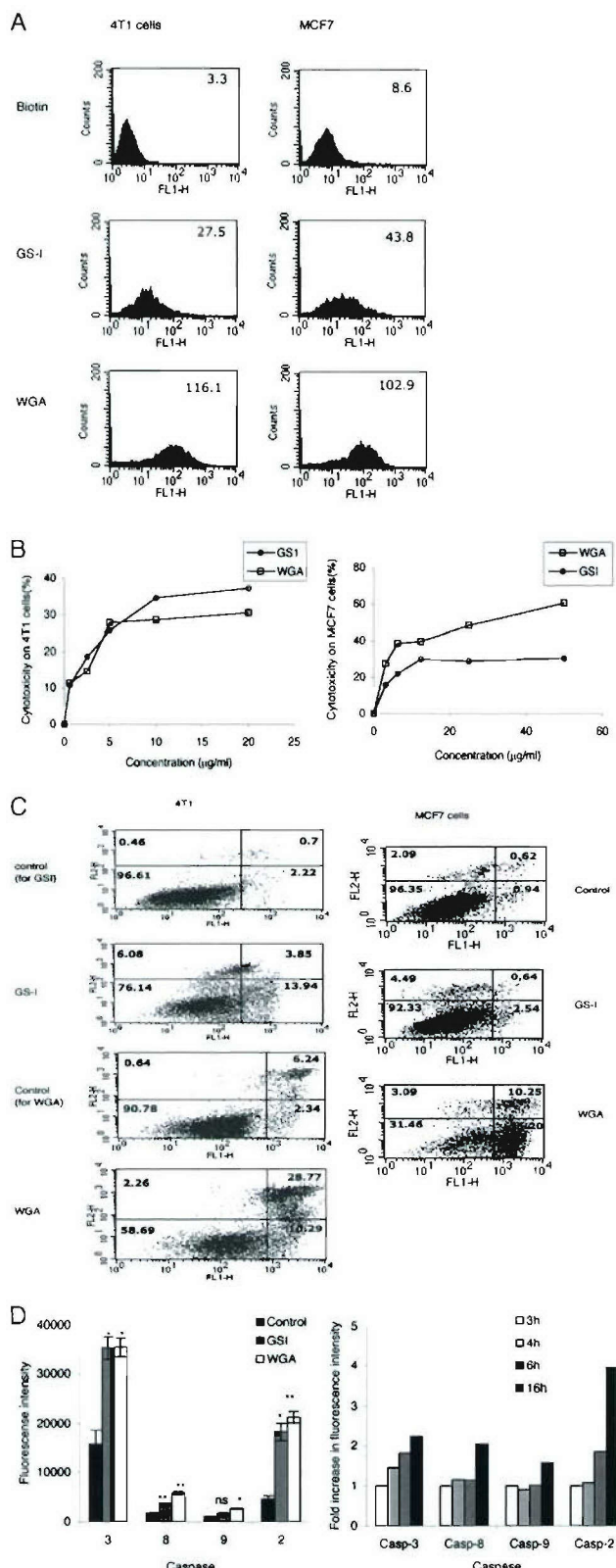


**FIGURE 1.** GS-I and WGA bound to the breast cell lines and mediated cytotoxicity and apoptosis. **A**, Lectins were coincubated with the indicated cell lines at 10 μg/ml for 30 min on ice. Similar amount of biotin was used as negative control. Binding was visualized with FITC-conjugated streptavidin using flow cytometry. Mean fluorescence intensity for each histogram is shown. **B**, Cells were seeded and coincubated with indicated concentration of the lectins overnight. Percentage of cytotoxicity was calculated based on the average of three replications as explained in Materials and Methods. **C**, Cells were incubated with or without lectins at 20 μg/ml for

**Table I. Peptides used in the study**

Peptide	Peptide Sequence
104	GGIMILLIFSLWFGGA
105	GGIYYPDIYYPYDIYYPD
106	GGIYWRYDIYWRYDIYWRD
107	GGIYYRYDIYRYDIYRYD
109	GGARVSPFWRYSSFAPTY

were consistently increased in treated cells compared with non-treated cells as depicted by fold increase of fluorescent intensity over a period of time (Fig. 1E), suggesting their critical role in cytotoxicity.

#### DNA immunization resulted in generation of carbohydrate-reactive serum Abs

We have defined peptides that mimic multiple carbohydrate Ags (6) that include peptides 105, 106, and 107 (Table I) or selected against specific carbohydrate-reactive Abs like peptides 104 and 109 (Table I) (23). Peptide 107 was chosen for our studies based on its consistent reactivity with both GS-I and WGA (Fig. 2A), further indicating that this peptide can functionally mimic multiple types of tumor-associated carbohydrate structures. In inhibition assays, we observed that peptide 107 binding to WGA was inhibited by GlcNAc (Fig. 2B) and that the peptide significantly inhibited GS-I lectin binding to 4T1 cells (C), suggesting that the peptide binds at or near the carbohydrate binding site of the two lectins.

We have previously shown that immunization with peptide mimotopes of carbohydrate Ags formulated as MAPs or as DNA vaccines can elicit carbohydrate-reactive IgM serum Abs (5, 24). To expand this latter strategy, the sequence of peptide 107 was translated into oligonucleotides and DNA constructs (Table II), and groups of mice were immunized with the 107-pSec DNA constructs and serum reactivity with carbohydrate probes was assayed (Fig. 2D). Serum IgM Abs from 107-pSec-immunized mice bound to Gal and GlcNAc oligosaccharides. We detected Ag-specific serum Abs of IgM isotype reactive with 4T1 and MCF7 cells by flow cytometry (Fig. 2, E and F), with no Ag-specific IgG isotype detected. Ag-specific serum IgM Abs were not detected against the myeloma cell line ARK cells (Fig. 2G) because reactivity of the preimmune serum to ARK cells was similar to the reactivity of serum from 107-pSec-immunized mice. The ARK cell line was not reactive with the GS-I lectin and only marginally with WGA (data not shown).

#### DNA immunization resulted in serum Abs capable of mediating apoptosis of tumor cells

To assess serum-mediated cell cytotoxicity, cells were coincubated with serum from peptide encoded DNA- or vector-alone-immunized mice (control), and the percentage of dead cells was detected

4 h. Cells were then harvested, washed, and stained with PI (FL-2) and annexin V (FL-1) as explained in Materials and Methods. Percentage of cells in each quadrant is shown. Both lectin-treated and nontreated cells were stained. Control stands for cells that were not treated with the lectin but were stained with PI and annexin V. In 4T1 cells, the experiments with WGA and GS-I were performed separately, so for each experiment we run a separate nontreated stained control. **D** and **E**, Cells were incubated with or without WGA and GS-I lectins at 10 μg/ml overnight and then were harvested, and caspase activity was measured. To compare the magnitude of activation over a period of time, fold increase of the activation, induced by GS-I lectin, as measured by fluorescence intensity of treated cells over nontreated cells at the same time point is presented (E). \*, p < 0.05; \*\*, p < 0.01; ns, not significant compared with control. All experiments above were repeated at least three times.

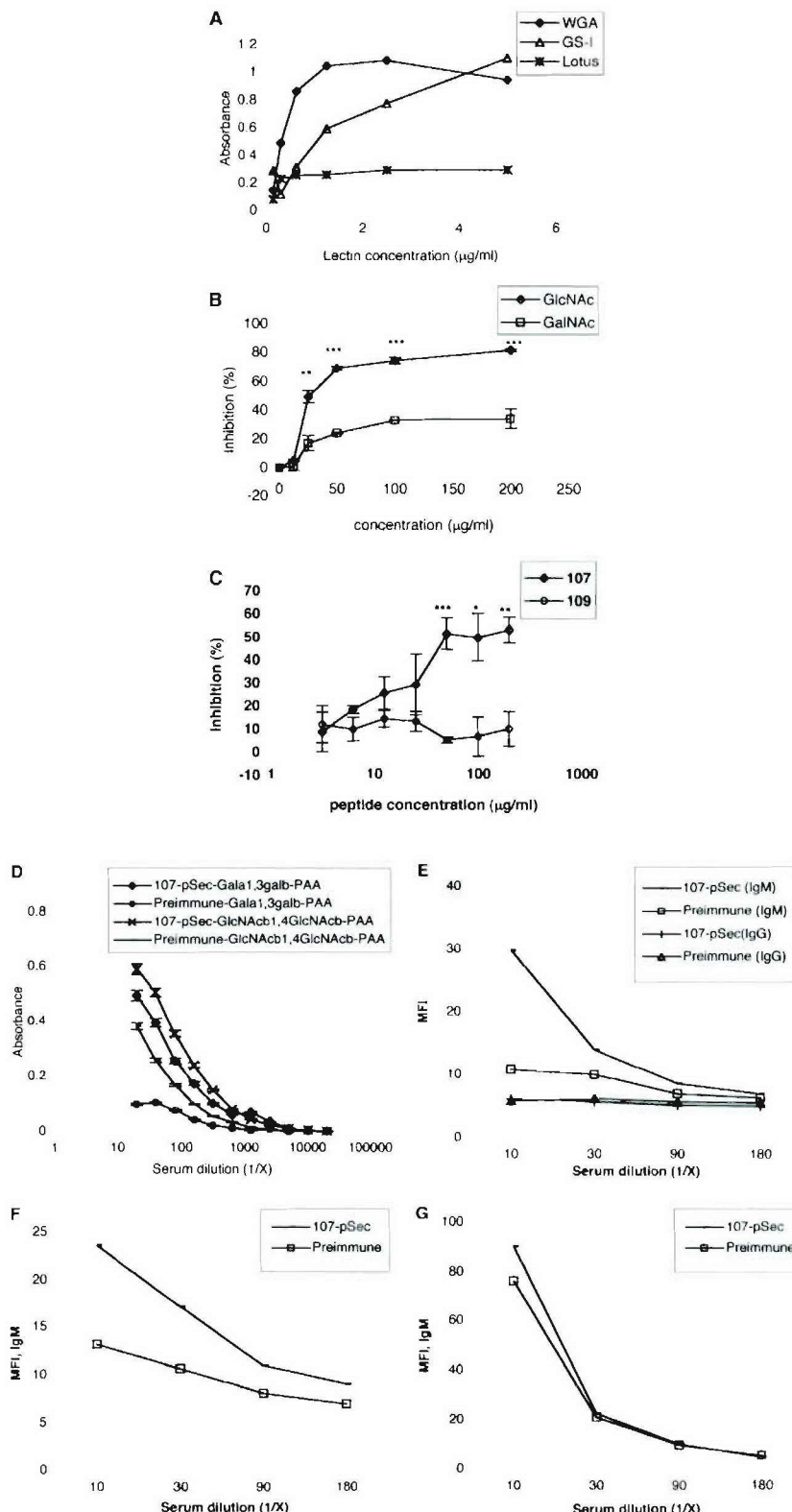


**FIGURE 2.** Peptide 107 reacted with the lectins in a specific manner, and immunization induced serum IgM Abs reactive with the carbohydrates and the cells. *A*, Plates were coated with the 107 peptide, and dose-dependent reactivity of indicated lectins was assessed. *B*, WGA binding to peptide 107 was inhibited by competitive carbohydrate GlcNAc. GalNAc was used as negative control. Results present the mean value  $\pm$  SD. \*\*,  $p < 0.01$ ; \*\*\*,  $p < 0.0005$  compared with inhibition of GalNAc at the same concentration. *C*, GS-I binding to the 4T1 cells was inhibited by peptide 107 as revealed in a FACS assay. Peptide 109 was used as the negative control. Bars show SD based on three replications. \*,  $p < 0.025$ ; \*\*,  $p < 0.01$ ; \*\*\*,  $p < 0.0005$  compared with inhibition of peptide 109 at the same concentration. *D*, Mice (10/group) were immunized three times with 107-pSec and the respective vector plasmid pSec. Animals were bled 10 days after the last boost. For each group, sera were pooled for 10 mice. ELISA plates were coated with indicated carbohydrates and reactivity of IgM Abs was detected. End-point Ab titer against Gal $\alpha$ 1,3Gal $\beta$ -PAA was 1:2560, whereas it was 1:1280 for GlcNAc $\beta$ 1,4GlcNAc $\beta$ -PAA. The titers were determined as the highest sera dilution with significantly higher OD compared with preimmune sera using paired Student's *t* test at  $p < 0.05$ . *E–G*, Binding of the serum to 4T1 (*E*), MCF7 (*F*), and ARK (*G*) cells was detected by flow cytometry and presented by mean fluorescence intensity (MFI).

after overnight coincubation. We observed  $\sim$ 20% dead cells in wells containing 107-pSec serum when wells supplemented with pSec (vector)-immunized serum were used as control. In concert with the GS-I and WGA effects, 107-pSec-immunized serum mediated apoptosis of both 4T1 and MCF7 cell lines with more pronounced effects on 4T1 cells (Fig. 3A). Paralleling the lectin cytotoxicity, we observed a significant increase in activation of caspases 2 and 3 after overnight incubation with serum from 107-

pSec-immunized mice (Fig. 3B). We estimated the fold increase in activation of caspases induced by 107-pSec-immunized mouse serum over normal mouse serum (Fig. 3C). Activation of caspases 2 and 3 was detected as early as 4 h postincubation with serum Abs from 107-pSec-immunized mice. After overnight incubation, we observed an increase in activation for all caspases studied; however, caspases 2 and 3 showed the highest fold increase in activation over normal-mouse serum-treated cells (Fig. 3C).

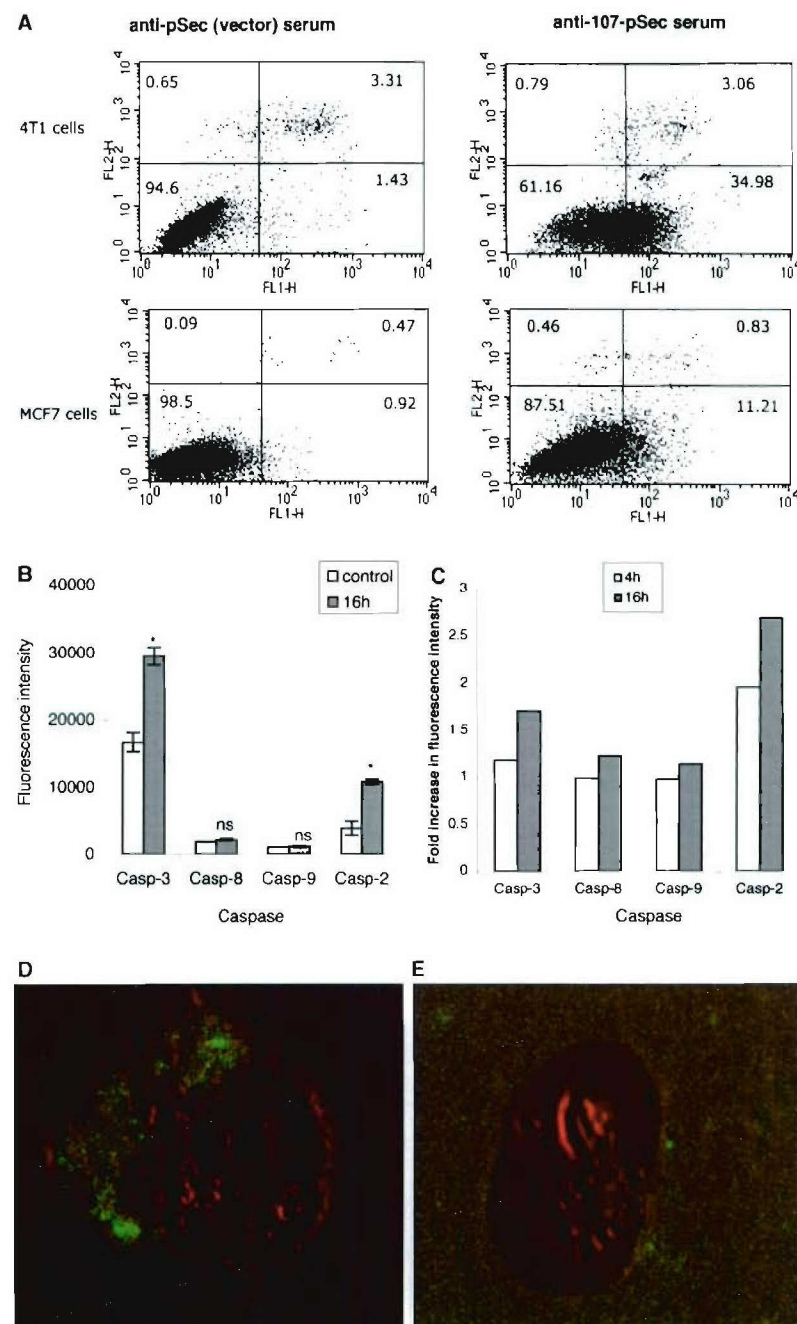
Table II. Oligonucleotide sequences used for cloning and making DNA constructs

Peptide	Oligonucleotide Sequences <sup>a</sup>
104	agcttGGCGGCATCATGATCCTGCTGATCTTCCTCGTGTGGTTGGGGCGCCATAA ggccgcTTAGGGCCCCGAACCAACAGCAGGGAGAAAGATCAGCAGGATCATGATGCC Ca
105	agcttGGCGGCATCTACTACCCCTACGACATCTACTACCCCTACGACATCTACTAC CCCTACGACTACGACTAACGACTAACGACTAACGACTAACGACTAACGACTAACG ggccgcTTAGTCGTAGGGTAGTAGATGTCGTAGGGTAGTAGATGTCGTAGGGTAG ATGTCGTAGGGTAGTAGATGTCGTAGGGTAGTAGATGTCGTAGGGTAGTAGATGCC Ca
107	agcttGGCGGCATCTACTACCGCTACGACATCTACTACCGCTACGACATCTACTAC CCGCTACGACTAACGACTAACGACTAACGACTAACGACTAACGACTAACGACTAACG ggccgcTTAGTCGTAGGGTAGTAGATGTCGTAGGGTAGTAGATGTCGTAGGGTAG TAGATGTCGTAGGGTAGTAGATGTCGTAGGGTAGTAGATGTCGTAGGGTAGTAGATGCC Ca

<sup>a</sup> Lowercase letters show sequence of the restriction sites used for cloning. Uppercase letters show the peptide-encoding sequences.

It is argued that the above-mentioned lectins trigger apoptosis via intracellular signaling following internalization (9, 14). To better understand the mechanism of apoptosis by serum, we investigated the possibility of internalization of serum Abs. Murine serum was mixed with FITC-conjugated anti-mouse IgM, and then the

mixture was added to cells, and fluorescence microscopy was used to visualize the binding pattern of murine IgM to cells. We observed that IgM Abs bound to the cell surface and that coincubation resulted in the appearance of IgM in small aggregates that were present in the interior of the cells due to internalization of the



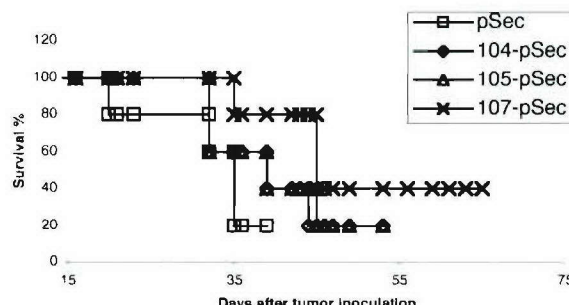


**FIGURE 4.** Immunization of tumor-bearing animals with DNA construct of the 107 peptide induced an increase in survival rate. Mice were inoculated with  $10^5$  cells s.c. in mammary ducts, and immunization was started 4 days later with 7-day intervals. The percentage of survival in immunized groups was estimated by the Kaplan-Meier method. Increase in the survival rate observed in 107-pSec-immunized mice is statistically significant at  $p = 0.021$  compared with pSec (vector)-immunized mice by log-rank test.

IgM Abs in endocytic vesicles (Fig. 3D). We did not detect internalization of anti-mouse IgM alone (Fig. 3E).

#### Therapeutic DNA immunization arrested liver metastasis

To assess whether vaccination with peptide 107 could arrest metastases, we established the 4T1 tumor in mammary fat pads and then started immunization with the plasmids containing the DNA sequences of 104, 105, and 107 mimotopes. Peptides 104 and 105 are carbohydrate mimics and induction of carbohydrate and cell-reactive functional serum Abs by immunization with these peptides has been shown in our previous works (23, 25, 26). Peptide 107 binds to both GS-I and WGA lectins, and the data suggest that this peptide may mimic multiple oligosaccharides involved in tumor cell apoptosis. To better evaluate peptide 107 as an antitumor apoptosis-mediated immunogen, we also included peptides 104 and 105 in the immunization regimen.

Immunization with 107-pSec plasmid induced slight tumor shrinkage in comparison to all other groups that was temporary (data not shown). However, 107-pSec immunization significantly ( $p < 0.021$ ) increased survival time of the tumor-bearing animals compared with immunization with vector (pSec) only (Fig. 4). At day 39, 80% of the 107-pSec-immunized mice were alive, whereas 80% of vector-immunized animals died, with the remaining 20% sacrificed at day 42 because of appearance of signs of morbidity based on the animal use protocol. At this same day point, 80% of 107-pSec-immunized mice were still alive. Although at day 56, no mice were alive in the 104-pSec- and 105-psec-immunized groups, 40% of the mice in the 107-pSec group were still alive in fair condition. These mice were later sacrificed at day 68 postinoculation due to a large tumor burden as required by the animal use protocol.

To further characterize the effects of immunization on metastases to distant organs, we repeated the challenge experiment as

**Table III.** Number of mice detected positive for distant organ metastasis of 12 total mice

Immunization	Organs	
	Lung	Liver
pSec (vector)	12	8
107-pSec	12	2*

\*.  $p = 0.018$  compared with vector immunized, by Fisher exact test.

above. Lung and liver samples were harvested, and the presence of metastatic cells was detected and quantified by clonogenic assay (Table III). The immunization regimen had no effect on lung metastases but had significant positive effects on reducing liver metastasis (Fisher exact test,  $p = 0.018$ ). Of 12 mice used for 107-pSec therapeutic DNA immunization, only 2 were found positive for tumor in the liver compared with 8 of 12 positive livers in pSec (vector)-immunized animals.

#### Prophylactic immunization with both DNA and the MAP peptide affected tumor growth and lung metastasis

Therapeutic immunization had no significant effect either on the size of primary tumor or on lung metastasis. To test whether earlier immunization and accumulation of Abs at the time of tumor challenge modified the outcome of immunization, in a follow-up study, mice were immunized before the challenge and after the challenge with either the peptide or DNA constructs. Mice were bled 7 days after the third prophylactic immunization and then challenged with 4T1 cells 3 days after blood collection. Serum was collected individually, and all sera were pooled for 10 mice in each group. Binding of pooled serum to 4T1 cells and its apoptotic activity was assayed (Table IV). As shown in Table IV, immunization with both peptide 107 and 107-pSec DNA vaccines generated serum Abs that bound to 4T1 cells and mediated their apoptosis. Peptide immunization generated Abs of higher end-point titer, which mediated a more pronounced apoptotic effect.

In both peptide and DNA-immunized animals, tumor grew significantly slower. All preimmunized mice developed tumor upon challenge; however, tumor growth was significantly slower in peptide 107-immunized animals (Fig. 5, A and B). In contrast to our therapeutic immunization regimen, in prophylactic immunization, we observed inhibition of primary tumor growth during the whole experiment. Examination of TUNEL-stained slides revealed significantly more apoptotic bodies per square millimeter in the primary tumors of immunized mice at 7 days post-tumor inoculation compared with control mice ( $p = 0.0072$ ; Fig. 5C).

To compare the effect of preimmunization on metastasis, we collected lungs at day 28 posttumor transplant from both DNA- and peptide-immunized mice and performed the clonogenic assay. In the peptide-immunized group (with 10 mice per group), 30% of 107-peptide-immunized animals were free of lung-associated tumor cells. In addition, comparison of the average of clonogenic lung metastases showed a significant reduction of lung metastatic cells in the 107-immunized group (Fig. 5D). In the DNA-immunized group, all mice tested had established lung metastasis; however, pSec-107-immunized mice had a smaller average of colonies than pSec-106 and pSec vector control (data not shown). Consistent with results from the clonogenic assay, metastatic lesions in the lungs from peptide 107-immunized group were significantly smaller than those from the naive group (Fig. 5, E and F).

#### Discussion

The presence of natural carbohydrate-reactive IgM Abs in humans capable of mediating apoptosis in tumor cells has been reported (1). In an effort to develop a strategy to induce sustained immunity targeting carbohydrate Ags on metastatic tumor cells, we have used lectins as a model template to further define and develop immunogens that elicit tumor-specific apoptosis triggering IgM Abs. GS-I consists of two isolectins, GS-I-B4 and GS-I-A4, with different carbohydrate specificity. GS-I-B4 is more specific for  $\alpha$ Gal, whereas the A4 isolectin has higher specificity toward  $\alpha$ GalNAc-containing ligands (27, 28). GS-I also binds to the neolacto-series Ags Lewis Y and Lewis b (our unpublished observation). WGA binds to both GlcNAc and sialic acid (29). Therefore, to

Table IV. Characterization of serum after DNA and peptide immunization

Test Description	Peptide Immunization			DNA Immunization			
	Naive	106	107	pSec (vector)	106-pSec	107-pSec	GS-1
End-point titer <sup>a</sup>		1:1280	1:2560		1:160	1:160	
Annexin binding <sup>b</sup>	184 ( $\pm$ 39)	228 ( $\pm$ 53) <sup>NS</sup>	436 ( $\pm$ 64) <sup>**</sup>	171.5 ( $\pm$ 43)	244.5 ( $\pm$ 32) <sup>NS</sup>	324 ( $\pm$ 36)*	902 ( $\pm$ 89) <sup>***</sup>
PI binding <sup>b</sup>	32 ( $\pm$ 3.8)	29.8 ( $\pm$ 1.2) <sup>NS</sup>	32 ( $\pm$ 2.9) <sup>NS</sup>	40.33 ( $\pm$ 3.2)	38.58 ( $\pm$ 4.1) <sup>NS</sup>	52.29 ( $\pm$ 4.5)*	111 ( $\pm$ 21)**

<sup>a</sup> Binding of IgM Abs to 4T1 cells was tested. Titer was determined based on mean fluorescence intensity of flow cytometry assay. The highest serum dilution with higher mean fluorescence intensity than the preimmune serum is shown as the end-point titer.

<sup>b</sup> Mean fluorescence intensity for annexin V and PI ( $\pm$ SD) is shown.

\* $p < 0.05$ ; \*\* $p < 0.025$ ; \*\*\* $p < 0.005$ ; NS, not significant compared with naive serum or pSec (vector) serum as negative controls. GS-1 was compared with either negative control.

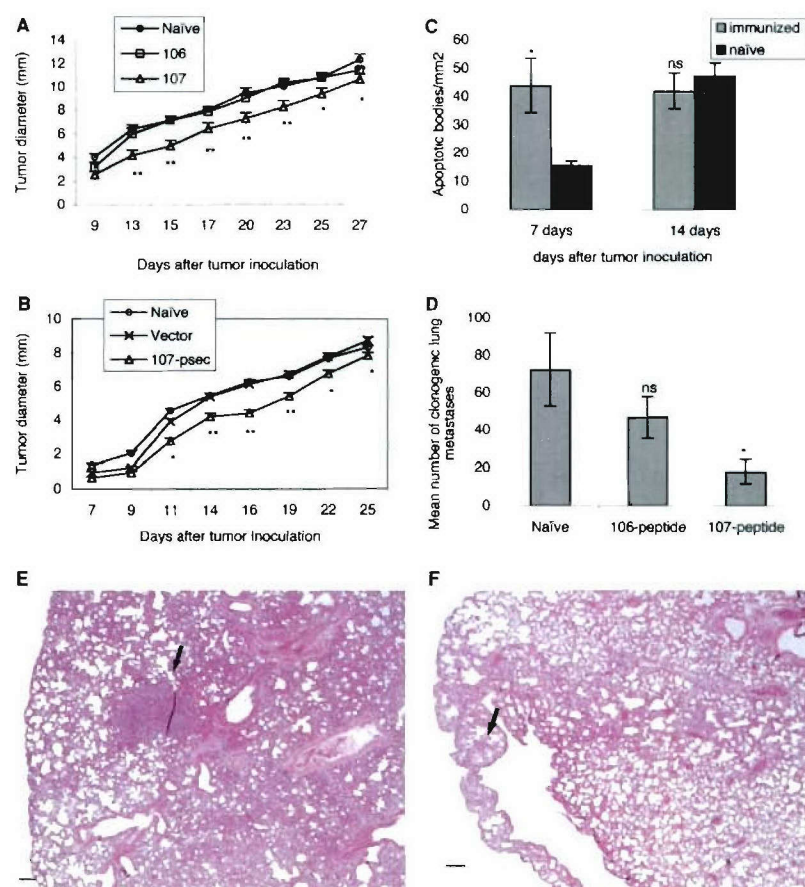
broaden the application, we decided to select for a peptide that could potentially mimic the various tumor-associated carbohydrate structures.

The 107-peptide was identified and selected based on its reactivity with both GS-I and WGA with an expectation that, upon immunization, serum Abs cross-reactive with multiple carbohydrate structures would be induced. The peptides 104, 106, 107, and 109 all bind to an anti-Lewis Y Ab (23, 25, 26) and induce serum Abs cross-reactive with Lewis Y-expressing breast cancer cells, which mediated tumor cell killing by a CDC mechanism (5). We have shown before that mimotopes of core structures of tumor-associated carbohydrate Ags are particularly advantageous to augment the cross-reactive carbohydrate immune response because they can function as priming agents to expand B cells to multiple carbohydrate Ags upon boosting with nominal Ag (30). Such peptides are considered as multiple Ag mimotopes and would simplify the vaccine strategy by obviating the need to develop multivalent immunogens based upon each individual immunogen.

Administration of the peptide and its genetic form (107-pSec construct) as vaccine induced serum IgM Abs that bound to cells and mediated apoptosis of both 4T1 and MCF7 cells, with a more pronounced effect on the murine cell line. This is not surprising in that MCF7 cells are not uniform in expressing full-length caspase 3 and display diminished susceptibility to apoptotic stimuli (31). Because the GS-I-reactive Gal epitope is not expressed on human cells, the observation that the serum Abs can trigger apoptosis of MCF7 cells suggests that  $\alpha$ GalNAc, GlcNAc, sialic acid moieties, and perhaps the Lewis Y Ag may be expressed on glycoproteins associated with signaling functions, and reactivity with these glycoproteins may mediate the internalization of the serum Abs.

Internalized serum IgM suggests that the mode of action of the induced Abs might be similar to the lectins. Like the lectins, specific binding to the cell surface oligosaccharides should be the prerequisite for the Ab-mediated cell killing. Internalized Abs can trigger a wide spectrum of intracellular signals that might contribute to apoptosis. For example, the serum Abs can induce their

**FIGURE 5.** Immunization with the peptide 107 inhibited tumor growth and reduced lung metastases. Mice (10 per group) were immunized with peptide (A) or DNA constructs (B) weekly for 3 wk and then inoculated with tumor at day 10 after the third immunization. Immunization was resumed at day 7 posttransplant and continued every week for 3 more weeks. Tumor size was measured during this period of time and are illustrated as the mean values  $\pm$  SD. \*,  $p < 0.025$ ; \*\*,  $p < 0.01$ , compared with 106 (A) or vector (B) immunization. C, Mice from peptide-immunized groups were sacrificed weekly, lungs and primary tumors were harvested, sections were prepared, and TUNEL staining was performed as described in Materials and Methods. Apoptotic bodies were counted in five randomly chosen microscopic fields in sections of primary tumors, and averages per square millimeter are shown. \*,  $p = 0.0072$ ; ns, not significant compared with naive tumor-bearing animals. D, Peptide-immunized mice were sacrificed at day 28, lungs were collected, and clonogenic assay was performed. The number of clonogenic cells was determined and illustrated as the mean values of 10 mice per group  $\pm$  SD. \*,  $p = 0.009$ ; ns, not significant compared with the naive mice. E and F, Groups of mice were left unimmunized (E) or were immunized as explained above (F) and then inoculated with the 4T1 tumor. Mice from each group were sacrificed weekly, lungs were harvested, sections were prepared, and H&E staining was performed on prepared slides. Slides prepared from mice sacrificed 21 days postinoculation are shown. Bars, 50  $\mu$ m.



effect via mitochondria activation as it has been proposed for the lectins (14). Internalized carbohydrate-reactive IgM via its interaction with rafts may lead to modulation of cellular ceramide, which results in the induction of apoptosis (32). Such mechanisms are currently under study. The caspase activation results further suggest a similarity between apoptosis mediated by the lectins and the serum Abs, because both predominantly mediated activation of caspases 2 and 3 in 4T1 cells.

We propose that immunization with peptide 107 generates serum Abs that bind to a subpopulation of cells that express the target lectin-defined carbohydrate epitopes on the 4T1 surface. Serum Ab binding is followed by internalization of the Abs, and apoptosis and lysis of cells, which appears as a temporary tumor regression because we observed only a marginal effect on the size of the tumor at the primary site of inoculation (data not shown). Ags released from lysed cells may still initiate an immune response, which inhibits further metastatic growth and a statistical increase in survival rate. Segregated analysis of the effects of therapy on metastasis to distant organs highlighted a definite influence on metastatic tumor in the liver. But why does the immunization affect only liver metastasis? Staining of tissues with lectins clearly showed that there are lectin-positive cells also in the lung and the solid tumor (data not shown). We postulate that by the time an effective level of the IgM titer is reached, tumor burden in the lung and at the site of primary inoculation exceeds a treatable limit. This is akin to studies in which treatment of cells with carbohydrate-reactive Ab are effective only a few days after tumor challenge (16). Likewise, vaccination efficacy has been implicated to be dependent on the size of tumor (7, 16, 19).

To account for timing, appearance, and the strength of the Ab response, and its influence on the outcome of the vaccination strategy, we immunized naive mice, and then challenged them with the tumor and continued the immunization. DNA immunization significantly slowed the growth of the solid tumor especially at the earlier stages. The *in situ* apoptosis assay revealed an increase in apoptosis of tumor cells from immunized mice at 7 days post-tumor transplant compared with controls. Peptide immunization produced a stronger Ab response, which strikingly blocked initiation of the lung metastasis in 30% of animals tested, with the number of lung metastasis also significantly reduced. This is a significant achievement because curing this tumor is difficult. Others showed that even prophylactic immunization in a cell-based vaccine targeting 4T1 cells with MHC and B7.1 transfectants, although effectively reducing lung metastasis, neither affected the growth of the primary tumor nor blocked lung metastasis (19, 33). IL-12 therapy proved to be an effective strategy in reducing the number of 4T1 lung metastases. However, it failed to affect primary tumor growth or afford protection against the initiation of tumor growth in the lung (34).

In patients with advanced stages of breast cancer, antitumor immune responses may still be present, and appropriate stimulation of immunity may have beneficial effects in immune augmentation leading to at least an increase of survival rate. Although the immunotherapy proposed here is not curative for aggressive tumors at advanced stages, it may postpone the progression of metastatic disease. It is generally recognized that treatment with mAbs or vaccines inducing Abs must be restricted to the adjuvant setting, where the targets are circulating tumor cells and micrometastases (16). Therefore, induction of apoptotic IgM Abs might be targeted as an endpoint in the development of vaccination strategies against cancer especially in the adjuvant setting for metastatic disease. Our findings point to the fact that cell apoptosis can be specifically targeted through a cross-reactive immune response to a surrogate

Ag, which has implications for the design of novel approaches for cancer vaccines.

## Acknowledgments

We thank Charlotte Read Kensil of Antigenics, Inc., for the QS-21

## Disclosures

The authors have no financial conflict of interest.

## References

- Brandlein, S., T. Pohle, N. Ruoff, E. Wozniak, H. K. Muller-Hermelink, and H. P. Vollmers. 2003. Natural IgM antibodies and immunosurveillance mechanisms against epithelial cancer cells in humans. *Cancer Res.* 63: 7995–8005.
- Lin, C. C., Y. C. Shen, C. K. Chuang, and S. K. Liao. 2001. Analysis of a murine anti-ganglioside GD2 monoclonal antibody expressing both IgG2a and IgG3 isotypes: monoclonality, apoptosis triggering, and activation of cellular cytotoxicity on human melanoma cells. *Adv. Exp. Med. Biol.* 491: 419–429.
- Yoshida, S., S. Fukumoto, H. Kawaguchi, S. Sato, R. Ueda, and K. Furukawa. 2001. Ganglioside G<sub>D2</sub> in small cell lung cancer cell lines: enhancement of cell proliferation and mediation of apoptosis. *Cancer Res.* 61: 4244–4252.
- Ravindranath, N. M., K. Nishimoto, K. Chu, and C. Shuler. 2000. Cell-surface expression of complement restriction factors and sialyl Lewis antigens in oral carcinoma: relevance to chemo-immunotherapy. *Anticancer Res.* 20: 21–26.
- Kieber-Emmons, T., P. Luo, J.-P. Qiu, T. Y. Chang, I. O. M. Blaszczyk-Thurin, and Z. Steplewski. 1999. Vaccination with carbohydrate peptide mimotopes promotes anti-tumor responses. *Nature Biotechnol.* 17: 660–665.
- Kieber-Emmons, T., B. Monzavi-Karbassi, B. Wang, P. Luo, and D. B. Weiner. 2000. Cutting edge: DNA immunization with minigenes of carbohydrate mimotopes induce functional anti-carbohydrate antibody response. *J. Immunol.* 165: 623–627.
- Monzavi-Karbassi, B., P. Luo, F. Jousheghany, M. Torres-Quinones, G. Cunto-Amesty, C. Artaud, and T. Kieber-Emmons. 2004. A mimic of tumor rejection antigen-associated carbohydrates mediates an antitumor cellular response. *Cancer Res.* 64: 2162–2166.
- Monzavi-Karbassi, B., S. Shamloo, M. Kieber-Emmons, F. Jousheghany, P. Luo, K. Y. Lin, G. Cunto-Amesty, D. B. Weiner, and T. Kieber-Emmons. 2003. Priming characteristics of peptide mimotopes of carbohydrate antigens. *Vaccine* 21: 753–760.
- Kim, M., M. V. Rao, D. J. Twardy, M. Prakash, U. Galili, and E. Gorelik. 1993. Lectin-induced apoptosis of tumour cells. *Glycobiology* 3: 447–453.
- Chen, Y. F., C. R. Boland, E. R. Kraus, and I. J. Goldstein. 1994. The lectin *Griffonia simplicifolia* I-A4 (GS I-A4) specifically recognizes terminal α-linked N-acetylgalactosaminyl groups and is cytotoxic to the human colon cancer cell lines LS174t and SW1116. *Int. J. Cancer* 57: 561–567.
- Schwarz, R. E., D. C. Wojciechowicz, A. I. Picon, M. A. Schwarz, and P. B. Paty. 1999. Wheatgerm agglutinin-mediated toxicity in pancreatic cancer cells. *Br. J. Cancer* 80: 1754–1762.
- Gorelik, E., U. Galili, and A. Raz. 2001. On the role of cell surface carbohydrates and their binding proteins (lectins) in tumor metastasis. *Cancer Metastasis Rev.* 20: 245–277.
- Valentiner, U., S. Fabian, U. Schumacher, and A. J. Leathem. 2003. The influence of dietary lectins on the cell proliferation of human breast cancer cell lines *in vitro*. *Anticancer Res.* 23: 1197–1206.
- Gastman, B., K. Wang, J. Han, Z. Y. Zhu, X. Huang, G. Q. Wang, H. Rabinowich, and E. Gorelik. 2004. A novel apoptotic pathway as defined by lectin cellular initiation. *Biochem. Biophys. Res. Commun.* 316: 263–271.
- Monzavi-Karbassi, B., G. Cunto-Amesty, P. Luo, and T. Kieber-Emmons. 2002. Peptide mimotopes as surrogate antigens of carbohydrates in vaccine discovery. *Trends Biotechnol.* 20: 207–214.
- Zhang, H., S. Zhang, N. K. Cheung, G. Ragupathi, and P. O. Livingston. 1998. Antibodies against GD2 ganglioside can eradicate syngeneic cancer micrometastases. *Cancer Res.* 58: 2844–2849.
- Knutson, K. L., M. R. Bishop, K. Schiffman, and M. L. Disis. 2002. Immunotherapy for breast cancer. *Cancer Chemother. Biol. Response Modif.* 20: 351–369.
- Chiriva-Internati, M., J. Du, M. Cannon, B. Barlogie, and Q. Yi. 2001. Myeloma-reactive allospecific cytotoxic T lymphocytes lyse target cells via the granule exocytosis pathway. *Br. J. Haematol.* 112: 410–420.
- Pulaski, B. A., and S. Ostrand-Rosenberg. 1998. Reduction of established spontaneous mammary carcinoma metastases following immunotherapy with major histocompatibility complex class II and B7.1 cell-based tumor vaccines. *Cancer Res.* 58: 1486–1493.
- Pulaski, B. A., and S. Ostrand-Rosenberg. 2000. Mouse 4T1 breast tumor model. In *Current Protocols in Immunology*, Vol. 3. J. E. Coligan, A. M. Kruisbeek, D. H. Margulies, E. Shevach, and W. Strober, eds. Wiley, New York, pp. 20.2.1–20.2.11.
- Aslakson, C. J., and F. R. Miller. 1992. Selective events in the metastatic process defined by analysis of the sequential dissemination of subpopulations of a mouse mammary tumor. *Cancer Res.* 52: 1399–1405.
- Monzavi-Karbassi, B., G. Cunto-Amesty, P. Luo, A. Lees, and T. Kieber-Emmons. 2001. Immunological characterization of peptide mimetics of carbohydrate antigens in vaccine design strategies. *Biologicals* 29: 249–257.
- Qiu, J., P. Luo, K. Wasmund, Z. Steplewski, and T. Kieber-Emmons. 1999. Towards the development of peptide mimotopes of carbohydrate antigens as cancer vaccines. *Hybridoma* 18: 103–112.

24. Prinz, D. M., S. L. Smithson, T. Kieber-Emmons, and M. A. Westerink. 2003. Induction of a protective capsular polysaccharide antibody response to a multipeptide DNA vaccine encoding a peptide mimic of meningococcal serogroup C capsular polysaccharide. *Immunology* 110: 242–249.

25. Luo, P., M. Agadjanyan, J. Qiu, M. Westerink, Z. Steplewski, and T. Kieber-Emmons. 1998. Antigenic and immunological mimicry of peptide mimotopes of Lewis carbohydrate antigens. *Mol. Immunol.* 35: 865–879.

26. Luo, P., G. Canziani, G. Cunto-Amesty, and T. Kieber-Emmons. 2000. A molecular basis for functional peptide mimicry of a carbohydrate antigen. *J. Biol. Chem.* 275: 16146–16154.

27. Wu, A. M., S. C. Song, J. H. Wu, and E. A. Kabat. 1995. Affinity of *Bandeiraea (Griffonia) simplicifolia* lectin-I, isolectin B4 for Gal $\alpha$ 1 $\rightarrow$ 4Gal ligand. *Biochem. Biophys. Res. Commun.* 216: 814–820.

28. Wu, A. M., J. H. Wu, S. C. Song, and E. A. Kabat. 1996. *Bandeiraea (Griffonia) simplicifolia* lectin-I, isolectin A4, reacting with Tn (GalNAc $\alpha$ 1 $\rightarrow$ Ser/Thr) or galabiose (Gal $\alpha$ 1 $\rightarrow$ 4Gal) containing ligands. *FEBS Lett.* 398: 183–186.

29. Gallagher, J. T., A. Morris, and T. M. Dexter. 1985. Identification of two binding sites for wheat-germ agglutinin on polylactosamine-type oligosaccharides. *Biochem. J.* 231: 115–122.

30. Cunto-Amesty, G., B. Monzavi-Karbassi, P. Luo, F. Jousheghany, and T. Kieber-Emmons. 2003. Strategies in cancer vaccines development. *Int. J. Parasitol.* 33: 597–613.

31. Chen, J. S., M. Konopleva, M. Andreeff, A. S. Multani, S. Pathak, and K. Mehta. 2004. Drug-resistant breast carcinoma (MCF-7) cells are paradoxically sensitive to apoptosis. *J. Cell. Physiol.* 200: 223–234.

32. Grazide, S., A. D. Terrisse, S. Lerouge, G. Laurent, and J. P. Jaffrezou. 2004. Cytoprotective effect of glucosylceramide synthase inhibition against daunorubicin-induced apoptosis in human leukemic cell lines. *J. Biol. Chem.* 279: 18256–18261.

33. Pulaski, B. A., V. K. Clements, M. R. Pipeling, and S. Ostrand-Rosenberg. 2000. Immunotherapy with vaccines combining MHC class II/CD80 $^+$  tumor cells with interleukin-12 reduces established metastatic disease and stimulates immune effectors and monokine induced by interferon- $\gamma$ . *Cancer Immunol. Immunother.* 49: 34–45.

34. Rakhimilevich, A. L., K. Janssen, Z. Hao, P. M. Sondel, and N. S. Yang. 2000. Interleukin-12 gene therapy of a weakly immunogenic mouse mammary carcinoma results in reduction of spontaneous lung metastases via a T-cell-independent mechanism. *Cancer Gene Ther.* 7: 826–838.

*Int. J. Cancer.* **117**, 398–408 (2005)  
© 2005 Wiley-Liss, Inc.

## Deficiency in surface expression of E-selectin ligand promotes lung colonization in a mouse model of breast cancer

Behjatolah Monzavi-Karbassi<sup>1</sup>, Tracy L. Whitehead<sup>1</sup>, Fariba Jousheghany<sup>1</sup>, Cecile Artaud<sup>1</sup>, Leah Hennings<sup>1</sup>, Saeid Shaaf<sup>1</sup>, Aubrey Slaughter<sup>1</sup>, Soheila Korourian<sup>1</sup>, Thomas Kelly<sup>1</sup>, Magdalena Blaszczyk-Thurin<sup>2</sup> and Thomas Kieber-Emmons<sup>1\*</sup>

<sup>1</sup>Arkansas Cancer Research Center and Department of Pathology, University of Arkansas for Medical Sciences, Little Rock, AR, USA

<sup>2</sup>Cancer Diagnosis Program, Division of Cancer Treatment & Diagnosis, National Cancer Institute, National Institutes of Health, Rockville, MD, USA

Expression of sialyl Lewis<sup>x</sup> (sLe<sup>x</sup>) and sLe<sup>a</sup> on tumor cells is thought to facilitate metastasis by promoting cell adhesion to selectins on vascular endothelial cells. Experiments supporting this concept usually bypass the early steps of the metastatic process by employing tumor cells that are injected directly into the blood. We investigated the relative role of sLe<sup>x</sup> oligosaccharide in the dissemination of breast carcinoma, employing a spontaneous murine metastasis model. An sLe<sup>x</sup>-deficient subpopulation of the 4T1 mammary carcinoma cell line was produced by negative selection using the sLe<sup>x</sup>-reactive KM93 MAb. This subpopulation was negative for E-selectin binding but retained P-selectin binding. Both sLe<sup>x</sup>-negative and -positive cells grew at the same rate; however, sLe<sup>x</sup>-negative cells spread more efficiently on plates and had greater motility in wound-scratch assays. Mice inoculated in the mammary fat pad with sLe<sup>x</sup>-negative and -positive variants produced lung metastases. However, the number of lung metastases was significantly increased in the group inoculated with the sLe<sup>x</sup>-negative variant ( $p = 0.0031$ ), indicating that negative selection for the sLe<sup>x</sup> epitope resulted in enrichment for a subpopulation of cells with a high metastatic phenotype. Cell variants demonstrated significant differences in cellular morphology and pattern of tumor growth in primary and secondary tumor sites. These results strongly suggest that loss of sLe<sup>x</sup> may facilitate the metastatic process by contributing to escape from the primary tumor mass.

© 2005 Wiley-Liss, Inc.

**Key words:** sialyl Lewis<sup>x</sup> antigen; metastasis; 4T1 cells; breast cancer

Tumor metastasis is a multistep process requiring detachment of malignant cells from the primary tumor, penetration of blood or lymph vessels, attachment to endothelium of distant organs and formation of new tumor foci.<sup>1,2</sup> Tissue invasion and metastasis of tumor cells are highly dependent on cell–cell interactions, many of which involve alterations in cell surface glycosylation patterns.<sup>3,4</sup> Although adhesion pathways utilized by tumor cells show considerable diversity, members of the selectin family of molecules and numerous neolactoseries antigens highly expressed on the tumor cell surface are involved in tumor metastasis by mediating binding of blood-borne tumor cells via E- and/or P-selectin to vascular endothelium.<sup>5–10</sup>

Much of what we know about selectin interactions comes from studies of leukocytes.<sup>11,12</sup> Functionally, the binding of selectins to leukocytes requires sialylated and fucosylated carbohydrate structures; their prototypes are SAα2–3Galβ1–4(Fucα1–3)GlcNAc and SAα2–3Galβ1–3(Fucα1–4)GlcNAc, referred to as sLe<sup>x</sup> and sLe<sup>a</sup>, respectively.<sup>13–15</sup> Both sLe<sup>x</sup> and sLe<sup>a</sup> are involved in selectin-mediated adhesion of cancer cells to vascular endothelium, and these determinants are thought to be closely associated with hematogenous metastasis of cancers.<sup>16–19</sup> These determinants not only are markers for cancer but also are functionally implicated in the malignant behavior of cancer cells.

Our understanding of the role of carbohydrate ligands for selectins on non-blood-borne “epithelial cell-like” cancer cells is still limited. Selectins are thought to function at a relatively late step in the metastatic cascade.<sup>16</sup> Determination of the mechanistic roles of selectin ligands in mediating tumor cell dissemination and organ colonization has relied almost exclusively on assessing metastasis by injecting tumor cells with altered expression of E- and P-selectin ligands directly into the bloodstream of experimen-

tal animals. Experimental metastasis models such as these exclude the early steps of the metastatic cascade that might be impacted by expression of selectin ligands. In this regard, Alpaugh *et al.*<sup>20</sup> showed in a human-SCID model of inflammatory breast carcinoma, which is a nonsyngeneic passive model, that the lack of sLe<sup>x/a</sup> promotes passive metastasis. It would be advantageous to use a syngeneic model in which tumor cells are injected into the orthotopic site and tumor cell dissemination and distant organ colonization are then assessed because in such a model tumor cells will be forced to complete all or most of the steps needed for metastasis that are completed by cells originating in the primary tumor. Moreover, such a model more closely mimics the situation in human patients, where metastases are thought to arise after seeding of distant organs with cells that originated in the organ hosting the primary tumor.

Here, we employed a syngeneic murine mammary tumor model with spontaneous metastatic behavior to examine how an important adhesion molecule with demonstrated roles in tumor dissemination can influence the metastasis process. The murine mammary carcinoma 4T1 is a highly metastatic cell line and has been used extensively as an animal model for spontaneous metastasis of advanced human breast cancer.<sup>21–23</sup> Using an sLe<sup>x</sup>-reactive MAb purported to bind to epitopes associated with E-selectin,<sup>24–26</sup> we employed negative selection by flow cytometry to generate 4T1 cells deficient in expression of the sLe<sup>x</sup> antigen, an approach that we believe better mimics the biologic route for enrichment of subpopulations. Our findings demonstrate that a marked decrease in surface sLe<sup>x</sup> expression and a subsequent reduction in E-selectin binding are associated with a morphologic phenotype showing enhanced lung-colonizing potential. Our studies emphasize the relative importance of sLe<sup>x</sup> in affecting the adhesion properties of tumor cells in primary and metastatic sites. By virtue of the cell line lacking E-selectin ligands, our studies also suggest that spontaneous lung metastasis by these breast cancer cells does not rely on E-selectin, in contrast to observations using murine melanoma cells injected directly into the blood.<sup>17,18,27</sup>

**Abbreviations:** ABL, *Agaricus bisporus* lectin; ACA, *Amaranthus caudatus* lectin; BNF, buffered neutral formalin; DAB, 3,3'-diaminobenzidine; DPBS, Dulbecco's PBS; ECL, *Erythrina cristaagali* lectin; GFP, green fluorescence protein; GS-I, *Griffonia simplicifolia*; H&E, hematoxylin and eosin; HUVEC, human umbilical vein endothelial cell; MAb, monoclonal antibody; NMR, nuclear magnetic resonance; OCT, optimal cutting temperature; PE, phycoerythrin; PHA, *Phaseolus vulgaris* agglutinin; PNA, *Arachis hypogaea* peanut agglutinin; SCID, severe combined immunodeficiency; RT, room temperature; sLe<sup>x</sup>, sialyl Lewis<sup>x</sup>; SNA, *Sambucus nigra* agglutinin; SWGA, succinylated WGA; TF, Thomsen-Friedreich; UEA-I, *Ulex europaeus* lectin; VVA, *Viscum album* agglutinin; WGA, wheat germ agglutinin.

Grant sponsor: U.S. Department of Defense; Grant number: DAMD17-01-0366; Grant sponsor: National Institutes of Health; Grant number: CA089480; Grant sponsor: ACS-IRG; Grant number: 271/G1-11262-01E.

\*Correspondence to: Arkansas Cancer Research Center, University of Arkansas for Medical Sciences, 4301 West Markham St., Slot #824, Little Rock, AR 72205, USA. Fax: +501-526-5934. E-mail: tke@uams.edu

Received 8 November 2004; Accepted after revision 16 March 2005

DOI 10.1002/ijc.21192

Published online 19 May 2005 in Wiley InterScience (www.interscience.wiley.com).

## Material and methods

### Cells and reagents

Murine 4T1 cells were purchased from the ATCC (Manassas, VA). The KM93 and CSLEX1 antibodies were purchased from Kamiya Biomedical (Seattle, WA) and BD Pharmingen (San Diego, CA), respectively. Anti-sLe<sup>x</sup> (BRA-4F1) and anti-sLe<sup>a</sup> (CA19-9) antibodies were purchased from Glycotech (Gaithersburg, MD). Lectins used in carbohydrate profiling were purchased from Vector (Burlingame, CA). Recombinant mouse E- and P-selectin/Fc (human IgG) chimera were purchased from R&D Systems (Minneapolis, MN) and used at 10 µg/ml in FACS assays. Conjugated secondary antibodies and streptavidin were purchased from Sigma (St. Louis, MO).

### Mice, tumor inoculation and metastasis assays

BALB/c female mice (6–8 weeks old) were purchased from the Jackson Laboratory (Bar Harbor, ME). NCR-nu/nu mice (4–6 weeks old, female) were obtained from Taconic Farms (Germantown, NY). To establish tumors, each mouse (10–12 mice/group) was inoculated s.c. in the abdominal mammary gland with 10<sup>4</sup> 4T1 cells. The 4T1 cell line was selected without mutagenesis for its resistance to 6-thioguanine.<sup>28</sup> The 4T1 tumor is highly tumorigenic and invasive; unlike most tumor models, it can spontaneously metastasize from the primary tumor in the mammary gland to multiple distant sites.<sup>22,28,29</sup> Lung metastatic cells in this model are detectable as soon as 14 days after transplant; however, at this stage, variability is high and, due to the low number of metastatic cells, serial dilution of a cell preparation is impossible. Culturing of serially diluted cells is very important in generating statistically meaningful data. Therefore, we waited 26 days to make certain that all mice had established lung metastases, which could be quantified by titration. With this timing, we had a tumor size of 8–10 mm with minimal signs of morbidity or stress in animals. Spontaneous metastases were measured by the methods described by Pulaski and Ostrand-Rosenberg<sup>22,29</sup> as clonogenic assays. Briefly, 26 days after tumor inoculation mice were killed and the lungs harvested. Lungs were washed in HBSS and finely minced. Minced samples were digested in 5 ml of enzyme cocktail containing PBS, 1 mg/ml collagenase type 4 and 6 units/ml elastase for 75 min at 4°C on a rotator. After incubation, samples were filtered through 70 µm nylon cell strainers and washed 3 times by HBSS. Following this, the number of clonogenic cells was determined by growing serially diluted cells in medium containing 6-thioguanine.<sup>28</sup> 6-Thioguanine kills all the normal mouse lung cells, and only tumor cells are able to establish colonies. Resistance to 6-thioguanine was stable, and cell sorting did not have any effect on this property.

### Flow cytometry and cell sorting

One- or 2-color flow cytometry was performed. Staining, acquisition and analysis were performed as described in a previous study.<sup>30</sup> In brief, cells were harvested using trypsin-free cell dissociation buffer (Invitrogen-GIBCO, Carlsbad, CA); resuspended in buffer containing DPBS, 1% BSA and 0.1% sodium azide (FACS buffer); and then incubated with biotinylated lectins or MAbs (10 µg/ml) for 30 min on ice. Following this, cells were stained with FITC- or PE-conjugated streptavidin (2 µg/ml) or antimouse IgM or IgG (Sigma) for an additional 30 min on ice. For cell sorting, sodium azide was removed from the buffer. Parental 4T1 cells were harvested as above, washed in sodium azide-free FACS buffer and coincubated with Km93 antibody (10 µg/ml in 10<sup>6</sup> cells). Antibody binding was visualized by antimouse IgM-FITC. Ten percent of the most reactive positive cells and 10% of the least reactive negative cells (2 extremes) were sorted out, and the procedure was repeated 3 more times. For visualization of E- and P-selectin, antimouse IgG-FITC (Sigma) was used as secondary antibody. Negative controls were set using either biotin-conjugated streptavidin or mouse IgG/IgM as primary antibody.

### Proliferation assay

*In vitro* proliferation assay of sLe<sup>x</sup>-positive and -negative cells was performed using Celltiter 96 Aqueous One Solution (Promega, Madison, WI) according to the manufacturer's instructions. Briefly, 5 × 10<sup>3</sup> cells were cultured in wells of 96-well plates, and every 24 hr the provided solution was added to each plate containing replicated wells for each cell variant and negative controls (only medium). Plates were incubated for 1 hr at 37°C and read by an ELISA reader at 490 nm. Cell cultures were closely monitored and maintained. The assay was performed every day until day 5 after seeding, when cells reached confluence.

### Histopathologic evaluation

Primary tumors from mice inoculated with sLe<sup>x</sup>-negative and -positive variants were harvested 15 days after inoculation, bisected, placed in 10% BNF and embedded in paraffin for histologic evaluation. Serial, 5 µm sections were mounted on glass slides. Every fifth section was stained with H&E and examined under a light microscope. For histochemical evaluation of E-selectin ligand expression, lungs were harvested from mice inoculated with sLe<sup>x</sup>-positive and -negative variants at 21 and 28 days postinoculation, placed in OCT compound (Ted Pella, Redding, CA) and frozen in liquid nitrogen. Frozen lung sections (5 µm) were fixed for 10 min in cold acetone, then washed with cold DPBS (Cellgro Mediatech, Herndon, VA). Endogenous peroxidase was blocked by immersion in 0.3% (w/v) hydrogen peroxide in absolute methanol for 15 min, followed by DPBS wash. Nonspecific binding was blocked by incubating with DPBS+1% BSA at RT for 20 min. Sections were then incubated with 30 µg/ml of anti-sLe<sup>x</sup> antibody (Kamiya Biomedical) or recombinant mouse E-selectin/human FC chimera (R&D Systems) for 30 min in DPBS+0.2% BSA at RT and washed in DPBS. Sections were incubated with antimouse IgM-peroxidase (1/150 dilution) or an antihuman IgG (Fc specific) peroxidase conjugate (1/300 dilution) for 15 min at RT, followed by DPBS wash. Sections were incubated with DAB solution for 5 min at RT, washed with distilled water, counterstained with methyl green, mounted and examined under a light microscope. Normal bronchial epithelium provided an internal positive control for sLe<sup>x</sup> expression. Primary antibody was omitted in negative controls to rule out nonspecific binding of the secondary antibody. Experimental conditions including concentration, dilution, washing and blocking were chosen based on preliminary experiments on lung tissue from several tumor-bearing and non-tumor-bearing animals. The best setting gave us no nonspecific staining when applied to tissues of naive mice.

### Lung *in situ* fluorescent microscopy

Tumor cells were transfected with an EGFP plasmid (pEGFP-1 from BD Biosciences/Clontech, Palo Alto, CA) to express GFP. After 3 rounds of sorting for the highest 5% GFP-expressing cells and cloning, green cells were sorted again with KM93 antibody in a 2-color FACS with PE-conjugated antimouse IgM as secondary antibody, as explained above to produce GFP-expressing sLe<sup>x</sup>-positive and -negative variants. NCR-nu/nu mice were then inoculated in the mammary fat pad with GFP-expressing sLe<sup>x</sup>-negative and -positive cells. Four weeks after transplant, mice were killed. The heart and lungs were exposed immediately, and the abdominal aorta was transected to allow drainage of blood. The needle tip of a 23 g butterfly catheter was placed into the right ventricle of the heart, and 30 µl of Dil-conjugated, acetylated low density lipoproteins (LDL) (Molecular Probes, Eugene, OR) in 10 ml of Krebs-Ringer bicarbonate solution were injected into the right ventricle over a period of 3–5 min to label pulmonary vascular endothelium. The heart and lungs were removed, the heart was trimmed from the lungs and the lungs were entirely scanned with an inverted confocal microscope (LSM 410; Zeiss, Thornwood, NY) to a tissue depth of approximately 70 µm. The tissue was screened thoroughly, and representative images were captured. Images were

TABLE I – MEAN FLUORESCENCE INTENSITIES OF LECTINS AND MAB REACTIVITY WITH CELL POPULATIONS BY FLOW CYTOMETRY

Lectin/MAbs	Specificity	Cell variant		
		4T1	sLe <sup>x</sup> -negative	sLe <sup>x</sup> -positive
Streptavidin <sup>1</sup>	Negative control for lectin staining	6.9 ( $\pm 3$ )	7.9 ( $\pm 4$ )	7.1 ( $\pm 3.9$ )
ABL	Galβ1,3GalNAc (TF) and NeuAcα2,3Galβ1,3GalNAc (sialylated TF)	5.2 ( $\pm 2.4$ ) <sup>2</sup>	5.7 ( $\pm 2.09$ )	5.6 ( $\pm 2.3$ )
ACA	TF, sialylated TF	8.8 ( $\pm 1.11$ )	8 ( $\pm 1.78$ )	7 ( $\pm 1.41$ )
SNA	NeuAcα2→6Gal/GalNAc	23.28 ( $\pm 5.45$ )	17.93 ( $\pm 2.8$ )	16.82 ( $\pm 2.22$ )
ECL	Galβ1→4GlcNAc	29.33 ( $\pm 2.36$ )	15.84 ( $\pm 1.76$ )	25.3 ( $\pm 2.49$ )
GS-I	α-Gal, α-GalNAc	28.6 ( $\pm 4$ )	30.6 ( $\pm 2.81$ )	33 (3.17)
PNA	Galβ1→3GalNAc	10.4 ( $\pm 1.76$ )	9.9 ( $\pm 0.9$ )	10.71 ( $\pm 1.5$ )
VVA	GalNAc	10.21 ( $\pm 1.29$ )	11.37 ( $\pm 2.18$ )	11.36 ( $\pm 0.76$ )
UEA-I	α (1→2)-linked fucose	43.28 ( $\pm 6.9$ )	29.84 ( $\pm 6.4$ )	78.35 ( $\pm 5.4$ )
WGA	Neu5Ac, GlcNAc	115.7 ( $\pm 4.5$ )	84.4 ( $\pm 6.6$ )	167.9 ( $\pm 6.9$ )
SWGA	GlcNAc	nd	42 ( $\pm 2.98$ )	39.2 ( $\pm 2.87$ )
L-PHA	β→6GlcNAc	110 ( $\pm 9$ )	101 ( $\pm 8.2$ )	112 ( $\pm 10.4$ )
IgG <sup>3</sup>	Negative control for antibody staining	5.8 ( $\pm 1.6$ )	5.05 ( $\pm 1.4$ )	5.33 ( $\pm 1.6$ )
IgM <sup>3</sup>	Negative control for antibody staining	6.6 ( $\pm 1.1$ )	7.14 ( $\pm 2.2$ )	6.36 ( $\pm 1.3$ )
CSLEX1	Sialyl Lewis <sup>x</sup>	6.1 ( $\pm 1$ )	5.28 ( $\pm 1.6$ )	6.96 ( $\pm 2.2$ )
BRA-4F1	Galβ1→4(Fucα1→3)GlcNAc (Lewis <sup>x</sup> )	6.5 ( $\pm 1$ )	5.78 ( $\pm 1$ )	5.26 ( $\pm 1$ )
FH6	Sialylated dimeric Lewis <sup>x</sup>	6.47 ( $\pm 1$ )	5.38 ( $\pm 1$ )	5.63 ( $\pm 0.8$ )
CA 19-9	NeuAcα2→3Galβ1→3(Fucα1→4)GlcNc	5.52 ( $\pm 1$ )	6.74 ( $\pm 0.5$ )	5.76 ( $\pm 1.18$ )
7LE	Galβ1→3(Fucα1→4)GlcNAc (Lewis <sup>y</sup> )	8.3 ( $\pm 2$ )	7.9 ( $\pm 1$ )	7.3 ( $\pm 1.2$ )
2-25LE	Fucα1→2Galβ1→3(Fucα1→4)GlcNAc (Lewis <sup>b</sup> )	9.2 ( $\pm 1.4$ )	8.6 ( $\pm 0.8$ )	8.6 ( $\pm 1.2$ )
BR55-2	Fucα1→2Galβ1→4(Fucα1→3)GlcNAc (Lewis <sup>y</sup> )	9.6 ( $\pm 2.4$ )	9.9 ( $\pm 2.7$ )	9 ( $\pm 2$ )

<sup>1</sup>Staining of cell with streptavidin-FITC/PE was used as negative control in all lectin experiments. Average of mean fluorescence intensities and standard deviations (SD) are calculated based on many independent experiments.<sup>2</sup>Average of mean fluorescence intensities  $\pm$  SD for lectins and antibodies based on 3 replications is shown. nd, not determined.<sup>3</sup>Mouse IgG and IgM were used as negative controls for antibody staining.

generated by collecting reflected light from the thin sections with the pinhole set to a small value.

#### Statistical analysis

The frequency of established lung tumors was compared using the Student *t*-test option in Excel (Microsoft Corp., Redmond, WA). Differences between groups were considered significant at  $p < 0.05$ . All experiments were repeated 3 times.

#### Results

##### Establishment of sLe<sup>x</sup>-negative and -positive tumor cell variants

First, we examined the binding profile of several MAbs against cell surface Lewis antigen-related epitopes known to be important in the metastasis process. Among the MAbs tested, only KM93 (which is directed against sLe<sup>x</sup>) reacted with 4T1 cells as assessed by FACS (Table I, Fig. 1a). Notably, the sLe<sup>x</sup>-reactive antibody, CA19-9, did not react with 4T1 cells (Table I). This observation is consistent with early studies which indicated that sLe<sup>x</sup> serves as a ligand associated with cancer cells derived from the lower digestive organs, while the sLe<sup>x</sup> determinant predominates in the adhesion of breast, ovarian and pulmonary cancer cells.<sup>31</sup> CSLEX1, which is another widely used anti-sLe<sup>x</sup> antibody, did not react with the 4T1 cells (Table I). It has been demonstrated that E-selectin reactivity might not always correlate with CSLEX1 binding.<sup>32,33</sup> The KM93 antibody<sup>34</sup> reacts with the sLe<sup>x</sup> antigen with broad specificity<sup>35</sup> and best correlates with E-selectin binding.<sup>24–26</sup> Binding assays indicated that this antigen was abundantly expressed on the surface of 4T1 cells.

To study the role of the sLe<sup>x</sup> antigen in the metastasis of the 4T1 cell line, cells were sorted based on 2 criteria (high binding and low binding) as determined via KM93 reactivity; and 2 segregated subpopulations were consequently produced. Following isolation, we tested the reactivity of the KM93 antibody with the cell variants (Fig. 1b), which indicated a differential pattern of staining for KM93 between the 2 subpopulations, in FACS analysis. These subpopulations were designated as sLe<sup>x</sup>-positive and sLe<sup>x</sup>-negative. The subpopulations were stable *in vitro*. Even after 1 month

of keeping them in culture, differences in KM93 binding were marked (data not shown).

##### sLe<sup>x</sup> is the major carbohydrate determinant that differs between cell variants

Theoretically, cell sorting could lead to enrichment of minor subpopulations that differ in other cell surface oligosaccharide structures associated with metastatic phenotypes.<sup>36,37</sup> To determine if this occurred, the cell surface glycosylation pattern of the subpopulations was probed using MAbs and a panel of plant lectins as illustrated in Table I and Figure 1c. ABL and ACA did not react with either the sLe<sup>x</sup>-positive or -negative variant, indicating that there was no expression of TF antigen, Galβ(1→3)GalNAc $\alpha$ , or sialylated TF on the cell surface. Similarly, the TF-specific lectin PNA did not react with either cell subpopulation. VVA, which has specificity toward the Tn antigen (GalNAc- $\alpha$ -R), did not distinguish between the cell variants, indicating similar levels of Tn antigen expression. Both GS-I and SNA lectins, which are specific for the α-Gal epitope and α(2→6)-linked sialic acid, respectively, reacted identically with both subpopulations. ECL showed an increase in reactivity with the sLe<sup>x</sup>-positive variant and was specific for Galβ(1→4)GlcNAc, suggesting that cells positively selected for the KM93 epitope express higher levels of type II chain LacNAc, a core structure for type II lactoseries oligosaccharides, including sLe<sup>x</sup>. On the contrary, a decrease of this substrate structure recognition by ECL lectin in the sLe<sup>x</sup>-negative variant suggests that these cells carry less of the type II LacNAc substrate, possibly because of modification with other glycosyltransferases competing for the same substrate. Increased cell surface N-linked β1→6(GlcNAcβ1→6Man is associated with increased metastatic properties.<sup>38–40</sup> L-PHA recognizes β(1→6) branching structures with high affinity and specificity. This lectin bound to all cell variants with no significant difference. Therefore, this observation rules out the possibility of higher expression of this epitope on sLe<sup>x</sup>-negative cells.

As shown in Figure 1c, WGA, which is specific for both GlcNAc and sialic acid, showed a significant increase in binding to sLe<sup>x</sup>-positive cells, suggesting elevated levels of either one or both of these carbohydrates. To distinguish between GlcNAc and

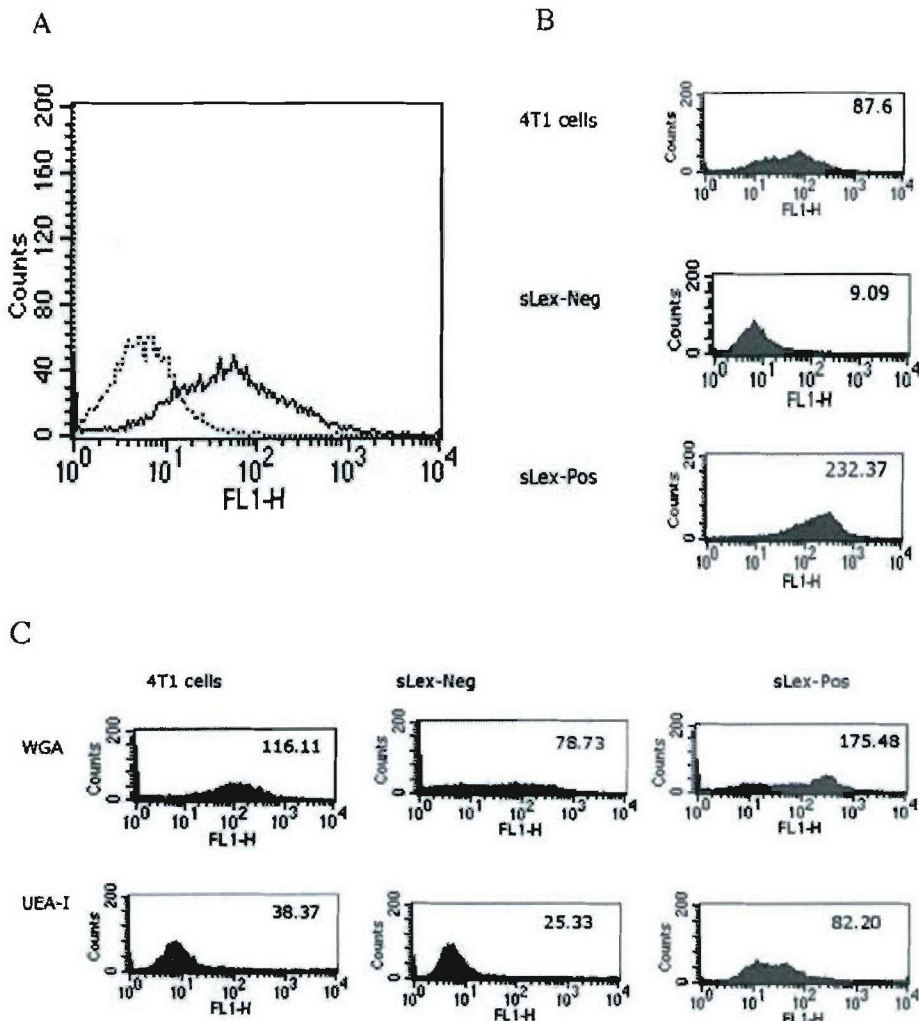


FIGURE 1 – (a) KM93 binds to parental 4T1 cells. Dotted line is murine IgM (10 µg/ml), which was used as negative control. Continuous line shows KM93 (10 µg/ml) reactivity. Antimouse IgM-FITC was used as secondary antibody. (b) KM93 staining of produced variants. 4T1 cells were sorted 4 times for generation of negative and highly positive KM93-reactive subpopulations. Expression of sLe<sup>x</sup> epitope was tested in original 4T1 as well as in sLe<sup>x</sup>-negative and sLe<sup>x</sup>-positive subpopulations. (c) WGA and UEA-I lectins react differently to the cell variants. Mean fluorescence intensity for each histogram is shown. Histograms are derived from a representative experiment out of at least 3 performed.

sialic acid, we tested the binding of SWGA (Table I), which binds only to GlcNAc residues and not sialic acid. SWGA did not differentiate significantly between the 2 subpopulations, implying that the higher WGA binding to the positive variant is most likely due to an increased level of terminal sialic acid residues. WGA and SNA binding data suggest that the decrease in sialic acid on the surface of the sLe<sup>x</sup>-negative variant is most likely that of the  $\alpha(2 \rightarrow 3)$  linkage.

UEA-I, which reacts mostly with terminal  $\alpha(1 \rightarrow 2)$ -linked fucose residues,<sup>41</sup> was also tested for binding (Fig. 1c) and displayed significantly higher reactivity with the sLe<sup>x</sup>-positive variant. Taken together, the lectin binding profile suggests that negative selection for the KM-93-reactive epitope resulted in a decrease in terminal sialic acid and of fucosylated structures. MAbs specific to Le<sup>x</sup> (BRA-4F1), sialylated dimeric Le<sup>x</sup> (FH6), sLe<sup>a</sup> (CA19-9), Le<sup>a</sup> (LE7), Le<sup>b</sup> (2-25LE) and Le<sup>y</sup> (BR55-2) did not show reactivity with the 4T1 cell line or its variants (Table I). Based on data obtained from MAbs, UEA-I, WGA and GS-1 binding, we believe that sLe<sup>x</sup>-negative cells are deficient in fucosylated or sialylated epitopes, which are subunits of sLe<sup>x</sup>, and that modification of a type II core structure by  $\alpha 1,2$ -fucosyltransferase or  $\alpha$ gal-transferase is not responsible for the decreased level of sLe<sup>x</sup>. NMR spectroscopy was employed to further characterize cell surface glycan structures. <sup>1</sup>H NMR spectra of intact cells confirmed a decrease in cell surface sialic acid in sLe<sup>x</sup>-negative cells, corrobor-

ating the WGA lectin binding data (data not shown). In sLe<sup>x</sup>-positive cells, the fucose resonance was more clearly observable than that in sLe<sup>x</sup>-negative cells (data not shown). Together these results suggest that the sLe<sup>x</sup> positive and -negative variants may have similar cell surface glycomic phenotypes except for sLe<sup>x</sup>.

#### E-selectin differentially recognized sLe<sup>x</sup>-negative and -positive cells

Murine 4T1 is a highly metastatic cell line, and based on its reactivity with KM93 MAb, the expression of E- or P-selectin ligand(s) on its surface is expected.<sup>26,42-44</sup> To investigate the functional significance of the different cell surface carbohydrate expression patterns, cells were tested for binding to E- and P-selectin. Cells were incubated with recombinant mouse E- and P-selectin/Fc (human IgG) chimeras, and binding was assayed by flow cytometry. E-selectin bound weakly to the original 4T1 cells, and its binding increased after positive selection for the KM93-reactive epitope (Fig. 2a). In contrast, E-selectin did not bind to the sLe<sup>x</sup>-negative variant. Reactivity of P-selectin with selected variants remained similar to the levels detected in binding to the parental 4T1 cells. These results indicate that binding of E-selectin to 4T1 cells correlates with the reactivity pattern of the KM93 antibody and that negative selection resulted in a cell variant deficient in the E-selectin-reactive ligand sLe<sup>x</sup>.

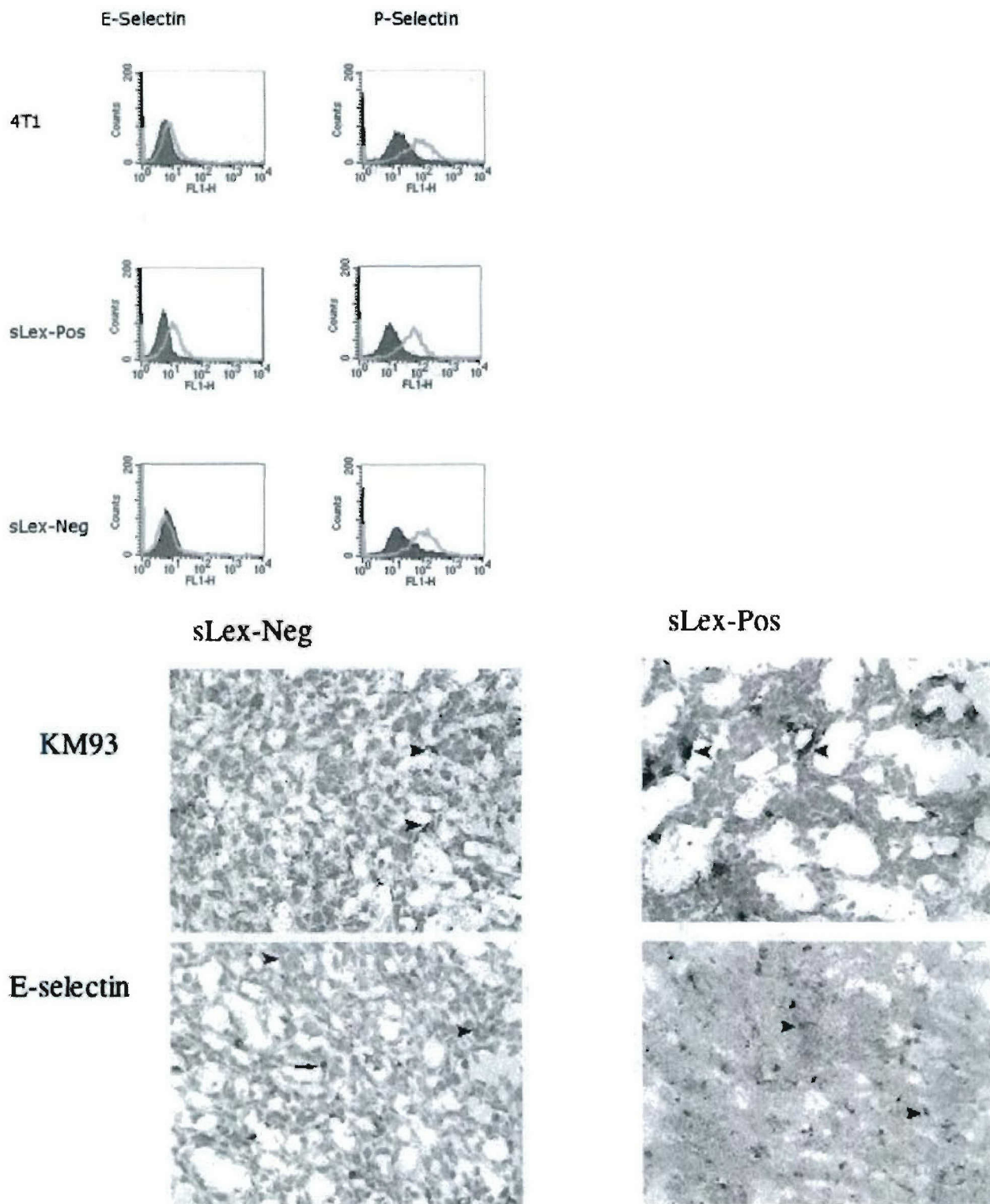


**FIGURE 2 – (a)** Analysis of mouse E- and P-selectin binding to the 4T1 cell line and its sLe<sup>x</sup>-negative and -positive variants by flow cytometry. Cells were first incubated with IgG-chimeric proteins and then stained with FITC-conjugated goat antihuman IgG (open histograms). Solid histogram shows binding in the presence of 20 mM EDTA. Experiment was repeated 3 times, and histograms of one representative are depicted. **(b)** Km93 and E-selectin histochemical binding in metastatic pulmonary tumors. sLe<sup>x</sup> antigen was expressed weakly on metastatic cells in lung sections from mice bearing sLe<sup>x</sup>-negative variant tumor, as assessed by KM93 antibody. sLe<sup>x</sup> antigen was strongly expressed on metastatic cells in lung sections (arrowheads) from mice bearing sLe<sup>x</sup>-positive tumor variant. E-selectin reactivity with lung metastatic cells from animals bearing sLe<sup>x</sup>-positive variant showed a diffuse moderate membranous pattern (arrowheads). In mice bearing sLe<sup>x</sup>-negative variant, metastatic cells (arrowheads) in lung sections rarely bind E-selectin, with a weak, granular membranous pattern. A few stromal cells with the morphology of endothelial cells are labeled (arrow).

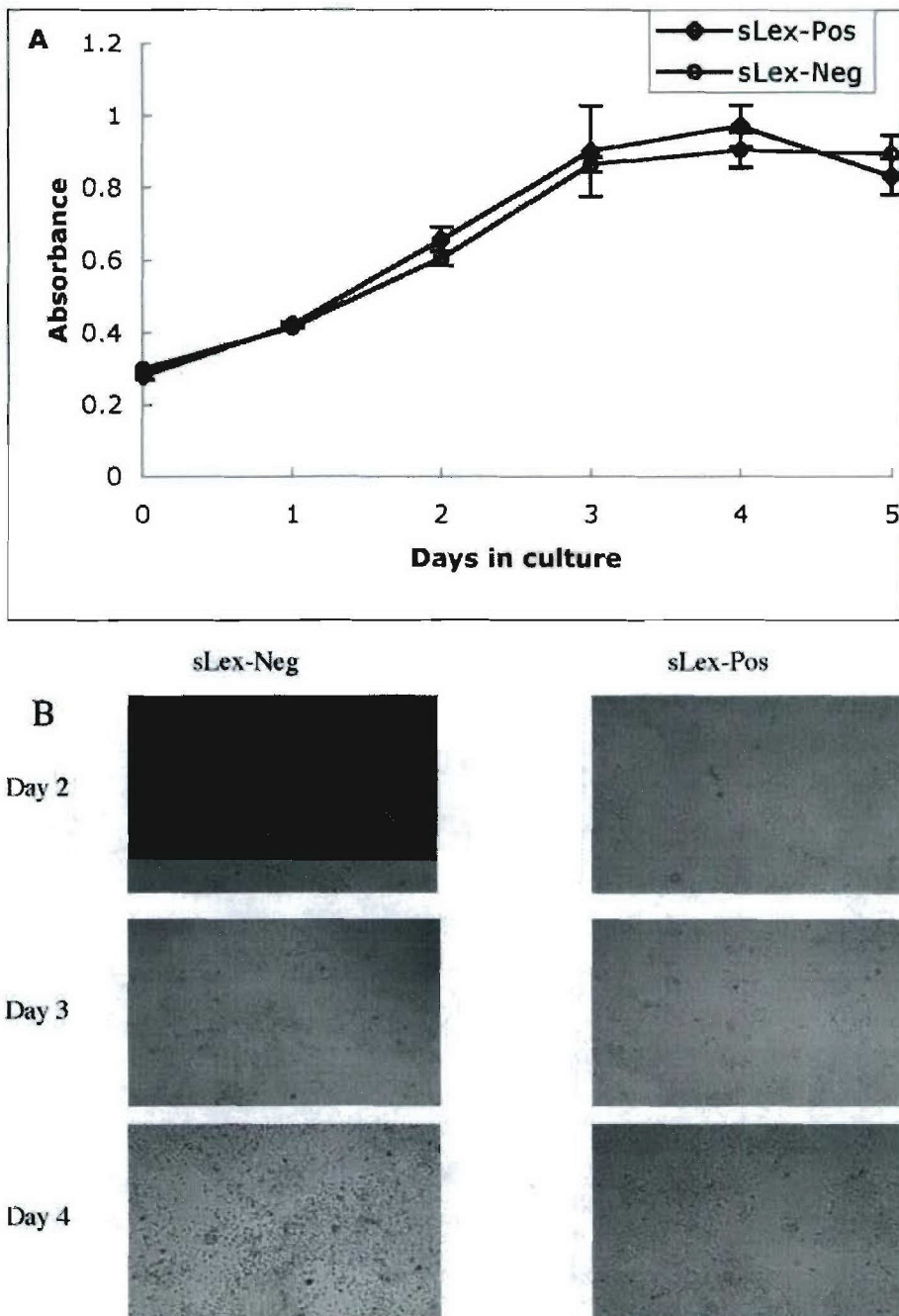


**FIGURE 3** – Phenotype of  $sLe^x$ -negative and -positive variants *in vitro*. (a) Cells (5,000/well) were seeded in wells of a 96-well plate at day 0 and cell proliferation was assessed using Celltiter 96 Aqueous One Solution, as described in Material and methods. Bars show SD of 3 replications. (b) Wells were photographed on days 2, 3 and 4; representative images are shown. (c) Cells were seeded into 100 mm tissue culture plates, and when they grew to confluence, the cell layer was scraped in the middle of the plate. Photographs were taken at the time of scraping and 24 and 48 hr later as indicated.

We further evaluated the stability of  $sLe^x$  expression by histochemical staining of the established lung tumor in  $sLe^x$ -negative and -positive tumor-bearing mice (Fig. 2b). In frozen lung sections, metastatic tumor cells from mice bearing the  $sLe^x$ -positive variant were strongly labeled with anti-KM93 antibody (Fig. 2b). Fewer cells in sections from mice bearing  $sLe^x$ -negative tumors were labeled, and they stained less intensely than their  $sLe^x$ -positive counterparts. We examined E-selectin binding characteristics of the cell variants *in vivo* by labeling frozen lung sections from mice bearing  $sLe^x$ -negative and -positive tumors with E-selectin. Metastatic tumor cells from mice bearing  $sLe^x$ -positive tumors stained diffusely with a membranous pattern (Fig. 2b). Metastatic cells from the  $sLe^x$ -negative variant were rarely labeled, and stain-

ing was less intense. Scattered stromal and pulmonary cells with the morphology of endothelial cells in both  $sLe^x$ -negative and -positive variants were labeled with E-selectin, consistent with expression of E-selectin ligands on endothelial cells. Taken together, these results indicate that the enriched cell variants retained the pattern of  $sLe^x$  expression *in vivo*.

*The  $sLe^x$ -negative variant displayed reduced cell-cell adhesion and enhanced motility *in vitro**

Comparison of cell growth *in vitro* revealed a similar growth rate for both  $sLe^x$ -negative and -positive subpopulations (Fig. 3a); however, a different growth pattern was observed (Fig. 3b). The  $sLe^x$ -positive variant, which is similar to the original 4T1, tended

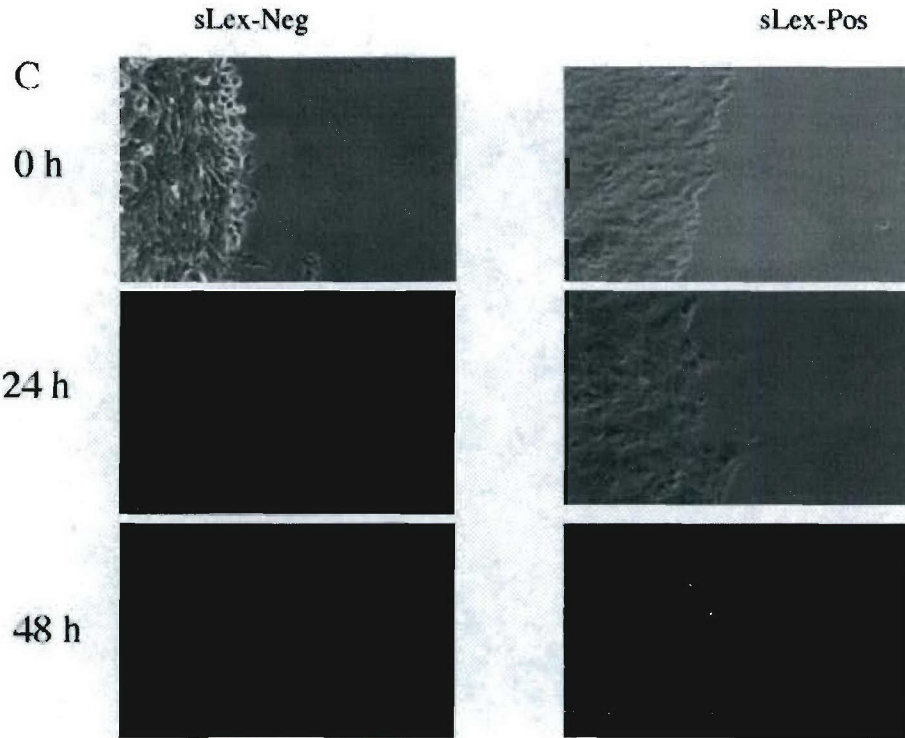


FIGURE 3 – CONTINUED.

to grow in clusters with high densities. While clusters were also visible in the sLe<sup>x</sup>-negative variant, this cell type had a tendency to spread out individually and quickly on the plate surface. Shortly after seeding the cells *in vitro*, sLe<sup>x</sup>-negative cells were observed to scatter and cover the surface, while sLe<sup>x</sup>-positive cells grew in separated clusters with surface void volume in between. To evaluate the rate of migration, we conducted a wound-healing experiment (Fig. 3c). As illustrated, 24 hr after scraping, sLe<sup>x</sup>-negative cells began to cover the scraped surface on the dish; and 48 hr later, the scratched surface of the dish was mostly covered. In the same time frame, sLe<sup>x</sup>-positive cells had yet to form separate colonies on the bare surface. These results suggest that sLe<sup>x</sup> oligosaccharide may affect the cell–cell adhesion and motility properties of the cells.

#### *Lung colonization in spontaneous metastasis was enhanced in sLe<sup>x</sup>-negative cells*

Tumor transplantation with the cell variants expressing different levels of sLe<sup>x</sup> was performed to evaluate their metastatic tendency. Groups of mice were inoculated with both the positively and negatively selected subpopulations to compare tumor metastasis (Fig. 4). We observed a statistically significantly ( $p = 0.0031$ ) higher number of colonies of metastatic cells in the lungs from animals injected with sLe<sup>x</sup>-negative cells (Fig. 4). Compared to the original 4T1 cell line, the number of colonies observed by clonogenic assay in mice inoculated with both the sLe<sup>x</sup>-positive and negative variants was significantly different in the same incubation time period.

Metastatic capacity of cell variants is related to the percentage of sLe<sup>x</sup>-positive or -negative cells present in the subpopulations. The percentage of sLe<sup>x</sup>-positive cells within each variant is negatively associated with the average number of tumor colonies observed in the clonogenic assay. As an average of multiple FACS assays, the percentage of sLe<sup>x</sup>-positive cells was about 50% of the parental line, while it was about 75% and 20% for the sLe<sup>x</sup>-positive and -negative variants, respectively. We observed a 2-fold

drop in the percentage of sLe<sup>x</sup>-negative cells after positive selection, whereas the percentage of sLe<sup>x</sup>-positive cells decreased 2.5-fold after negative selection. We observed average numbers of tumor colonies of 67 for the 4T1 parental line, 27.1 for the sLe<sup>x</sup>-positive variant and 139 for sLe<sup>x</sup>-negative variant. The 2.5-fold decrease of clonogenic lung metastatic cells after positive selection and the 2.1-fold increase after negative selection correspond to the fold increase or decrease in sLe<sup>x</sup>-positive cells, respectively. These findings are consistent with the conclusion that over the entire metastatic process sLe<sup>x</sup>-negative cells have an advantage over sLe<sup>x</sup>-positive cells. The results indicate that in any primary tumor mass with positive staining for sLe<sup>x</sup> oligosaccharide, an sLe<sup>x</sup>-negative subpopulation might exist that does metastasize very efficiently.

#### *sLe<sup>x</sup> expression affected the morphology of the primary tumor mass and lung micrometastases*

To detect morphologic differences in tumor cells and in the interaction of tumor cells with blood vessels within primary tumors, 8 sections from tumors in sLe<sup>x</sup>-positive and -negative inoculated mice, taken at approximately 20  $\mu$ m intervals, were evaluated histologically. Tumors from both variants had similar morphology, with a similar mitotic rate and degree of intratumoral necrosis. Cells were highly polymorphic and arranged in rows or small clusters, with scant fibrous stroma. In 7 of 8 sections examined, sLe<sup>x</sup>-positive cells exhibited a strong tendency to elongate with the long axis of the cells parallel to capillaries and arterioles, forming streams and often whirling around vessels (Fig. 5a). In contrast, sLe<sup>x</sup>-negative cells were more randomly oriented and not observed to whirl around vessels (0 of 8 sections examined) (Fig. 5b). However, another pattern of cellular architecture was observed in tumors of sLe<sup>x</sup>-negative cells. In 4 of 8 sections, cuboidal tumor cells were occasionally arranged in 1 or 2 irregular rows along capillaries and arterioles (Fig. 5b). In these areas, individual tumor cells appeared to be polarized with respect to the

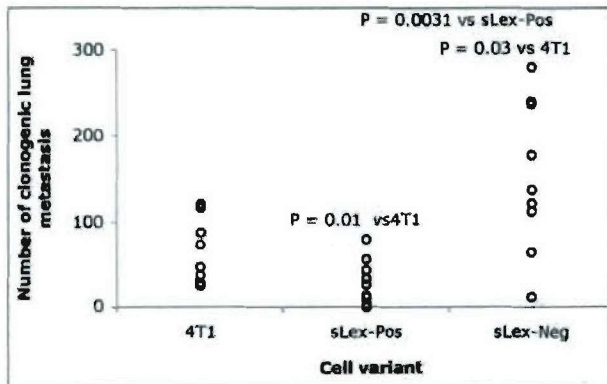


**FIGURE 4 –** sLe<sup>x</sup>-negative cells metastasize to the lung more than sLe<sup>x</sup>-positive and original 4T1 cells. Mice (10/group) were inoculated in the mammary fat and killed at day 26, organs were removed and cell suspensions were prepared and cultured. The number of clonogenic lesions was plotted. The experiment was repeated 3 times (10–12 mice/group) with similar results. Each circle corresponds to an individual mouse.

basement membrane of the blood vessel. This pattern was not observed in sections from sLe<sup>x</sup>-positive tumors.

Using 4T1 cells as a spontaneous pulmonary metastasis model, it was shown that extravasation was not a prerequisite for metastatic growth.<sup>45</sup> The authors showed that tumor cells proliferated in blood vessels and then proliferating tumor cells massively extravasated *via* outgrowing the blood vessel. In our model, the differences observed in the morphology of growth patterns in the primary tumor suggest that modification in a carbohydrate epitope and a subsequent alteration in cell-cell adhesion might impact the pattern of micrometastases. Therefore, in the next step of our investigation, we examined the morphology of lung micrometastases.

Fluorescent microscopy was performed on the lungs of tumor-bearing animals injected with GFP-expressing sLe<sup>x</sup>-negative or positive tumor cells. At 4 weeks after tumor transplant, mice (4/group) were killed and the entire lung surface was scanned in search of fluorescent tumor cells. In both sets of animals, several large tumor colonies (>200 µm, diameter) were detected. We screened areas in between the large lesions for small clusters of cells to compare morphology of tumor cell growth in early metastases. In more than 20 fields screened randomly, sLe<sup>x</sup>-negative tumor cells tended to be seen as individual cells or loosely organized groups of 2–3 cells without extensive membranous contact (Fig. 5c). However, small clusters of tumor cells were easily visualized in most of the fields screened in mice injected with sLe<sup>x</sup>-positive cells (Fig. 5d). Also, metastatic clusters of sLe<sup>x</sup>-positive cells were extended in a typical linear form from within capillaries. Such a linear intracapillary form of solitary tumor was not found in lung sections of sLe<sup>x</sup>-negative-injected animals. Therefore, consistent with the observed *in vitro* growth pattern of cells, sLe<sup>x</sup>-negative and -positive variants demonstrated significant differences in cellular morphology and pattern of tumor growth in the primary and secondary tumor sites.

## Discussion

The involvement of both sLe<sup>x</sup> and sLe<sup>a</sup> in metastasis *via* interaction with E- and P-selectins is addressed in the literature.<sup>8,9,17</sup> While we observed that the 4T1 cell line was deficient in sLe<sup>a</sup>, we specifically selected a subpopulation with markedly diminished expression of sLe<sup>x</sup> based on KM93 antibody binding, which is specific for this epitope. We show in this report that negative

selection for the sLe<sup>x</sup> epitope resulted in enrichment for a subpopulation of 4T1 cells with a high metastatic phenotype. Others investigating the basis underlying the metastatic properties of inflammatory breast carcinoma also showed, consistent with our data, that a decrease or lack of sLe<sup>x/a</sup> promotes passive metastasis of tumor cells in a xenograft model.<sup>20,46</sup> Together such findings indicate that the conventional belief that metastatic tendency is increased by upregulation of sialylated Lewis oligosaccharides and a subsequent increase in tumor cell–endothelial cell adhesion might be restricted to metastatic events associated with blood-borne tumor cells.

An increasing body of evidence indicates that the reduction in cell adhesion correlates with tumor invasion and metastasis.<sup>47–49</sup> Our results demonstrating differences in growth pattern and cell morphology *in vitro* clearly indicate that these properties have been modified upon negative selection for the sLe<sup>x</sup> epitope. We also observed, *in situ*, that cell variants had a tendency to interact distinctly with the tumor vasculature. The polarization of sLe<sup>x</sup>-negative cells with respect to the basement membrane of capillaries and small arterioles may indicate a greater propensity for vascular invasion compared to sLe<sup>x</sup>-positive cells, which tended to grow in elongated, streaming bundles parallel to blood vessels. Wyckoff *et al.*<sup>50</sup> described similar vascular polarization in metastasis-prone *vs.* nonmetastasizing cell lines using *in situ* fluorescence microscopy of primary tumors.

We also observed differences between the cell variants in the morphology of pulmonary metastases. Tumor cells from the sLe<sup>x</sup>-positive variant were observed growing as small clusters in a linear fashion within capillaries. This is in accordance with the results of Wong *et al.*,<sup>45</sup> who demonstrated similar intravascular growth in spontaneous metastasis of the murine 4T1 cell line. Tumor cells from the sLe<sup>x</sup>-negative variant were observed within capillaries as single cells adjacent to endothelium or as loose clusters of 2–3 cells without strong cell–cell interaction, and linear growth within capillaries was not observed. These findings suggest that sLe<sup>x</sup>-negative metastatic cells may have a reduced tendency to grow as intravascular clusters and may undergo extravasation more frequently.

Cell surface carbohydrate profiling indicates major differences in the expression of sialic acid and fucose residues, which are constituents of sLe<sup>x</sup>, based on different degrees of recognition using lectins. Although the detailed structural delineation of oligosaccharides has not been established, we ruled out core structural modification and sialic acid replacement by either  $\alpha$ (1→2)-linked fucose or  $\alpha$ Gal. We did not detect significant differences in the expression of  $\beta$ -1→6-GlcNAc and of  $\beta$ -1→4-GlcNAc between the cell variants based on lectin profile analysis. While the lectin binding data suggest that major modification involves sLe<sup>x</sup> epitope loss, we do not dismiss the possible contribution of other factors on the surface of the sLe<sup>x</sup>-negative variant, which may compensate for the lack of sLe<sup>x</sup> epitope.

Since the composition of oligosaccharides contributes to the folding, stability and biologic function of glycoproteins, expression of sLe<sup>x</sup> oligosaccharide could affect the adhesive properties of cells in an indirect way *via* affecting molecules important in adhesion. For instance, it has been proposed that the lack of sLe<sup>x</sup> enhanced formation of tumor embolus *via* stronger E-cadherin interaction within each embolus, which led to more efficient metastatic dissemination.<sup>20</sup> However, we did not observe any difference in anti-E-cadherin antibody binding to the cell variants (data not shown) or emboli formation among the sLe<sup>x</sup>-negative subpopulation *in vitro* or *in situ*, similar to the phenotype reported by Barsky's group.<sup>20</sup> A phenotype similar to what we observed has been associated with an increase in  $\beta$ -1→6-GlcNAc branching structures on complex N-linked carbohydrates.<sup>51</sup> Replacing  $\beta$ -1→6 branching structures with bisecting GlcNAc has led to enhanced homotypic adhesion of tumor cells *via* increased functional expression of E-cadherin.<sup>52</sup> It has also been suggested that integrins are involved in lung metastasis and that the tumor  $\alpha_3\beta_1$

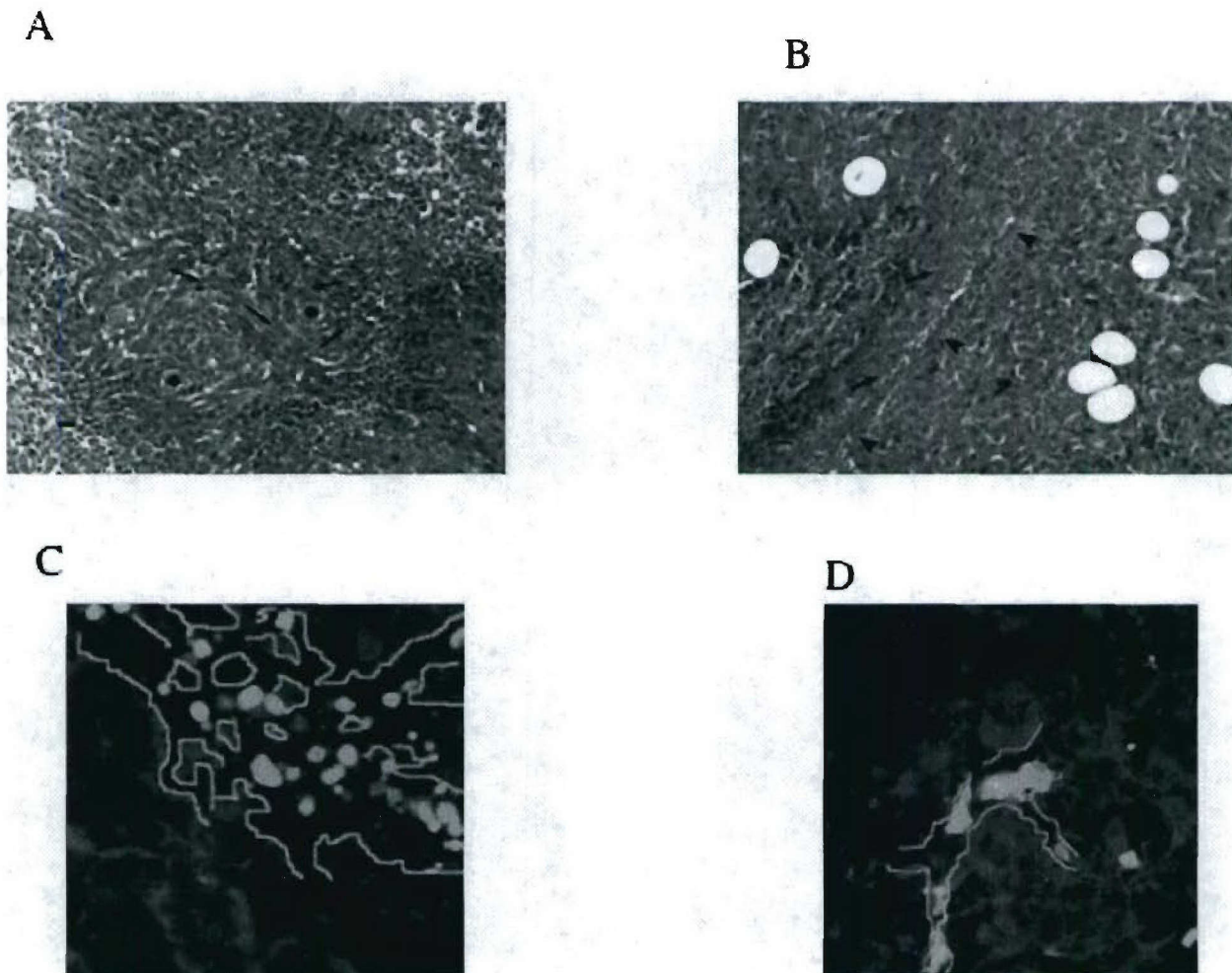


**FIGURE 5** – Histology of the primary tumor and *in situ* microscopy of lung in mice (4/group) inoculated with sLe<sup>x</sup>-positive (*a,d*) and -negative (*b,c*) cells. (*a,b*) Tumor-bearing mice were killed 15 days after transplant; serial sections of solid tumors were prepared, stained with H&E and examined under a light microscope; and images were taken at  $\times 20$  magnification. In sLe<sup>x</sup>-positive tumor mass (*a*), arrow shows streams of tumor cells parallel to and whirling around capillaries (stars). In sLe<sup>x</sup>-negative tumor mass (*b*), tumor cells (arrow) are polarized in 1 or 2 irregular rows along a capillary (arrowhead). Scale bar = 20  $\mu$ m. (*c,d*) Mice were inoculated with GFP-expressing sLe<sup>x</sup>-negative (*c*) and -positive (*d*) tumor cells. Twenty-eight days after the transplant, mice were killed and lungs were prepared for scanning using a Zeiss LSM410 laser scanning microscope. Images were taken at  $\times 63$  magnification. sLe<sup>x</sup>-negative tumor cells are present as individual cells or loosely associated groups of 2 or 3 cells within capillaries (*c*), in contrast to sLe<sup>x</sup>-positive cells, which exhibit linear clusters within capillaries (*d*). Lines indicate inner margins of capillary walls.

integrin makes an important contribution in tumor arrest in the lung.<sup>53</sup> The glycosylation profile of integrins has been implicated in the modulation of their function.<sup>54,55</sup> Therefore, sLe<sup>x</sup> expression may modify the adhesion abilities of either E-cadherin or integrins involved in metastasis. Further studies are needed to investigate these possibilities.

The sLe<sup>x</sup> antigen, as an adhesion molecule, is thought to play a crucial role in the metastatic cascade. Many studies have proposed measuring the surface expression of this antigen as a prognostic marker<sup>6,56-59</sup> or as a target in treating metastasis through antiadhesion therapy.<sup>17,27</sup> A review of studies performed on the role of sLe<sup>x</sup> oligosaccharide in metastasis brings up an important issue. What is the role of the sLe<sup>x</sup> carrier or other coexpressed molecules on the functional involvement of this antigen? The use of sLe<sup>x</sup> as a prognostic indicator or a target makes more sense if it is combined with the state of disseminated cancer cells or the status of other markers, like nm23-H1 or CD24.<sup>60-62</sup> For example, CD24 is a P-selectin ligand and can mediate rolling of carcinoma cells on P-selectin *in vitro*.<sup>63,64</sup> It has been suggested that CD24 expression

might be considered as a prognostic marker.<sup>65</sup> However, to create a functional P-selectin ligand, CD24 should be modified with sLe<sup>x</sup> and the expression of neither CD24 nor sLe<sup>x</sup> alone is sufficient to facilitate P-selectin binding and accumulation of tumor cells in the lung.<sup>62</sup> Our results suggest that while sLe<sup>x</sup> is an important tumor-associated antigen, there seems to be a substantial need to characterize potential molecules carrying this oligosaccharide and that evaluation of this oligosaccharide alone might have limited clinical application.

Our findings support the concept that metastatic dissemination may be facilitated as a consequence of increased tumor tissue disaggregation mediated by reduction in sLe<sup>x</sup> expression on tumor cells. We speculate that absence of the sLe<sup>x</sup> oligosaccharide promotes the metastatic behavior of the 4T1 cell line, possibly through decreased adhesion at the primary tumor site, which increases individual cell dissemination, resulting in increased micrometastases. Entry into the circulation has also been addressed by others as a critical step for dissemination of tumor cells to distant organs.<sup>30,66</sup> The results also suggest that the advan-

tages that sLe<sup>x</sup>-expressing cells may have in the later steps of the metastatic process due to more efficient extravasation do not compensate for the increased efficiency of escape of tumor cells from the primary lesion. Our results also suggest that any limiting role for the E-selectin receptor<sup>8</sup> or other undefined sLe<sup>x</sup> receptors<sup>18</sup> and the sLe<sup>x</sup> ligand itself in the hematogenous part of the metastasis cascade in this model does not affect the end point of the metastasis process. Instead, sLe<sup>x</sup>-independent P-selectin-ligand interactions with the P-selectin receptor on either endothelium or platelets may play a role in the homing of metastatic cells in our model. P-selectin ligands are expressed on human carcinomas<sup>67,68</sup>

and play a role in metastasis.<sup>9,69</sup> P-selectin was observed to bind very well to all of our subpopulations. In conclusion, our data indicate that subpopulations in the primary tumor mass, which are low or negative for sLe<sup>x</sup> expression, should be considered as a potential source for micrometastases.

### Acknowledgements

This study was supported by a DOD grant (DAMD17-0101-0366) and an NIH grant (CA089480) to T.K.E. and by an ACS-IRG pilot grant (271/G1-11262-01E) to T.L.W.

### References

- Liotta LA, Steeg PS, Stetler-Stevenson WG. Cancer metastasis and angiogenesis: an imbalance of positive and negative regulation. *Cell* 1991;64:327-36.
- Fidler IJ. The pathogenesis of cancer metastasis: the "seed and soil" hypothesis revisited. *Nature Rev Cancer* 2003;3:453-8.
- Dennis JW, Granovsky M, Warren CE. Protein glycosylation in development and disease. *Bioessays* 1999;21:412-21.
- Granovsky M, Fata J, Pawling J, Muller WJ, Khokha R, Dennis JW. Suppression of tumor growth and metastasis in Mgtat5-deficient mice. *Nat Med* 2000;6:306-12.
- Nelson RM, Venot A, Bevilacqua MP, Linhardt RJ, Stamenkovic I. Carbohydrate-protein interactions in vascular biology. *Annu Rev Cell Dev Biol* 1995;11:601-31.
- Renkonen J, Paavonen T, Renkonen R. Endothelial and epithelial expression of sialyl Lewis<sup>x</sup> and sialyl Lewis<sup>a</sup> in lesions of breast carcinoma. *Int J Cancer* 1997;74:296-300.
- Kim YJ, Varki A. Perspectives on the significance of altered glycosylation of glycoproteins in cancer. *Glycoconj J* 1997;14:569-76.
- Ohyama C, Tsuboi S, Fukuda M. Dual roles of sialyl Lewis<sup>x</sup> oligosaccharides in tumor metastasis and rejection by natural killer cells. *EMBO J* 1999;18:1516-25.
- Kim YJ, Borsig L, Varki NM, Varki A. P-selectin deficiency attenuates tumor growth and metastasis. *Proc Natl Acad Sci USA* 1998;95:9325-30.
- Majuri ML, Niemela R, Tiisala S, Renkonen O, Renkonen R. Expression and function of α2, 3-sialyl- and α1, 3/1, 4-fucosyltransferases in colon adenocarcinoma cell lines: role in synthesis of E-selectin counter-receptors. *Int J Cancer* 1995;63:551-9.
- McEver RP, Moore KL, Cummings RD. Leukocyte trafficking mediated by selectin-carbohydrate interactions. *J Biol Chem* 1995;270:11025-8.
- Kansas GS. Selectins and their ligands: current concepts and controversies. *Blood* 1996;88:3259-87.
- Varki A. Selectin ligands: will the real ones please stand up? *J Clin Invest* 1997;100:S31-5.
- Lowe JB, Ward PA. Therapeutic inhibition of carbohydrate-protein interactions in vivo. *J Clin Invest* 1997;100:S47-51.
- McEver RP, Cummings RD. Role of PSGL-1 binding to selectins in leukocyte recruitment. *J Clin Invest* 1997;100:S97-103.
- Kannagi R, Izawa M, Koike T, Miyazaki K, Kimura N. Carbohydrate-mediated cell adhesion in cancer metastasis and angiogenesis. *Cancer Sci* 2004;95:377-84.
- O I, Otvos L, Kieber-Emmons T, Blaszczyk-Thurin M. Role of SA-Le<sup>a</sup> and E-selectin in metastasis assessed with peptide antagonist. *Peptides* 2002;23:999-1010.
- Zhang J, Nakayama J, Ohyama C, Suzuki M, Suzuki A, Fukuda M, Fukuda MN. Sialyl Lewis<sup>x</sup>-dependent lung colonization of B16 melanoma cells through a selectin-like endothelial receptor distinct from E- or P-selectin. *Cancer Res* 2002;62:4194-8.
- Kishimoto T, Ishikura H, Kimura C, Takahashi T, Kato H, Yoshiki T. Phenotypes correlating to metastatic properties of pancreas adenocarcinoma in vivo: the importance of surface sialyl Lewis<sup>a</sup> antigen. *Int J Cancer* 1996;69:290-4.
- Alpaugh ML, Tomlinson JS, Ye Y, Barsky SH. Relationship of sialyl Lewis<sup>a</sup> underexpression and E-cadherin overexpression in the lymphovascular embolus of inflammatory breast carcinoma. *Am J Pathol* 2002;161:619-28.
- Miller FR, Miller BE, Heppner GH. Characterization of metastatic heterogeneity among subpopulations of a single mouse mammary tumor: heterogeneity in phenotypic stability. *Invasion Metastasis* 1983;3:22-31.
- Pulaski BA, Ostrand-Rosenberg S. Reduction of established spontaneous mammary carcinoma metastases following immunotherapy with major histocompatibility complex class II and B7.1 cell-based tumor vaccines. *Cancer Res* 1998;58:1486-93.
- Parviz M, Chin CS, Graham LJ, Miller C, Lee C, George K, Bear HD. Successful adoptive immunotherapy with vaccine-sensitized T cells, despite no effect with vaccination alone in a weakly immunogenic tumor model. *Cancer Immunol Immunother* 2003;52:739-50.
- Liu F, Zhang Y, Zhang XY, Chen HL. Transfection of the *nm23-H1* gene into human hepatocarcinoma cell line inhibits the expression of sialyl Lewis<sup>a</sup>, α1,3 fucosyltransferase VII, and metastatic potential. *J Cancer Res Clin Oncol* 2002;128:189-96.
- Guo P, Zhang Y, Zhang XY, Chen HL, Wang H, Narimatsu H. Analysis of Lewis antigens on cell surface and α1, 3-fucosyltransferase subtypes in H7721 human hepatocarcinoma cells. *J Exp Clin Cancer Res* 2003;22:135-9.
- Nemoto Y, Izumi Y, Tezuka K, Tamatani T, Irimura T. Comparison of 16 human colon carcinoma cell lines for their expression of sialyl Le<sup>x</sup> antigens and their E-selectin-dependent adhesion. *Clin Exp Metastasis* 1998;16:569-76.
- Fukuda MN, Ohyama C, Lowitz K, Matsuo O, Pasqualini R, Ruoslahti E, Fukuda M. A peptide mimic of E-selectin ligand inhibits sialyl Lewis<sup>x</sup>-dependent lung colonization of tumor cells. *Cancer Res* 2000;60:450-6.
- Aslakson CJ, Miller FR. Selective events in the metastatic process defined by analysis of the sequential dissemination of subpopulations of a mouse mammary tumor. *Cancer Res* 1992;52:1399-405.
- Pulaski BA, Ostrand-Rosenberg S. Mouse 4T1 breast tumor model. In: Coligan JE, Kruisbeek AM, Margulies DH, Shevach E, Strober W, eds. *Current protocols in immunology*, vol. 3. New York: John Wiley & Sons, 2000;20.2.1-20.2.16.
- Monzavi-Karbassi B, Cunto-Amesty G, Luo P, Shamloo S, Blaszczyk-Thurin M, Kieber-Emmons T. Immunization with a carbohydrate mimicking peptide augments tumor-specific cellular responses. *Int Immunopharmacol* 2001;13:1361-71.
- Takada A, Ohmori K, Yoneda T, Tsuyuoka K, Hasegawa A, Kiso M, Kannagi R. Contribution of carbohydrate antigens sialyl Lewis<sup>a</sup> and sialyl Lewis<sup>x</sup> to adhesion of human cancer cells to vascular endothelium. *Cancer Res* 1993;53:354-61.
- Wagers AJ, Stoolman LM, Craig R, Knibbs RN, Kansas GS. An sLe<sup>x</sup>-deficient variant of HL60 cells exhibits high levels of adhesion to vascular selectins: further evidence that HECA-452 and CSLEX1 monoclonal antibody epitopes are not essential for high avidity binding to vascular selectins. *J Immunol* 1998;160:5122-9.
- Wagers AJ, Stoolman LM, Kannagi R, Craig R, Kansas GS. Expression of leukocyte fucosyltransferases regulates binding to E-selectin: relationship to previously implicated carbohydrate epitopes. *J Immunol* 1997;159:1917-29.
- Hanai N, Shitara K, Yoshida H. Generation of monoclonal antibodies against human lung squamous cell carcinoma and adenocarcinoma using mice rendered tolerant to normal human lung. *Cancer Res* 1986;46:4438-43.
- Dohi T, Nemoto T, Ohta S, Shitara K, Hanai N, Nudelman E, Hakomori S, Oshima M. Different binding properties of three monoclonal antibodies to sialyl Le<sup>x</sup> glycolipids in a gastric cancer cell line and normal stomach tissue. *Anticancer Res* 1993;13:1277-82.
- Hakomori S. Tumor malignancy defined by aberrant glycosylation and sphingo(glyco)lipid metabolism. *Cancer Res* 1996;56:5309-18.
- Hakomori S. Glycosylation defining cancer malignancy: new wine in an old bottle. *Proc Natl Acad Sci USA* 2002;99:10231-3.
- Dennis JW, Laferte S, Waghamore C, Breitman ML, Kerbel RS. β1-6 branching of Asn-linked oligosaccharides is directly associated with metastasis. *Science* 1987;236:582-5.
- Yagel S, Feinmesser R, Waghamore C, Lala PK, Breitman ML, Dennis JW. Evidence that β1-6 branched Asn-linked oligosaccharides on metastatic tumor cells facilitate invasion of basement membranes. *Int J Cancer* 1989;44:685-90.
- Seberger PJ, Chaney WG. Control of metastasis by Asn-linked, β1-6 branched oligosaccharides in mouse mammary cancer cells. *Glycobiology* 1999;9:235-41.
- Nemoto-Sasaki Y, Mitsuki M, Morimoto-Tomita M, Maeda A, Tsuji M, Irimura T. Correlation between the sialylation of cell surface

Thomsen-Friedenreich antigen and the metastatic potential of colon carcinoma cells in a mouse model. *Glycoconj J* 2001;18:895–906.

42. Kanoh A, Ota M, Narimatsu H, Irimura T. Expression levels of *FUT6* gene transfected into human colon carcinoma cells switch two sialyl-Lewis<sup>x</sup>-related carbohydrate antigens with distinct properties in cell adhesion. *Biochem Biophys Res Commun* 2003;303:896–901.
43. Misugi E, Kawamura N, Imanishi N, Tojo SJ, Morooka S. Sialyl Lewis<sup>x</sup> moiety on rat polymorphonuclear leukocytes responsible for binding to rat E-selectin. *Biochem Biophys Res Commun* 1995;215:547–54.
44. Liu F, Qi HL, Zhang Y, Zhang XY, Chen HL. Transfection of the *c-erbB2/neu* gene upregulates the expression of sialyl Lewis<sup>x</sup>, α1,3-fucosyltransferase VII, and metastatic potential in a human hepatocarcinoma cell line. *Eur J Biochem* 2001;268:3501–12.
45. Wong CW, Song C, Grimes MM, Fu W, Dewhirst MW, Muschel RJ, Al-Mehdi AB. Intravascular location of breast cancer cells after spontaneous metastasis to the lung. *Am J Pathol* 2002;161:749–53.
46. Alpaugh ML, Tomlinson JS, Kasraeian S, Barsky SH. Cooperative role of E-cadherin and sialyl-Lewis<sup>x/a</sup>-deficient MUC1 in the passive dissemination of tumor emboli in inflammatory breast carcinoma. *Oncogene* 2002;21:3631–43.
47. Behrens J. The role of cell adhesion molecules in cancer invasion and metastasis. *Breast Cancer Res Treat* 1993;24:175–84.
48. Cavallaro U, Christofori G. Cell adhesion in tumor invasion and metastasis: loss of the glue is not enough. *Biochim Biophys Acta* 2001;1552:39–45.
49. Hirohashi S, Kanai Y. Cell adhesion system and human cancer morphogenesis. *Cancer Sci* 2003;94:575–81.
50. Wyckoff JB, Jones JG, Condeelis JS, Segall JE. A critical step in metastasis: in vivo analysis of intravasation at the primary tumor. *Cancer Res* 2000;60:2504–11.
51. Yoshimura M, Nishikawa A, Ihara Y, Taniguchi S, Taniguchi N. Suppression of lung metastasis of B16 mouse melanoma by *N*-acetylglucosaminyltransferase III gene transfection. *Proc Natl Acad Sci USA* 1995;92:8754–8.
52. Yoshimura M, Ihara Y, Matsuzawa Y, Taniguchi N. Aberrant glycosylation of E-cadherin enhances cell–cell binding to suppress metastasis. *J Biol Chem* 1996;271:13811–5.
53. Wang H, Fu W, Im JH, Zhou Z, Santoro SA, Iyer V, DiPersio CM, Yu QC, Quaranta V, Al-Mehdi A, Muschel RJ. Tumor cell α<sub>5</sub>β<sub>1</sub> integrin and vascular laminin-5 mediate pulmonary arrest and metastasis. *J Cell Biol* 2004;164:935–41.
54. Pochee E, Litynska A, Amoresano A, Casbarra A. Glycosylation profile of integrin α<sub>5</sub>β<sub>1</sub> changes with melanoma progression. *Biochim Biophys Acta* 2003;1643:113–23.
55. Isaji T, Gu J, Nishiuchi R, Zhao Y, Takahashi M, Miyoshi E, Honke K, Sekiguchi K, Taniguchi N. Introduction of bisecting GlcNAc into integrin α<sub>5</sub>β<sub>1</sub> reduces ligand binding and down-regulates cell adhesion and cell migration. *J Biol Chem* 2004;279:19747–54.
56. Murata K, Egami H, Shibata Y, Sakamoto K, Misumi A, Ogawa M. Expression of blood group-related antigens, ABH, Lewis<sup>a</sup>, Lewis<sup>b</sup>, Lewis<sup>x</sup>, Lewis<sup>y</sup>, CA19-9, and CSLEX1 in early cancer, intestinal metaplasia, and uninvolved mucosa of the stomach. *Am J Clin Pathol* 1992;98:67–75.
57. Grabowski P, Mann B, Mansmann U, Lovin N, Foss HD, Berger G, Scherubl H, Riecken EO, Buhr HJ, Hanski C. Expression of sialyl-Le<sup>x</sup> antigen defined by MAb AM-3 is an independent prognostic marker in colorectal carcinoma patients. *Int J Cancer* 2000;88:281–6.
58. Nakagoe T, Fukushima K, Sawai T, Tsuji T, Jibiki M, Nanashima A, Tanaka K, Yamaguchi H, Yasutake T, Ayabe H, Arisawa K, Ishikawa H. Increased expression of sialyl Lewis<sup>x</sup> antigen as a prognostic factor in patients with stage 0, I, and II gastric cancer. *Cancer Lett* 2002;175:213–21.
59. Nakagoe T, Fukushima K, Itoyanagi N, Ikuta Y, Oka T, Nagayasu T, Ayabe H, Hara S, Ishikawa H, Minami H. Expression of ABH/Lewis-related antigens as prognostic factors in patients with breast cancer. *J Cancer Res Clin Oncol* 2002;128:257–64.
60. Yamaguchi A, Ding K, Machara M, Goi T, Nakagawara G. Expression of *nm23-H1* gene and sialyl Lewis<sup>x</sup> antigen in breast cancer. *Oncology* 1998;55:357–62.
61. Sumikura S, Ishigami S, Natsugoe S, Miyazono F, Tokuda K, Nakajo A, Okumura H, Matsumoto M, Hokita S, Aikou T. Disseminated cancer cells in the blood and expression of sialylated antigen in gastric cancer. *Cancer Lett* 2003;200:77–83.
62. Friederichs J, Zeller Y, Hafezi-Moghadam A, Grone HJ, Ley K, Altevogt P. The CD24/P-selectin binding pathway initiates lung arrest of human A125 adenocarcinoma cells. *Cancer Res* 2000;60:6714–22.
63. Aigner S, Ramos CL, Hafezi-Moghadam A, Lawrence MB, Friederichs J, Altevogt P, Ley K. CD24 mediates rolling of breast carcinoma cells on P-selectin. *FASEB J* 1998;12:1241–51.
64. Aigner S, Stoeber ZM, Fogel M, Weber E, Zarn J, Ruppert M, Zeller Y, Vestweber D, Stahel R, Sammar M, Altevogt P. CD24, a mucin-type glycoprotein, is a ligand for P-selectin on human tumor cells. *Blood* 1997;89:3385–95.
65. Kristiansen G, Winzer KJ, Mayordomo E, Bellach J, Schluns K, Denkert C, Dahl E, Pilarsky C, Altevogt P, Guski H, Dietel M. CD24 expression is a new prognostic marker in breast cancer. *Clin Cancer Res* 2003;9:4906–13.
66. Zijlstra A, Mellor R, Panzarella G, Aimes RT, Hooper JD, Marchenko ND, Quigley JP. A quantitative analysis of rate-limiting steps in the metastatic cascade using human-specific real-time polymerase chain reaction. *Cancer Res* 2002;62:7083–92.
67. Mannori G, Crottet P, Cecconi O, Hanasaki K, Aruffo A, Nelson RM, Varki A, Bevilacqua MP. Differential colon cancer cell adhesion to E-, P-, and L-selectin: role of mucin-type glycoproteins. *Cancer Res* 1995;55:4425–31.
68. Stone JP, Wagner DD. P-selectin mediates adhesion of platelets to neuroblastoma and small cell lung cancer. *J Clin Invest* 1993;92:804–13.
69. Varki NM, Varki A. Heparin inhibition of selectin-mediated interactions during the hematogenous phase of carcinoma metastasis: rationale for clinical studies in humans. *Semin Thromb Hemost* 2002;28:53–66.